

# Field observations of geomorphic change during artificial estuary openings

---

**Report prepared for:**  
Corangamite Catchment Management Authority (CCMA)

v 2.0 Feb 2020



**This report should be cited as:**

McSweeney, S.L., and Stout, J.C. (2019) Field observations of geomorphic change during artificial estuary openings. Report prepared for: Corangamite Catchment Management Authority (CCMA). December 2019.

**Corresponding author:**

Dr. Sarah McSweeney

School of Geography

The University of Melbourne

[sarah.mcsweeney@unimelb.edu.au](mailto:sarah.mcsweeney@unimelb.edu.au)

## Table of Contents

List of Tables .....	2
List of Figures.....	2
Acknowledgements .....	3
1.0 Project brief .....	5
2.0 Executive Summary .....	6
3.0 Introduction.....	8
3.1 Background.....	8
3.2 Project aims .....	9
4.0 Literature review of opening processes .....	10
4.1 Natural openings .....	10
4.2 Artificial openings and conditions favouring a successful opening .....	12
4.3 Geomorphic change during artificial openings .....	13
4.4 Physiochemical change during artificial openings and fish deaths.....	15
5.0 Methods .....	16
5.1 Water level thresholds for natural openings .....	16
5.2 Field work.....	16
5.2.1 Study sites .....	16
5.2.1 Monitoring of artificial openings.....	18
5.2.2 Hydraulic gradient .....	20
5.3 Historic hydraulic gradients for successful openings.....	20
5.4 Controls on basin drainage .....	21
5.5 Physiochemical change .....	21
6.0 Results .....	22
6.1 Water levels for natural openings.....	22
6.2 Field observations during artificial openings .....	23
6.1.1 Aire River 1: 01/02/19 .....	24
6.1.2 Gellibrand River: 09/03/19.....	26
6.1.3 Aire River 2: 01/05/19 .....	28
6.1.4 Spring Creek: 31/05/19 .....	30
6.1.5 Curdies Inlet 1: 16/06/19 .....	33
6.1.6 Curdies Inlet 2: 17/01/19 .....	35
6.1.7 Painkalac Creek: 08/08/19 .....	36
6.1.8 Anglesea River: 14/08/19 .....	39
6.3 Timescales of geomorphic change during artificial openings .....	41
6.4 Thresholds for successful openings .....	42
6.5 Predicting estuary drainage rates .....	45
6.6 Physiochemical change during artificial openings .....	46
7.0 Discussion .....	46
7.1 Geomorphic controls on the success of artificial openings .....	46
7.2 Recommendations for ensuring a successful opening.....	48
7.3 Controls on basin drainage rates .....	49
7.4 Can we slow estuary drainage rates to avoid fish strandings? .....	50
7.5 Where this study fits within the current management procedure.....	51
8.0 Conclusion .....	52
9.0 References .....	54
Appendix 1: Natural opening water levels .....	56
Appendix 2: Field data for 2019 artificial openings.....	58
Appendix 3: Historic hydraulic gradients, water levels, and drainage details for known openings .....	65
Appendix 4: Physiochemical change vs morphological change at the mouth .....	68

## List of Tables

Table name	Page
<b>Table 1.</b> Historic water levels at which natural openings occur at different sites.	21
<b>Table 2.</b> Historic hydraulic gradients at which natural openings occur at different sites.	22
<b>Table 3.</b> Summary of artificial estuary entrance openings monitored in the field as part of this study.	24
<b>Table 4.</b> Min and mean HG for a successful opening for estuaries that had >5 openings recorded.	44
<b>Table 5.</b> Summary of observed geomorphic stages during an artificial opening.	47

## List of Figures

Figure name	Page
<b>Figure 1a-d.</b> Flooding prior to artificial opening and artificial openings being undertaken	8
<b>Figure 2a-b.</b> Natural openings of Gellibrand River and Sherbrook River	9
<b>Figure 3a-c.</b> Natural opening of the Aire River 2014	11
<b>Figure 4.</b> Conditions favouring natural opening via seepage/liquefaction of the berm	12
<b>Figure 5.</b> Illustration of the hydraulic gradient	13
<b>Figure 6a-c.</b> Pilot channel stage during an artificial opening	14
<b>Figure 7a-c.</b> Rapid expansion stage during an artificial opening	14
<b>Figure 8a-c.</b> River flow stage during an artificial opening	15
<b>Figure 9.</b> Conceptual stages during the artificial opening sequence	15
<b>Figure 10a-g.</b> Map of study sites and locations and equipment placement	17
<b>Figure 11a-c.</b> Open ocean wave heights and directions for study sites	18
<b>Figure 12a-d.</b> Measurement methods to obtain geomorphic data in the field	19
<b>Figure 13.</b> Example EstuaryWatch data used to calculate hydraulic gradient	20
<b>Figure 14.</b> Distributions of water levels at which natural openings occur	22
<b>Figure 15.</b> Basin drainage and timing of morphological monitoring at Aire River opening 1	24
<b>Figure 16a-d.</b> Morphological change during Aire River opening 1	25
<b>Figure 17a-f.</b> Photos of morphological change during Aire River opening 1	25
<b>Figure 18.</b> Basin drainage and timing of morphological monitoring at Gellibrand River opening	26
<b>Figure 19a-d.</b> Morphological change during Gellibrand River opening	27
<b>Figure 20a-f.</b> Photos of morphological change during Gellibrand River opening	27
<b>Figure 21.</b> Basin drainage and timing of morphological monitoring at Aire River opening 2	28
<b>Figure 22.</b> Surveys of entrance cross section change during Aire River opening 2	29
<b>Figure 23a-f.</b> Morphological change during Aire River opening 2	29
<b>Figure 24a-d.</b> Photos of morphological change during Aire River opening 2	30
<b>Figure 25.</b> Basin drainage and timing of morphological monitoring at Spring Creek opening	31
<b>Figure 26.</b> Surveys of entrance cross section change during Spring Creek opening	31
<b>Figure 27a-d.</b> Morphological change during Spring Creek opening	32
<b>Figure 28a-f.</b> Photos of morphological change during Spring Creek opening	33
<b>Figure 29.</b> Change in surveyed long profile during Curdies Inlet opening 1	34
<b>Figure 30.</b> Photos of morphological change during Curdies Inlet opening 1	34
<b>Figure 31a-c.</b> Flooding prior to opening and reduction in flooding at Curdies Inlet	34
<b>Figure 32a-b.</b> Basin drainage and timing of morphological monitoring at Curdies openings 1 and 2	35
<b>Figure 33.</b> Morphological change during opening 2 at Curdies Inlet	35
<b>Figure 34a-d.</b> Pictures from artificial opening 2 at Curdies Inlet	36

<b>Figure 35.</b> Basin drainage and timing of morphological monitoring at Painkalac Creek	37
<b>Figure 36a-d.</b> Morphological change during opening of Painkalac Creek	37
<b>Figure 37.</b> Surveys of entrance cross section change during opening of Painkalac Creek	38
<b>Figure 38a-d.</b> Pictures from artificial opening of Painkalac Creek	38
<b>Figure 39.</b> Basin drainage and timing of morphological monitoring at Anglesea River	39
<b>Figure 40.</b> Surveys of entrance cross section change during opening of Anglesea River	39
<b>Figure 41a-d.</b> Morphological change during opening of Anglesea River	40
<b>Figure 42a-d.</b> Pictures from artificial opening of Anglesea River	40
<b>Figure 43a-b.</b> Conceptual change in channel width, area, discharge, velocity and water level	41
<b>Figure 44a-h.</b> Field data showing change in channel width, area, discharge, velocity and water level	42
<b>Figure 45a-d.</b> Hydraulic gradient and grade at which estuaries have been successfully opened	43
<b>Figure 46a-b.</b> Artificial opening of Aire River 01/05/14 that failed due to swell size	44
<b>Figure 47.</b> Berm length vs hydraulic head that openings are likely to be successful	44
<b>Figure 48a-d.</b> Correlation between HG at time of opening and estuary drainage rate and duration	45
<b>Figure 49.</b> Sequence and stages of geomorphic change during an opening	46
<b>Figure 50a-b.</b> Distribution of HG and grades at which estuary openings are likely to be successful.	47
<b>Figure 51.</b> Example recording sheet that could be used to calculate HG/grade at the time of opening	49
<b>Figure 52.</b> How study results can work alongside EEMSS for estuary opening decision making	52

## Acknowledgements

This project was funded by the Corangamite Catchment Management Authority and Department of Environment, Land, Water and Planning (DELWP) as grant # FIN PRO 035-F005.

Thanks to EstuaryWatch, Glenelg Hopkins CMA, and Corangamite CMA for providing entrance condition records. Thank you to Judy Spafford for providing photos and updates about the entrance condition and morphology of the Gellibrand River estuary.

Thank you to all Melbourne university students and friends who helped monitor estuary entrance morphology and physiochemical data in the field.

Thanks for staff from Parks Victoria, Surf Coast Shire Council, and the Great Ocean Road Coast Committee for allowing us to monitor on site after artificial estuary openings.

## Glossary

**AHD:** Australian height Datum. The Australian Height Datum is a vertical datum in Australia used as a consistent elevation reference. The mean sea level for 1966-1968 was assigned the value of 0.00 m on the Australian Height Datum from thirty tide gauges around the coast of the Australia.

**Berm:** A nearly horizontal plateau on the beach face or backshore. The berm is formed by the deposition of beach material by wave action. The berm is located between the estuary lagoon and the ocean.

**Berm crest:** The highest point of a beach berm.

**Berm length:** The distance between the nearshore water level and the landward crest of the berm - in this case marked by the seaward edge of the estuarine lagoon.

**Estuary basin:** The lagoonal area and main central water body of an estuary located landward of the estuary mouth and behind the beach berm.

**H<sub>s</sub>:** Significant wave height. The statistical basis for all wave heights presented in forecasts and map displays. H<sub>s</sub> is calculated as the average height of the highest one-third of the waves.

**Hydraulic head:** Hydraulic head is a specific measurement of liquid above a vertical datum. It is usually measured as the liquid surface elevation (i.e. in m).

**Hydraulic gradient:** The Hydraulic Gradient is a vector gradient between two or more hydraulic head measurements over the length of the flow path.

**Perched estuary:** When an estuary is perched, the water surface elevation of the lagoon is super-elevated above mean sea level.

## 1.0 Project brief

This report summarises the results of a desktop and field analysis comprising Part II of the project: *A geomorphic prediction module for intermittently open/closed estuaries (IOCE) in Victoria (Australia)*. This research was funded by Corangamite Catchment Management Authority (CCMA) and the Department of Land, Water, and Environmental Planning (DELWP) Victoria.

The project as a whole has focused on better understanding the geomorphic processes which control estuary entrance opening and closure. This report focuses on understanding why some artificial openings are successful and others are not. It also identifies how geomorphic change at the mouth (i.e. breach growth) influences the rate of basin drainage and physiochemical conditions within the lagoon.

### **The specific aims of this project were to:**

- (1) Determine the water levels and at which different estuaries are likely to naturally open;
- (2) Gain a high-resolution field dataset that enables us to better understand what changes in entrance morphology occur during an opening and what the timescales of these changes are in relation to basin drainage;
- (3) Determine under what conditions an artificial opening is likely to be successful or unsuccessful;
- (4) Understand what factors control the rates and total amount of estuary drainage occurring during artificial openings to determine if we can slow down drainage rates to avoid fish strandings.

**The project involved:** intensive field work undertaken during 2019 where geomorphic change was monitored during eight artificial openings. This report presents the results of that field work and uses this data to address the above aims. In addition, historic water levels and hydraulic gradients at which estuaries have successfully opened were analysed from existing data sourced from the Estuary Entrance Management Support System (EEMSS) and EstuaryWatch.

**A main outcome of the study is:** that the hydraulic gradient at the time of opening was identified as the primary control on the success of artificial openings. It also dictates the rate and duration of estuary basin drainage. From historic data, the specific hydraulic gradients at which estuary openings tend to be successful have been defined. As an attachment to this report, a simple cost-effective method (as an Excel spreadsheet) is presented where managers can calculate the hydraulic gradient prior to artificial openings from easily obtainable data. To do this, managers simply need to input the: (a) berm length, (b) estuary water level, and (c) tidal elevation. The calculated hydraulic gradient value can then be compared to the known minimum threshold for a successful opening to assess the likelihood of success.

**The calculation of hydraulic gradient prior to opening should can be incorporated into EEMSS or used alongside it to assess the likelihood of openings being successful.** Collating this data can also help refine thresholds in future and between sites. Additionally, the geomorphic prediction tool produced in Part I of this project could be used simultaneously to predict the estuary opening duration given the current and forecast marine and fluvial conditions. This provides a complete management procedure to assess the feasibility of implementing artificial openings that would complement the existing EEMSS process.

A supporting grant was received from Melbourne University to link the impact of changes in estuary entrance morphology during artificial openings to changes in basin physiochemistry. Physiochemical data was collected in the field during four artificial openings in 2019 where depth profiles were able to be taken. The analysis of physiochemical change during artificial openings is ongoing. This work is part of a wider project being undertaken in collaboration with researchers at Griffith University. The data obtained during the 2019 field work as part of this project will also be analysed in more detail as part of an honours project at Melbourne University in 2020. The preliminary results from this aspect of the work are presented in this report (see Appendix 4).

## 2.0 Executive Summary

Intermittently Open/Closed Estuaries (IOCE) are a subtype of wave dominated estuary with entrances which periodically close to the ocean. They are common globally and are the dominant estuary type in Victoria, Australia. Entrance closures occur when there is low river flow and a beach berm builds across the estuary entrance to separate the estuary from the ocean. If the estuary remains closed for a long time, any freshwater inflow will accumulate behind the berm and raise the estuary water level. As water levels increase, flooding of low-lying land and infrastructure can occur. To alleviate flooding risk to human assets, estuary managers artificially open estuaries to allow floodwaters to drain towards the ocean.

**The issue:** While artificial openings are usually effective as a short-term flood reduction strategy, sometimes openings will not achieve their goals of sustaining an open entrance or reducing land and property inundation by decreasing the estuary water level. An implication of this is that artificial openings must often be reimplemented, costing thousands of dollars at a time. A second issue is that fish deaths can sometimes occur after artificial openings. Fish deaths can result from the loss of oxygen rich water when the estuary is stratified, or fish strandings during openings that rapidly drain the basin. Understanding the geomorphic conditions where openings will be successful in maintaining a connection to the ocean is imperative to reduce the need for reimplementation. As geomorphic change at the mouth (i.e. entrance dimensions and discharge) is intrinsically linked to drainage rates and physiochemical change in the lagoon, gaining event-scale data during artificial openings is essential to quantify the timescales and magnitudes of these changes. This project aims to tackle this problem by intensively monitoring geomorphic change at the mouth during artificial openings to link to changes in the estuary as a whole.

### **This primary aims of the project are as follows:**

- (1) To obtain a high-resolution field dataset that enables us to understand what changes in entrance morphology occur during an opening and how these changes affect the rates of basin drainage.
- (2) To determine under what conditions an artificial opening is likely to be successful;
- (3) To identify the water levels and at which different estuaries are likely to naturally open.

A secondary aim of the project is to use field data to understand how changes in estuary entrance morphology control physiochemical conditions within the estuary basin.

**What was done:** During 2019, field work was undertaken at six IOCE in west Victoria - Anglesea River, Painkalac Creek, Spring Creek, Aire River, Gellibrand River, and Curdies Inlet. Field work involved continuously monitoring the change in entrance morphology, water level, and basin physiochemistry during eight artificial openings. This represents the first known study to continuously monitor change at the mouth during multiple artificial openings across different sites. Historic data from McSweeney (2016), Estuary Entrance Management Support System (EEMSS), and EstuaryWatch were used to calculate the hydraulic gradient at which 65 historic openings occurred. The hydraulic gradient is representative of the energy slope between the estuary and the sea. This is calculated as the total head difference between the estuary lagoon and the ocean divided by the berm length. Hydraulic gradient values were compared between openings to obtain the range of gradients/grades at which artificial openings tend to be successful. For 14 estuaries with records of natural openings, the water level and hydraulic gradient prior to natural openings were extracted to determine thresholds of natural opening for different IOCE sites.

### **The main findings of the study are:**

- (1) **The hydraulic gradient at the time of opening controls the success of an artificial opening.** Artificial openings have historically been successful when the hydraulic gradient is  $>0.019$  m/m (Figure 1a). This equates to a minimum grade of 1:53 (Figure 1b). Openings have been unsuccessful when the hydraulic gradient is  $<0.015$  m/m (grade of 1:67) and have had mixed success when 0.015-0.019 m/m (Figure 1a-b). This provides a threshold for successful opening and a zone of risk when openings could go either way depending on the offshore wave height, winds, and tidal stage.



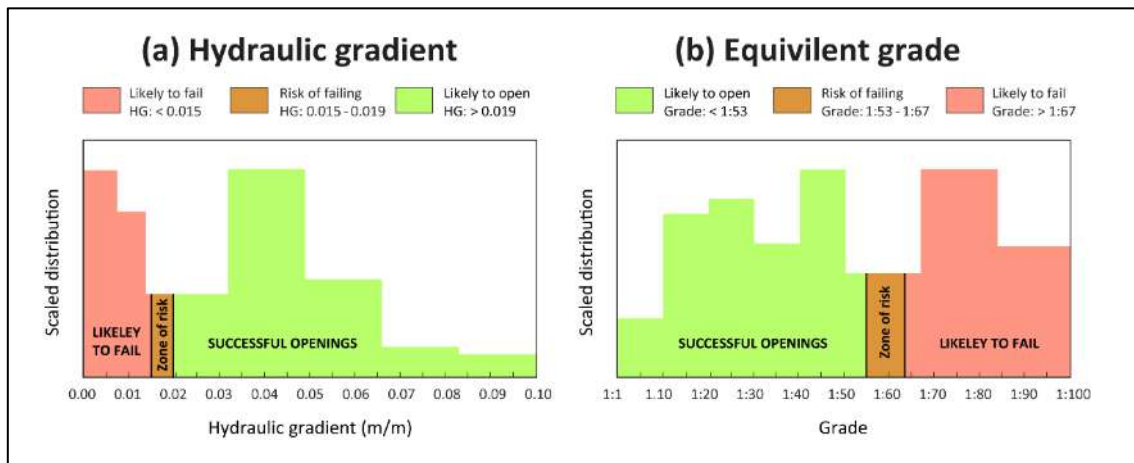


**Figure 1a-b.** (a) Hydraulic gradient; and (b) equivalent grade at which artificial openings are likely to be successful, unsuccessful, and at risk of failing - based on distributions from historic data (n = 63).

**(2) The rate and duration of basin drainage is also a function of the hydraulic gradient at the time of opening (Figure 2a-b).** Once an estuary reaches a critical velocity, drainage cannot be slowed down. This threshold is typically reached early (~3hrs) into the opening sequence. To slow basin drainage, estuaries must be opened at a lower hydraulic gradient, or the period of initial slow outflow could be extended via strategic placement of spoil, so it enters the channel before a critical velocity is reached. This means that any intervention to decrease drainage rates to avoid fish strandings must occur before peak outflow velocity is reached.

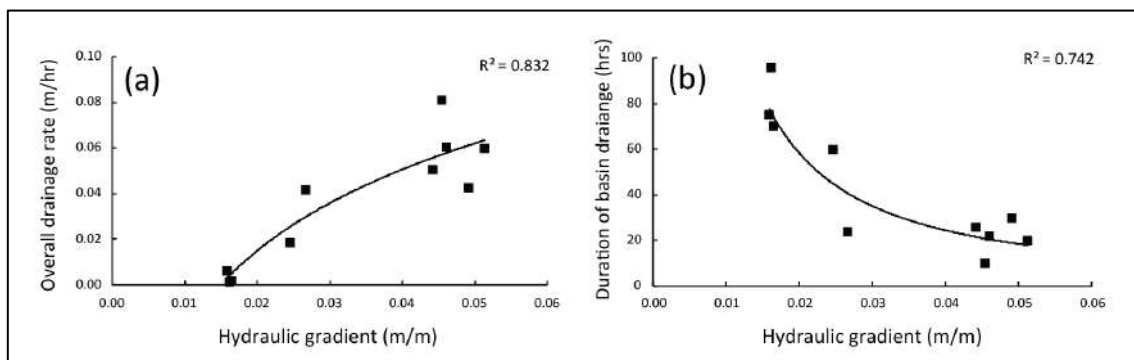


**Figure 2a-b.** The correlation between hydraulic gradient and (a) drainage rate and (b) drainage duration.

- (3) The hydraulic gradient should be used to predict the proximity to natural openings - not just the water level.** Estuaries naturally open when the gradient is >0.022 m/m (grade: 1:46).
- (4) Hydraulic gradients can be easily quantified at a low cost** and calculated using only the estuary water level, offshore tidal elevation, and berm length. It should be included in estuary opening assessments to gauge the likelihood of success. Data should be also collected to quantify the hydraulic gradient to refine thresholds for individual estuaries in future. An example spreadsheet to calculate it is attached.
- (5) Temporal asymmetry exists in rates of change in outflow velocity, cross-sectional area, and discharge during an opening.** Parameters increase rapidly on the rising limb of the hydrograph with a gradual decline after a max value is reached. Changes in water level lag geomorphic change at the mouth. The max outflow velocity and channel width are reached before the max cross-sectional area and discharge. Peak discharge and rapid basin drainage occur only when the channel reaches an equilibrium width.

**Calculating the hydraulic gradient is a cost-effective and easy way to assess the likely success of artificial openings. Ultimately this will reduce the need for reimplementatation. The hydraulic gradient can also be used to predict drainage rates and determine when natural openings are likely to occur.**



### 3.0 Introduction

#### 3.1 Background

Artificial estuary entrance openings are a common management action undertaken in Victoria (Barton et al., 2008; McSweeney et al., 2018) and many locations globally (e.g. South Africa, the U.S.A, and New Zealand). A main purpose of artificial openings is to alleviate the flooding of property and infrastructure which occurs when an estuary entrance is closed for a long period of time (Figure 1a-b). When an estuary is closed, freshwater inflow accumulates behind the berm. Over time, the basin water level can increase in response to inflows and inundate low lying land surrounding the basin. Artificial openings involve the mechanical excavation of the berm to reconnect the estuary to the ocean (Figure 1c-d). After excavation, the channel will continue to incise and widen, allowing water within the basin to gradually drain to the sea.



**Figure 1a-d.** (a) Flooding at the Barham and (b) Anglesea River estuaries prior to artificial opening; (c-d) artificial openings being undertaken at the Gellibrand River estuary. Photos from EstuaryWatch (2019).

**While artificial openings are mostly effective as a short-term flood reduction strategy, sometimes openings will not achieve their goals of: (a) reconnecting the estuary to the ocean and sustaining an open entrance, or (b) reducing land and property inundation by decreasing the estuary water level.**

An implication of this is that artificial openings must often be reimplemented. This can cost thousands of dollars at a time. Artificial openings are typically unsuccessful (i.e. a connection to the ocean is not maintained past excavation) when the hydraulic head between the estuary and the ocean is low or when offshore waves are high. Hydraulic head is the elevation difference between the estuary water level and the ocean (Slinger, 2017). If an estuary is opened with low head, there is a lack of potential energy, which translates to very weak outflow though the channel (Morris and Turner, 2010). As a result, outflow has insufficient velocity to erode sand offshore, and the channel typically infills from wave-driven deposition within hours to days of opening (McSweeney et al., 2018).

Openings that maintain an open entrance but do not drain the basin enough to alleviate flooding are again those which are right at the threshold of having sufficient hydraulic head to maintain an opening. Following excavation, outflow expends more energy in widening the channel as opposed to incising it. As the channel bed remains high above AHD, drainage rates are very slow, and the estuary is likely to close again within days to weeks without any substantial decrease in water level. The length of the berm/excavated channel is also important as a longer channel can slow outflow and also equates to a larger volume of sand that must be eroded.

Under certain conditions, artificial openings can sometimes result in fish deaths. While our understanding of the physiochemical conditions and factors that can cause fish deaths is improving, this is still limited by a lack of historic event-scale data. Fish deaths can occur either by the loss of oxygen rich water when the estuary is stratified prior to opening (Becker et al., 2009), or by a rapid decline in water level which can leave fish stranded on the floodplain (Whitfield and Cowley, 2018). A good example of this second process is the fish death that occurred at Curdies Inlet in July 2017. After an artificial opening, the estuary drained very rapidly and left many fish stranded upstream. There is therefore an interest in determining whether we can predict or slow estuary drainage rates in order to avoid fish strandings in future.

A key component of understanding the thresholds for successful openings and being able to predict basin hydrodynamics and physiochemical change is linking the geomorphic change occurring at the mouth to processes within the estuary basin (i.e. mixing and drainage). This is because the morphology and discharge at the mouth are essentially geomorphic controls affecting many processes upstream. For instance, if the entrance cross-sectional area is large, it can allow for a higher volume of water to drain seaward and thus increase drainage rates. If the estuary is draining quickly, there may then be more potential for fish strandings or a loss of oxygen rich water within the basin. The interaction of processes at the mouth and within the basin are currently poorly understood due to a lack of data at sufficient time scales (McSweeney et al., 2018). This is because it is challenging in practice to continuously monitor geomorphic change at the mouth as the entrance morphology rapidly changes. In addition, estuary drainage, physiochemistry, and entrance morphology have typically been assessed independently (Suara et al., 2018). This project aims to tackle this problem by intensively monitoring the geomorphic processes at the mouth during artificial openings and linking this to change across the whole estuary.

One further issue is that the water levels at which estuaries tend to naturally open are largely unknown. This is important because if an estuary is close to naturally opening, it can be worth avoiding human intervention to maintain ecological integrity of the system. Thus, this project will draw upon existing data from the Estuary Entrance Management Support System (EEMSS) and EstuaryWatch citizen science program to extract historic water levels at which different estuaries tend to naturally open.

### **3.2 Project aims**

#### **The specific aims of this project are as follows:**

- (1) To determine the water levels and at which different estuaries are likely to naturally open;
- (2) To gain a high-resolution field dataset that enables us to better understand what changes in entrance morphology occur during an opening and what the timescales of these changes are in relation to basin drainage;
- (3) To determine under what conditions an artificial opening is likely to be successful or unsuccessful;
- (4) To determine what factors control the rates and total amount of estuary drainage occurring during artificial openings and if we can slow down drainage rates to avoid fish strandings.

**A secondary aim of the project is:**

- (5) To use field data to understand how changes in estuary entrance morphology control physiochemical conditions within the estuary basin.

## 4.0 Literature review of opening processes

### 4.1 Natural openings

IOCE naturally open when the water surface elevation of the backing lagoon becomes higher than that of the berm crest. This can occur via three mechanisms: (1) overtopping from the catchment side; (2) overtopping from the ocean side; and (3) by seepage and/or liquefaction of the berm.

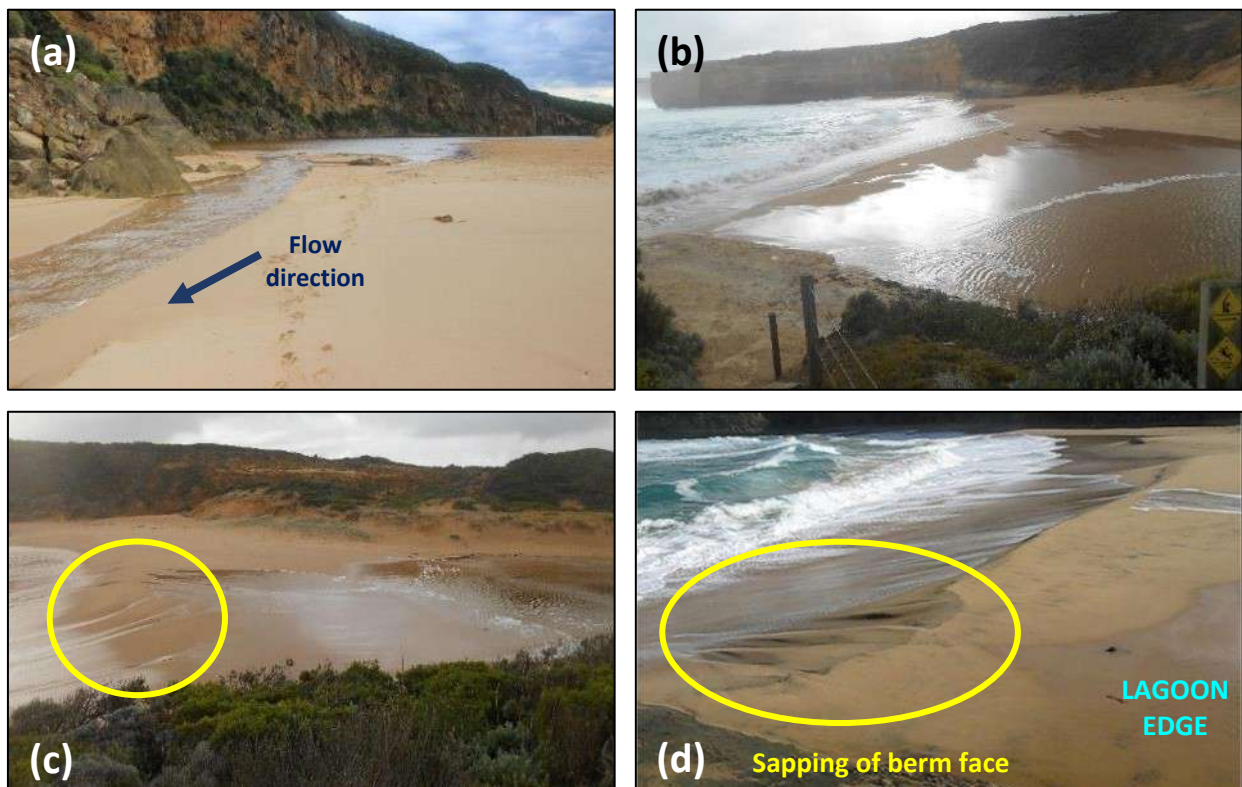


**Figure 2a-d.** (a) Opening of Gellibrand River via increased fluvial inflow. The lagoon has spilled over the berm and incised a channel seaward; (b) natural opening of Sherbrook River via ocean wave overtopping. The lagoon is full and with each consecutive wave, more water is delivered into the estuary which resulted in an opening; (c-d) saturation of the berm resulting in sapping at the Sherbrook River.

#### **(1) Overtopping from the catchment side (Figure 2a).**

Here the estuary will open in response to a period of increased fluvial inflow. This is the most common mode of natural opening for IOCE. Fluvial inflow raises the basin water surface elevation to a critical point where it can overtop the berm. Overtopping of the berm typically occurs as a thin sheet of outflow which creates a knickpoint at the seaward edge of the berm (Figure 3a). After the berm elevation is lowered, a preferred scour channel develops from the crest (Figure 3b). Outflow velocities then increase, and the channel rapidly widens and incises (Figure 3c). The duration from the initiation of berm overtopping to peak velocities in the channel to be reached is described by Gordon (1990) to take ~280 mins at small lagoons (e.g. Narrabeen Lagoon and Dee Why Lagoon, (New South Wales (NSW), Australia) but hours-days at larger estuaries (e.g. Aire River, VIC (Figure 3); Lake Wollumboola, NSW (Aber and Downey, 1989)



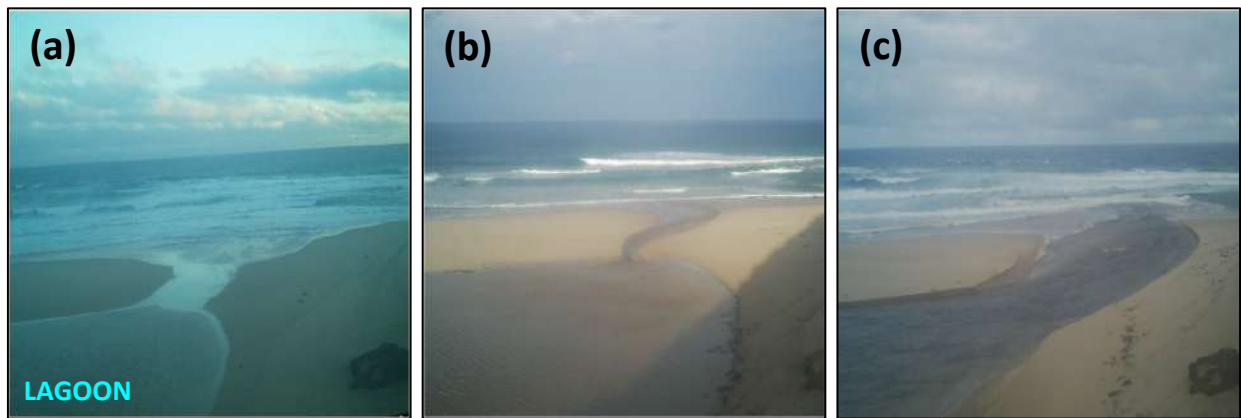


**Figure 3a-c.** Natural opening of the Aire River 2014. (a) Outflow initiates as a thin sheet 10 am 21/05/14; (b) a scour channel forms 10 am 22/05/14; (c) peak outflow and an expanding channel 8 am 23/05/14.

### **(2) Overtopping from the ocean side (Figure 2b).**

This mechanism of natural opening involves wave overtopping of the berm crest from the ocean side. As waves overtop the berm, they add water to the basin which eventually raises the water level to a point where it can overtop the berm. An estuary will typically only open via ocean water overtopping when the berm is narrow or when the lagoon water surface elevation is very close to that of the berm crest to begin with (Hart, 2009). Natural openings via wave overtopping are most common at perched estuaries and result in the near-complete drainage of the basin over rapid (i.e. hourly) timescales. Estuaries that are perched have water levels above mean sea level (MSL). They tend to occur on coastlines with steep, reflective beaches where high wave run-up gives rise to berms that are several meters above high tide levels. Perched estuaries essentially empty when they breach due to the steep gradient between the estuary and the ocean (i.e. short berm length and perched water level) (Parkinson and Stretch, 2007).

### **(3) Seepage and/or liquefaction of the berm (Figure 2c-d).**

The breaching of perched estuaries can also be triggered by seepage and liquefaction of the berm following inundation by waves (Kraus and Walmsley, 2003; Kraus, 2003). This is likely to occur when the berm is high and narrow, the lagoon is full and perched high above mean sea level, and the high tide wave runup point is close to the berm crest elevation (due to large swells or high tides) (Kraus et al. 2002). Here wave runup over the berm saturates the front face of the berm and reduces its structural integrity (Figure 4). The phreatic line below the berm surface provides an envelope where sediment is vulnerable to offshore movement or collapse via sapping. Downslope seepage can occur through porous sediment which can liquefy the sediment and allow material to be transported seaward as a slurry (Kraus, 2003). This mode of opening is more common at perched estuaries and those which have berms comprised of more porous (i.e. larger) sediment (Gordon, 1990).

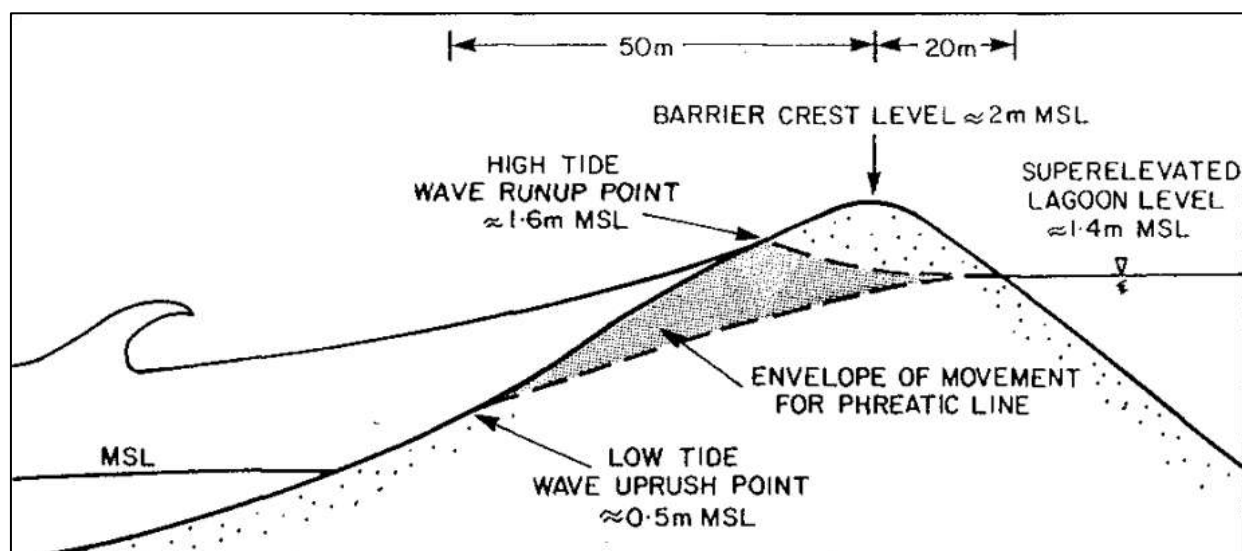


**Figure 4.** Conditions favouring natural openings via seepage and/or liquefaction of the berm. The phreatic line, also known as the seepage line or saturation line, is an imaginary line which separates the unstable saturated zone from unsaturated zone (Gordon 1990: pp. 2884).

Overall, natural openings are not as well documented as artificial openings. This is likely due to their variable nature and the difficulty in instrumenting estuaries prior to an opening. Thus, the timescales and rates of geomorphic change and drainage have not been well quantified or compared between sites.

**The main controls on the likelihood of a natural opening occurring are:**

- **Berm crest elevation vs estuary water level** - the critical control on whether overtopping will occur;
- **Hydraulic head and berm length** - natural openings tend to occur when hydraulic head is high and the distance between the estuary and the ocean is short. This equates to a steeper energy slope between the estuary and the ocean is steeper;
- **Degree of saturation of the berm** - for perched estuaries, a more saturated berm will favour an opening occurring via seepage and liquefaction;
- **Wave runup and tidal limit** - a higher nearshore water level will increase the landward extent of berm inundation and is more likely to add water into the basin of a perched estuary.

**4.2 Conditions favouring successful artificial openings**

The geomorphic conditions which favour a successful opening (i.e. where a connection to the ocean is maintained past excavation) are described to vary between sites (Haines, 2006). While this may be the case when considering swell conditions and fluvial inflow, which vary regionally, at the scale of the mouth, three factors are most important and can be consistently quantified between openings and sites:

**(1) Hydraulic head between the estuary and the ocean**

This is the total elevation difference between the estuary water surface elevation (i.e. water level) and the nearshore sea level (Figure 5) (Slinger, 2017). Opening at a higher hydraulic head provides more potential energy which results in faster outflow and increases the likelihood of openings being successful.

**(2) The berm length**

The berm length is the distance between the lagoon and the nearshore water line (Figure 5). Openings tend to be successful when the berm length is shorter. This is because a shorter berm: (a) equates to a lower volume of sand that has to be eroded; and (b) means the energy slope between the estuary and the ocean is generally steeper.

### (3) Offshore swell conditions

Openings are more likely to be successful under lower offshore wave heights as wave-driven deposition is lower and does not overwhelm outflow within the channel and the net offshore sediment transport.

The **hydraulic gradient** is a parameter which uses the hydraulic head and berm length to quantify the energy slope between the estuary and the ocean (Figure 5). If this slope is steeper (i.e. a higher hydraulic gradient), there is more potential energy behind the berm, and it is likely that outflow will reach faster velocities more rapidly thus resulting in higher rates of in-channel erosion.

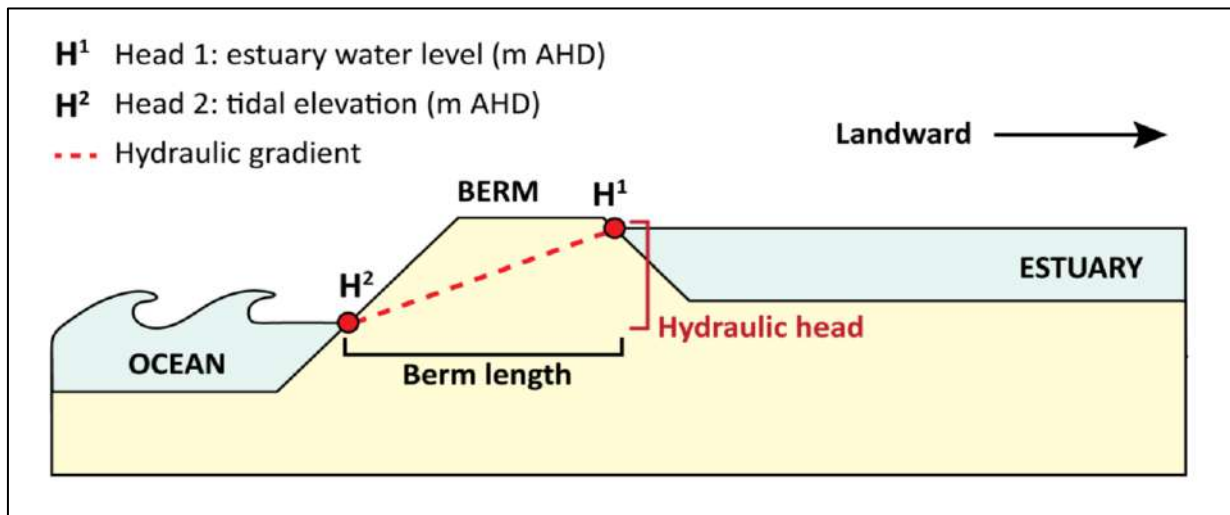


**Figure 5.** Hydraulic gradient - the energy slope between the basin water surface elevation and the ocean.

**While the success of an opening is controlled by these factors, the estuary opening duration becomes a function of the relative balance between onshore vs offshore sediment transport at the mouth once the basin has drained and hydraulic head is removed. Thus, if a long opening duration is a main management goal, the forecast streamflow and swell conditions should also be considered.**

#### 4.3 Geomorphic change during artificial openings

From a summary of relevant literature (Gordon, 1990; Odd et al., 1995; Haines, 2006; Parkinson and Stretch, 2007; Wainwright and Baldock, 2015; McSweeney, 2016), the sequence of geomorphic change during artificial openings can be broadly considered to comprise three main stages:

**STAGE 1: Pilot channel:** small, initial channel created by excavation; low outflow velocity; no basin drainage;

**STAGE 2: Rapid expansion:** rapidly expanding channel; very fast outflow; basin starts draining rapidly;

**STAGE 3: River flow:** channel expansion ceases; outflow velocity decreases; basin continues to slowly drain.

##### STAGE 1: Pilot channel:

Stage 1 represents a low energy state where rates of channel expansion and outflow velocity are initially low - but increase rapidly at the end of the stage. Stage 1 commences after excavation and a shallow, rectangular channel exists (Figure 6a-b). Channel dimensions are dictated by excavation, but the channel typically remains 2-10 m wide and 0.2-0.5 m deep throughout Stage 1. Outflow velocity is low, being between 0.5-1.5 m/s. Outflow gradually scours a deeper channel into the downstream face of the berm while the upstream crest remains more intact. Initially, erosion rates are low because sediment transport threshold conditions are only marginally exceeded. A series of knickpoints migrate up the channel. During Stage 1, there is no change in basin water level as drainage lags channel expansion and discharge through the mouth is minimal. Stage 1 lasts for ~80-100 mins and ends when the knickpoints reach the lagoon. When this occurs, rates of channel expansion rapidly increase. The duration of Stage 1 is a function of the hydraulic gradient between the estuary and the ocean and the channel dimensions (Gordon, 1990).

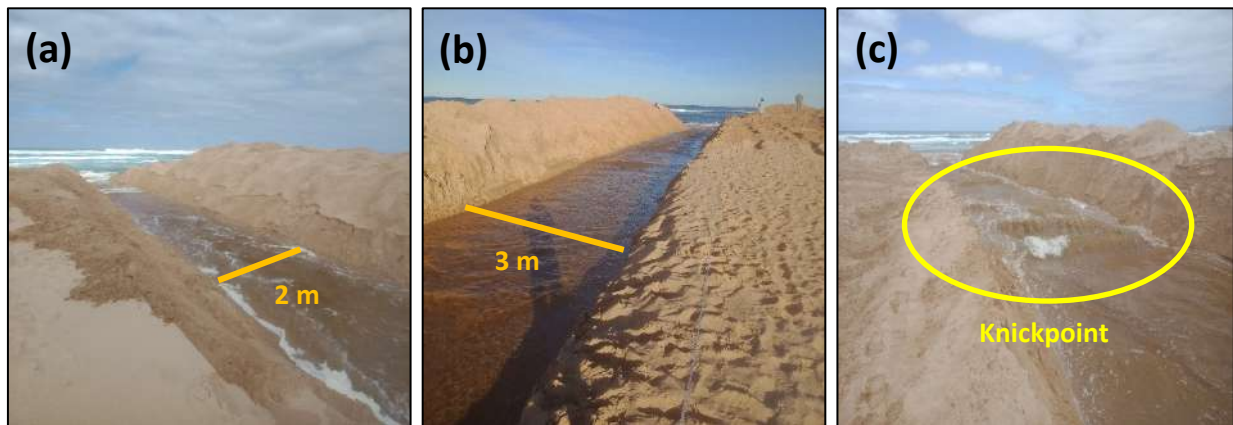


**Figure 6a-c.** Pilot channel stage: (a) Aire River; (b) Curdies Inlet; (c) knickpoint migrating up the channel.

**STAGE 2: Rapid expansion:**

Stage 2 commences as the knickpoints reach the basin and scouring lowers the upstream berm crest (Figure 7). As this occurs, the volume of water entering the channel increases which in turn increases erosion rates. The estuary enters a high-energy state where geomorphic change becomes rapid. A weir may form early in this stage at the seaward edge of the lagoon. Outflow velocity increases to 1.5-5 m/s and becomes supercritical with standing waves and antidunes present. Rates of channel incision and expansion increase dramatically with widening occurring via bank collapse (Wainwright and Baldock, 2015). The channel can reach 10-100m or more in width and is typically 0.5-3 m deep. Peak velocity and channel width are reached, and the channel then maintains an equilibrium width. As discharge increases, the basin water level decreases rapidly. Stage 2 lasts between 4-20 hrs and the duration is influenced by: adjustment of the hydraulic gradient to decreasing basin water level and the maximum cross-sectional area of the channel. Wave action has little impact on entrance morphology as outflow dominates any onshore sediment transport. Stage 2 ends once the channel has reached its maximum discharge and the outflow hydrograph enters the falling limb. By this time, basin water levels have decreased substantially.



**Figure 7a-c.** Rapid expansion stage: (a) Aire River; (b) Spring Creek; (c) Painkalac Creek - with weir present and scouring of the upstream crest of the berm.

**STAGE 3: River flow:**

Stage 3 consists of the falling limb of the discharge hydrograph (Figure 8) and the estuary enters a lower energy state. Here the estuary water level has decreased substantially to reduce hydraulic head. This causes the outflow velocity, discharge, and in-channel erosion rates to progressively decrease. Velocity falls below 1.5 m/s and the channel stops incising and widening. Standing waves disappear and flow becomes subcritical. Stage 3 will persist until the estuary stops draining. Late in Stage 3, waves may move into the mouth at high tide coinciding with low outflow velocities. Waves may travel into the lower basin resulting in an influx of salt water. The duration of Stage 3 is between 4-30 hrs or more and depends on



the total volume of water being discharged through the entrance as a function of the storage volume of the basin. The duration of Stage 3 is longer for estuaries with a larger volume of water in the basin.



**Figure 8a-c.** River flow stage: (a) Aire River; (b) Curdies Inlet; and (c) Painkalac Creek with wave intrusion.

After the basin has completely ceased draining (i.e. the water level is no longer decreasing), the estuary becomes tidally influenced. Tidal oscillations may be evident in the basin. Channel infill will commence via wave processes with infill rates increasing with higher wave conditions and reduced inflow. At smaller estuaries, infill may commence on the first high tide after drainage (Perissinotto et al., 2010).

**The change in channel dimensions, water level, and discharge during the opening sequence is shown in Figure 9. This provides a working hypothesis for predicting geomorphic change during the field work.**

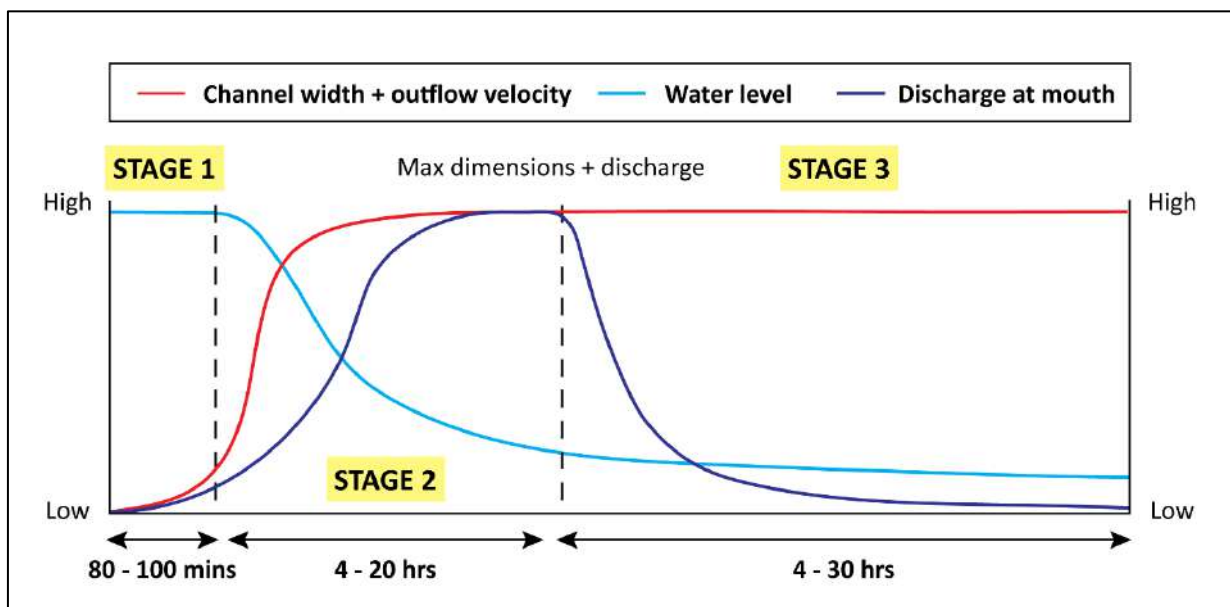


**Figure 9.** Conceptual diagram showing the three stages within the sequence of entrance opening and the relative timing of changes in the estuary channel dimensions, basin water level, and discharge/outflow.

#### 4.4 Physiochemical change during artificial openings and fish deaths

Fish deaths have been noted to occur in ICOE after artificial openings in many regions globally (Whitfield, 1995; Sloan and Kamer, 2005). They have been linked to changes in salinity, temperature, and oxygen (Becker et al., 2009), as well as rapid drainage which can leave fish stranded on the floodplain or surrounding the basin (Whitfield and Cowley, 2018).

Fish deaths occurring due to changes in estuary physiochemistry following artificial openings are most commonly linked to the rapid seaward movement of oxygen rich water which occurs when the estuary is opened in a stratified condition. When stratified, oxygen rich water sits on the top layer of the estuary and deoxygenated (salt) water sits as a wedge along the bottom. When an estuary is opened, the top layer drains off first leaving behind anoxic water (Whitfield, 1995; Hoeksema et al., 2006). This process is well summarised by Becker et al., (2009pp. 576) in reference to changes in estuary physiochemistry after artificial opening that resulted in a fish death in the Surrey River estuary (Victoria) in 2005:

*“When an estuary becomes stratified during the closed mouth phase, isolated waters below the halocline have stagnated and become anoxic. As a result, only waters above the halocline contain oxygen concentrations capable of sustaining most fish. It appears that if a mouth opening happens under low flow conditions, a shearing effect occurs within the water column where surface water flow out to sea leaving deeper water behind. This results in only anoxic waters being present after opening.”*

A good example of a recent fish death occurring via this process occurred at Tallow Creek (NSW) in 2019. Here the estuary was artificially opened when it was stratified with low dissolved oxygen in the basin ([www.abc.net.au/news/2019-06-19/thousands-of-fish-killed-after-council-opens-lagoon-in-byron-bay/11223734](http://www.abc.net.au/news/2019-06-19/thousands-of-fish-killed-after-council-opens-lagoon-in-byron-bay/11223734)). Following opening, thousands of fish died as a result of anoxic conditions. Anoxia was increased by a lack of rainfall prior to and following the opening. In Victoria, a similar process has resulted in fish deaths - with notable examples occurring at the Surrey and Gellibrand River estuaries.

Fish deaths can also occur when an estuary rapidly drains after an artificial opening (Russell, 1994). Here the rapid drop in water level causes fish to become stranded on the upstream floodplain. A good example of this process occurred at Curdies Inlet in 2017. Thus, to avoid fish deaths occurring via this process, understanding the geomorphic controls on the rate and duration of estuary drainage is essential. This exemplifies how geomorphic change at the mouth (i.e. an increase discharge) links to changes in the basin. Fish can also become stranded in aquatic vegetation as the estuary water level falls and vegetation becomes exposed. This process has been documented in the West Kleinemonde Estuary (South Africa) (Whitfield and Cowley, 2018). Here established supratidal aquatic macrophyte beds became exposed after an opening when the estuary drained rapidly. As the estuary had been closed for two years prior, fish living in the estuary prior to the opening lacked the experience of entering estuarine littoral areas on the flood tide and retreating back into the channel on the ebb tide.

## 5.0 Methods

### 5.1 Water level thresholds for natural openings

EEMSS and EstuaryWatch provide the dates of historic natural openings and the water level at which natural openings occur. Curdies Inlet and the Powlett, Gellibrand, and Anglesea River estuaries also have permanent water level gauges installed in their basins as part of the DELWP stream gauge network (<http://data.water.vic.gov.au/static.htm>). For 14 estuaries with records of natural openings, the water level prior to natural openings were extracted from the above databases. Descriptive statistics were calculated to determine historic water levels at which these sites have naturally opened. Boxplots were also used to show the distribution of water levels at which each site has naturally opened in the past.

### 5.2 Field work

#### 5.2.1 Study sites

During 2019, field work was undertaken at six IOCE in west Victoria (Figure 10a-g). Field work involved monitoring geomorphic and hydrodynamic change during eight artificial openings. Sites monitored included: Anglesea River, Painkalac Creek, Spring Creek, Aire River, Gellibrand River, and Curdies River estuaries. Study sites have a range of morphologies with the Gellibrand and Curdies Inlet being the largest

and Spring Creek being the smallest (Figure 9a-g). Wave energy is highest at the Gellibrand, Curdies, and Aire Rivers, and decreases eastward at Painkalac Creek, Anglesea River, and Spring Creek (Figure 11a-c). All estuaries are exposed to swells coming from the southwest. Study sites were selected because: (a) artificial openings occurred during the timeframe of the study making fieldwork logistically possible; and (b) artificial openings are ongoing and thus there is a management interest in these estuaries.

The change in estuary entrance morphology, hydrodynamics, and basin water level were monitored continuously prior to and during artificial openings. At the Gellibrand River, Spring Creek, Anglesea River, and Curdies Inlet, changes in physiochemical conditions were also monitored (Figure 10b; d; f; g). Data was used to identify the timescale of geomorphic change at the mouth to then link this to changes in estuary lagoon drainage rates and variability in physiochemical conditions. This data was then compared between openings. The eight artificial openings monitored during this study include:

- |                                  |                                  |
|----------------------------------|----------------------------------|
| (1) Aire River 01: 01/02/2019;   | (5) Curdies Inlet 02: 16/06/2019 |
| (2) Gellibrand River: 09/03/2019 | (6) Curdies Inlet 02: 17/06/2019 |
| (3) Aire River 02: 01/05/2019    | (7) Painkalac Creek: 08/08/2019  |
| (4) Spring Creek: 31/05/2019     | (8) Anglesea River: 14/08/2019   |

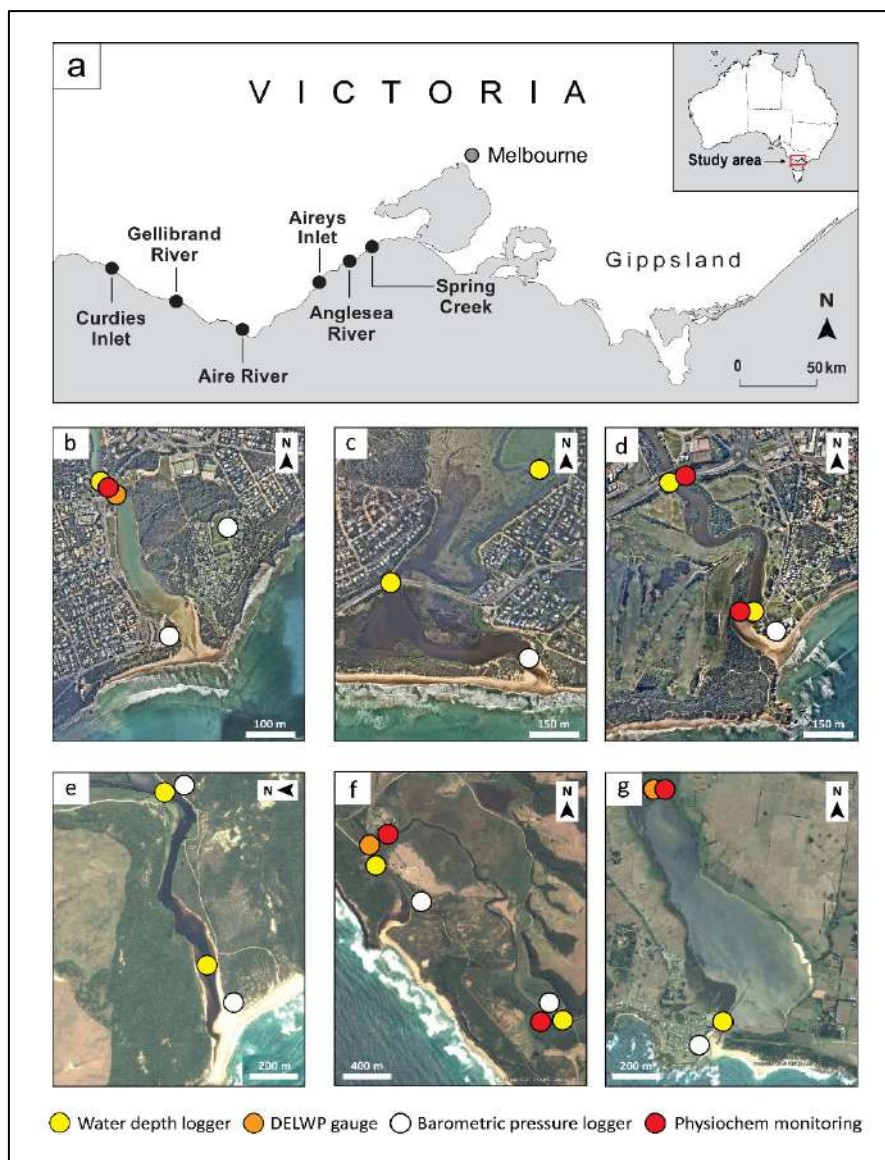


**Figure 10a-g.** (a) Study site locations in Victoria and entrance morphology and equipment placement at (b) Anglesea River; (c) Aireys Inlet; (d) Spring Creek; (e) Aire River; (f) Gellibrand River; (g) Curdies Inlet.

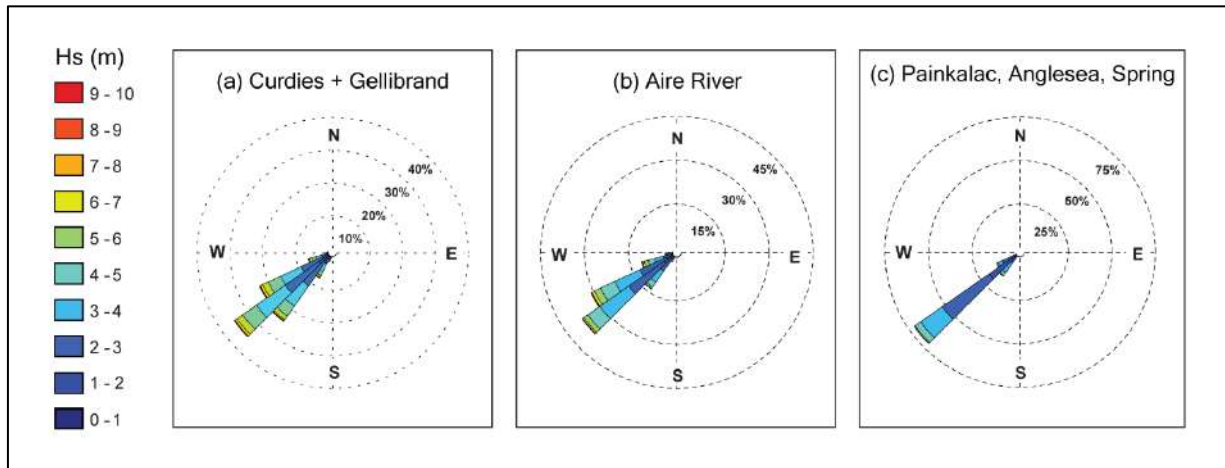


**Figure 11a-c.** Open ocean wave direction roses (Hs is significant wave height) (NOAA WaveWatch III data).

### 5.2.1 Monitoring of artificial openings

Estuary entrance morphology was measured via topographic surveying using a Real Time Kinematic (RTK) GPS. Repeat surveying occurred along a fixed cross-section at the inlet throat (Figure 12a-c). The inlet throat is the area of the channel where the greatest discharge and most rapid geomorphic change occur. This area is effectively a geomorphic control point that determines how much water can flow out through the mouth. Here cross-sectional area and channel depth are largest. When strong outflow prevented crossing of the channel, the channel width was measured using a laser range finder and the depth was measured with a stadia pole. A long profile was surveyed from the swash zone, over the berm, and into the lagoon prior to opening to obtain the berm height and length. Surveying occurred continuously following excavation until the estuary basin had ceased draining. The cessation of basin drainage was determined by the water level no longer declining but either stabilising at a minimum depth or becoming tidally influenced. All survey data was post processed to be relative to Australian height Datum (AHD).

From the survey data, the following parameters were calculated:

- **Channel width (m):** how wide the channel is across from one bank to the other;
- **Channel water depth (m):** how deep the water is in the channel;
- **Cross-sectional area (m<sup>2</sup>):** the area of a river's cross-section taken here at the inlet throat;
- **Channel bed depth (m AHD):** lowest elevation of the channel bed at the former berm position;
- **Berm length (m):** the horizontal length distance from the lagoon edge to the ocean.
- **Berm crest elevation (m AHD):** the maximum elevation of the berm crest prior to opening.



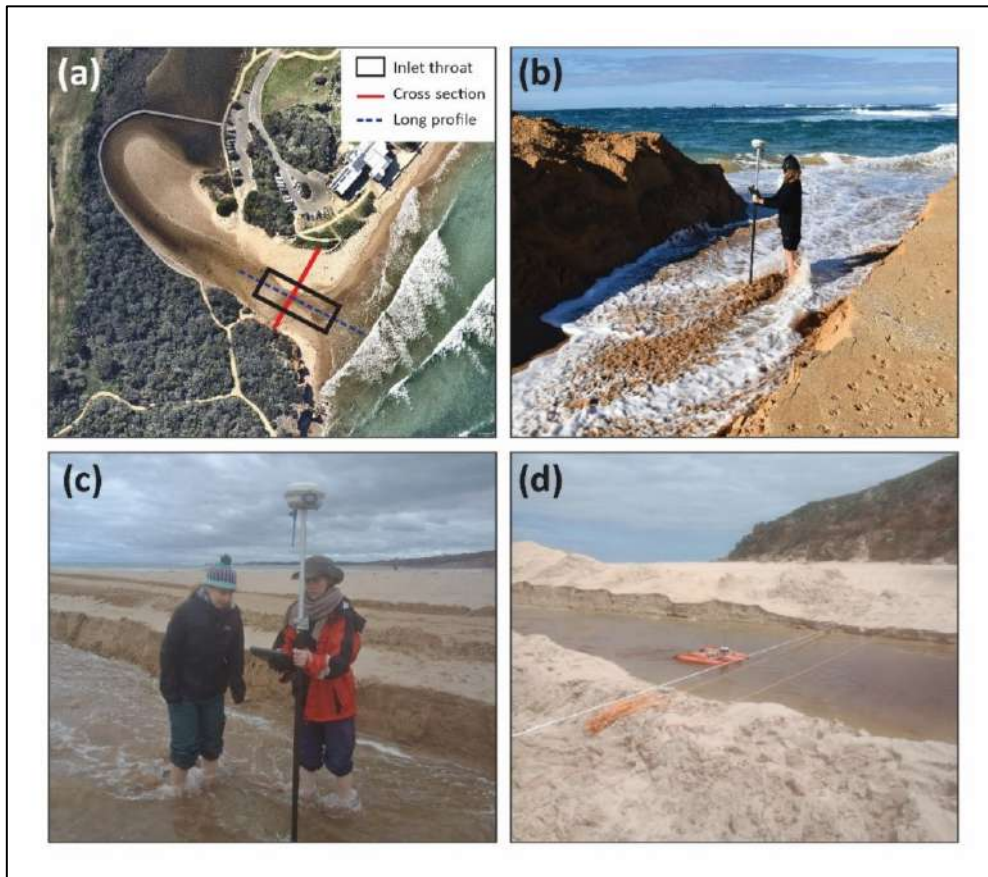


**Figure 12a-d.** (a) Measurement of geomorphic data at the estuary mouth including (b-c) topographic surveying with an RTK GPS and (d) an ADCP mounted on a River Ray raft coupled with the RTK GPS unit.

Estuary outflow velocity was measured at the inlet throat corresponding with the timing of morphological surveys. Velocities were measured in the centre of the channel using a Marsh-McBirney Portable Flow Meter mounted on a wading rod. When strong outflow prevented readings being taken directly in the channel, floats were used to measure outflow velocities. At least three velocity measurements were taken each time and then averaged. Discharge was then calculated using the estuary cross-sectional area calculated from morphological surveys and the outflow velocity as per Equation 1 where Q is discharge.

$$Q \text{ (m}^3\text{/s}^{-1}\text{)} = \text{cross sectional area (m}^2\text{)} * \text{velocity (m/s)} \quad \text{(Equation 1)}$$

An Acoustic Doppler Current Profiler (ADCP) was used to measure outflow velocities and channel morphology when possible (Figure 12d). An ADCP is a hydroacoustic current meter (similar to a sonar) used to measure water current velocities using the Doppler effect of sound waves scattered back from particles in the water column. The ADCP was paired with a second RTK GPS to ensure morphological measurements were relative to AHD. The ADCP was mounted on a River Ray raft and pulled across the channel via a cable and pulley system (Figure 12d). Standing waves in the channel largely limited the use of the ADCP as did high velocity outflow. The ADCP could also only be used when the channel was at least 0.50 m deep so it could not be used in several shallow openings. ADCP data was post processed using WinRiver™ software to obtain measurements of channel area, velocity, and discharge at the mouth.

The change in estuary basin water level was measured continuously using pressure sensors (Solinst LevelLogger 30001 model) anchored to the channel bed. Pressure sensors were installed at locations upstream of the estuary mouth including in the central basin (Figure 10b-g). Data was logged at 1-5 min intervals to allow for maximum storage. A barometric pressure logger was installed within a 2 km radius of all loggers and logger data was corrected for variations in atmospheric pressure. All water level data



## 5.4 Controls on basin drainage

The estuary basin drainage rate can be influenced by the HG at the time of opening and the entrance morphology (i.e. channel dimensions and discharge at the mouth). Estuary drainage rates and durations were calculated for 10 openings where artificial openings were successful in draining the basin. This included six estuary openings monitored in 2019 supplemented with data collected during four openings from McSweeney (2016). The total duration of drainage was defined as from the time of opening until the basin had ceased decreasing in water level. The overall drainage rate and duration was calculated for each opening. Also calculated was the average drainage rate and duration of Stage 2 (Figure 8) using the thresholds from literature to identify the duration of Stage 2. Stage 2 is when the estuary enters a state of rapid morphological change and drainage. Therefore, this is the time where the rapid reduction in water level could influence fish strandings and basin mixing processes. Drainage rates and durations were correlated with the maximum channel cross-sectional area, width, discharge, and velocity during an opening, as well as the HG at the time of opening, and the basin water volume at the time of opening to determine the key controls on the rate and duration of basin drainage.

## 5.5 Physiochemical change

As a secondary part of this project, physiochemical change in the estuary basin after artificial openings was monitored in conjunction with changes in estuary entrance morphology and water level.

Physiochemical data was collected for four artificial openings in 2019:

- (a) Gellibrand River artificial opening 09/03/2019;
- (b) Spring Creek artificial opening 31/05/2019;
- (c) Curdies Inlet artificial opening 02 17/06/2019;
- (d) Anglesea River artificial opening 14/08/2019.

Physiochemical monitoring was undertaken at approximately the same time as morphological measurements at the mouth. Data was obtained from locations as shown in Figure10b-g and supplemented with data from DELWP water level gauges when available (Figure10b-g). Monitoring involved taking measurements as depth profiles at 0.3-0.5 m depth intervals using a HI9829 Multiparameter Meter. The meter was calibrated prior to each opening. For each depth profile the total water depth was recorded, and the following parameters were measured: pH, temperature, dissolved oxygen (% saturation and concentration - ppm), turbidity, conductivity, and salinity. The flow velocity was measured at the top (i.e. 20 % of the water depth) and bottom (bottom 20 % depth) of the water column using a Marsh-McBirney Flow Meter. Changes in estuary physiochemistry were analysed in relation to the timing and magnitude of change in entrance morphology and discharge at the mouth with the idea that change at the mouth influences change within the basin.

As a second component of the physiochemical analysis, a desktop analysis was undertaken using historic data. Water level and physiochemical data was compared for historic openings at two sites: the Gellibrand and Curdies River estuaries. Data was analysed to compare conditions which resulted in fish deaths vs when fish deaths did not occur. For Curdies Inlet, the fish death in focus occurred in 2017 where fish were stranded on the floodplain after a period of rapid drainage. Three fish deaths at the Gellibrand were analysed and compared to multiple other openings which suffered no fish deaths.

The timing of fish deaths was extracted from EstuaryWatch. Water level and physiochemical data was obtained from DELWP gauges installed in the basins of both estuaries. Data therefore does not represent the estuary as a whole. For each opening, the hourly change in estuary water level, salinity, temperature, conductivity, and dissolved oxygen were analysed. Data was extracted for a 3-day period prior to the opening and extending until approximately 1-week after the opening to ensure the whole period of drainage was included. Hydraulic gradients prior to opening were calculated from EstuaryWatch data.



## 6.0 Results

### 6.1 Water levels for natural openings

Natural openings occur when the water surface elevation within the estuary is higher than that of the berm crest. Water level statistics and thresholds for natural openings were calculated for 14 estuaries across the GHMA, CCMA and WGMA regions that had sufficient records of water levels occurring prior to natural openings (Table 1; Figure 14). Full details of natural openings are included in Appendix 1.

**Table 1.** Descriptive statistics for sites with records of historic water levels prior to natural openings.

CMA region	Estuary	n openings	Min WL (m)	Max WL (m)	Median WL (m)	Mean WL (m)
GHCMA	Glenelg River	4	1.04	1.54	1.32	1.31
GHCMA	Fitzroy River	13	0.63	1.46	1.07	1.07
GHCMA	Surrey River	25	0.55	1.71	1.04	1.16
GHCMA	Eumerella River	10	0.50	1.79	1.06	1.07
GHCMA	Merri River (RC)	4	1.08	2.00	1.55	1.55
GHCMA	Hopkins River	16	0.74	1.90	1.30	1.31
CCMA	Curdies Inlet	1	1.98	1.98	1.98	1.98
CCMA	Gellibrand River	12	1.01	2.02	1.41	1.45
CCMA	Aire River	5	1.45	2.50	1.62	1.76
CCMA	Barham River	37	1.10	2.30	1.62	1.57
CCMA	Painkalac Creek	4	1.43	1.66	1.55	1.55
CCMA	Anglesea River	10	1.23	2.00	1.60	1.59
CCMA	Spring Creek	3	1.65	1.95	1.90	1.83
WGMA	Powlett River	3	2.05	2.35	2.21	2.20

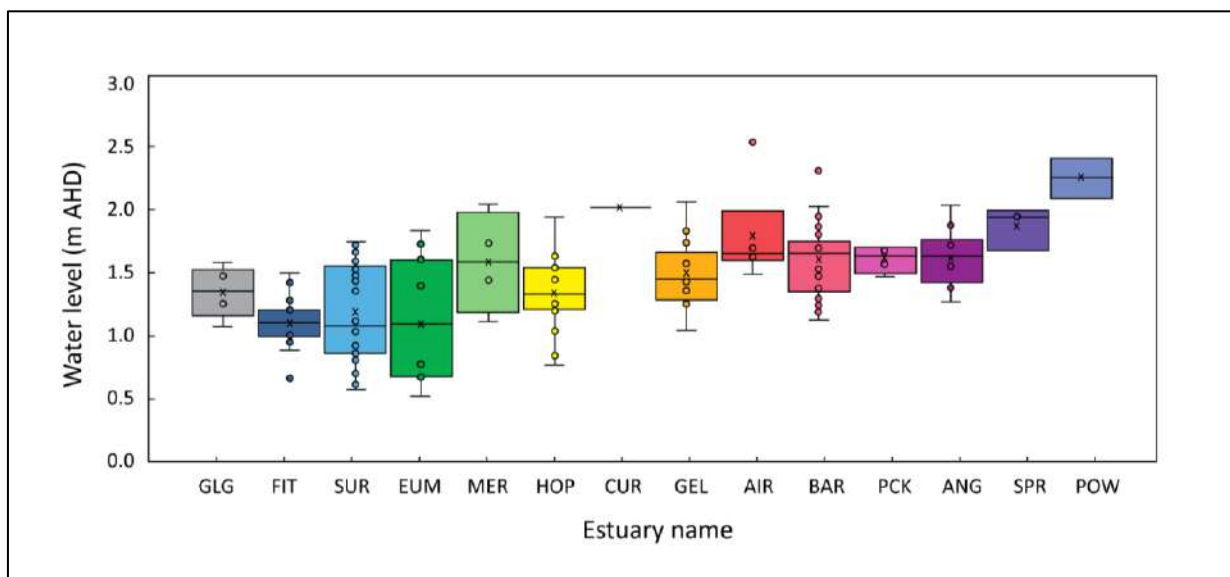


**Figure 14.** Distributions of water levels at which estuaries naturally open. GLG (Glenelg); FIT (Fitzroy); SUR (Surrey); EUM (Eumeralla); MER (Merri at Rutledges Cutting); HOP (Hopkins); CUR (Curdies); GEL (Gellibrand); AIR (Aire); BAR (Barham); PCK (Painkalac); ANG (Anglesea); SPR (Spring); and POW (Powlett).

As the estuary water level is only one part of the picture for assessing natural opening thresholds, HG values were also calculated for historic natural openings which had the berm length recorded via EstuaryWatch (Table 2). These were compared to the values for all artificial openings with HG data. From the available data, estuaries tend to naturally open when the HG 0.022 m/m (grade: 1:46) or above. The average HG for natural openings is 0.052 m/m (grade: 1:19). This is steeper than the average for artificial openings which is 0.033 m/m (grade: 1:30). Natural openings also occur with a slightly shorter berm length and lower berm height on average compared to artificial openings. Interestingly, natural openings occur at a similar water level on average compared to artificial openings but the head between the estuary and ocean is higher (Table 2). This is likely to be related to the offshore tidal elevation (i.e. stage) at the timing of natural openings where a lower tide would equate to higher relative hydraulic head.

**Table 2.** HG values for natural openings with sufficient water level and berm data and a comparison to values for known artificial openings. Berm\_L = berm length, Berm\_H = berm height, and WL = water level)

Natural openings	Date_open	Berm_L (m)	Berm_H (m AHD)	WL (m AHD)	Head (m)	HG (m/m)	Grade
Curdies Inlet	18/06/18	80	2.00	1.98	2.48	0.031	1:32
Wreck_Creek_01	08/11/19	79	2.15	2.10	1.86	0.024	1:43
Wreck_Creek_02	01/12/17	89	2.10	1.98	2.04	0.023	1:44
Merricks_Creek_01	21/06/19	91	2.10	2.01	2.16	0.024	1:42
Merricks_Creek_02	09/07/18	30	2.07	1.96	1.91	0.064	1:16
Gellibrand_River_01	06/01/19	50	-	1.10	1.10	0.022	1:46
Gellibrand_River_02	31/05/17	15	1.89	1.79	1.89	0.126	1:8
Gellibrand_River_03	01/05/15	35	1.60	1.60	1.68	0.048	1:21
Gellibrand_River_04	06/02/15	14	1.60	1.25	1.46	0.104	1:10
<b>Mean_nat_openings</b>	-	<b>53.67</b>	<b>1.94</b>	<b>1.75</b>	<b>1.84</b>	<b>0.052</b>	<b>1:19</b>
<b>Median_nat_openings</b>	-	<b>50.00</b>	<b>2.04</b>	<b>1.96</b>	<b>1.89</b>	<b>0.034</b>	<b>1:29</b>
Mean_artificial openings	-	60.55	2.29	1.78	1.71	0.033	1:30
Median_artificial openings	-	51.50	2.18	1.74	1.70	0.030	1:33

## 6.2 Field observations during artificial openings

This section provides a summary of field observations from eight artificial openings monitored during 2019 (Table 3). Field measurements include the continuous change in entrance morphology, outflow velocity, discharge, and estuary water level. Table 3 summarises the dates and characteristics of artificial openings monitored during the fieldwork.

For an estuary opening to be '**successful**' the channel had to maintain an open entrance after excavation and enter a stage of rapid outflow, expansion, and drainage. This represents "success" in Table 3.

For an opening to have '**drained the basin**' it had to decrease the basin water level by >10 % of the starting water level and/or achieve its purpose of alleviating flooding. This represents the column "drains" in Table 3 (on the next page).

**Full details of changes in channel morphology for each opening are presented in Appendix 2.**

**Table 3.** Summary of artificial estuary entrance openings monitored in the field as part of this study.

#	Site/opening	Date	HG (m/m)	WL (m AHD)	Decrease in WL (m)	Time to drain (hrs)	Opening duration	H <sub>s</sub> (m)	Success	Drains
1	Aire River 1	01/02/19	0.022	+1.52	-1.00	24	24 days	2.59	Yes	Yes
2	Gellibrand River	09/03/19	0.016	+1.52	-0.13	70	5 days	3.31	Yes	No
3	Aire River 2	01/05/19	0.010	+1.60	-0.00	-	4 days	2.02	Yes	No
4	Spring Creek	31/05/19	0.051	+1.90	-1.20	16	Unknown	0.83	Yes	Yes
5	Curdies Inlet 1	16/06/19	0.015	+1.34	-0.00	-	0 days	2.86	No	No
6	Curdies Inlet 2	17/06/19	0.025	+1.38	-1.10	42	16 days	2.17	Yes	Yes
7	Painkalac Creek	08/08/19	0.045	+2.11	-0.81	16	38 days	2.44	Yes	Yes
8	Anglesea River	14/08/19	0.016	+1.76	-0.47	100	7 days	1.41	Yes	Yes

### 6.1.1 Aire River 1: 01/02/19

**Opening at the Aire River was successful and the opening achieved its purpose of draining the basin.**

Opening occurred at 9 am on 01/02/19 on a falling high tide (0.60 m). At the time of opening, the berm was 70 m long, the estuary water level was +1.52 m AHD (Figure 15), and HG 0.027 m/m (grade of 1:37). On 01/02, offshore H<sub>s</sub> was moderate at 2.59 m and fluvial discharge (Q) low (36.45 ML/day). The ADCP was set up to be pulled across the channel however high velocity outflow and standing waves inhibited its use. Geomorphic change was steady over the first hour and entered a stage of rapid channel expansion and incision 1.5 hrs after opening coinciding with an outflow velocity >1.50 m/s (Figure 16; Figure 17). Peak velocity (3.07 m/s) and channel width (35.11 m) were reached 4 hrs after opening and peak cross-sectional area (58 m<sup>2</sup>) and discharge (174 m<sup>3</sup>/s<sup>-1</sup>) occurred 4.7 hrs after opening (Figure 16). 6 hrs after opening, velocity (2.2 m/s) and discharge (114 m<sup>3</sup>/s<sup>-1</sup>) had started to decrease. 8 hrs after opening, the channel maintained a similar width (34 m) but velocity had decreased further to 1.60 m/s and the channel had stopped incising. 8 hrs after opening, the basin water level had decreased by -0.31 m to +1.21 m AHD (Figure 15). The estuary ceased draining to the ocean ~24 hrs after the opening with the water level stabilising at +0.52 m AHD (Figure 15; Figure 17d). Aire River remained open for 24 days until 25/02/19.

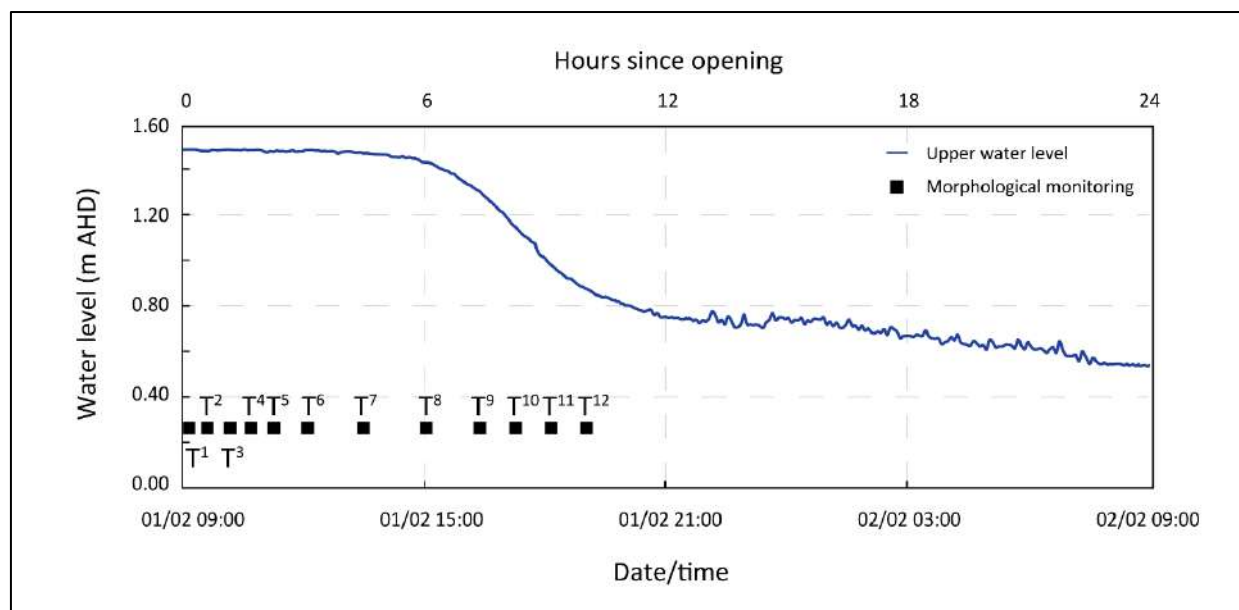


**Figure 15.** Basin water level (every 5 min) and the timing of morphological monitoring at the Aire River.

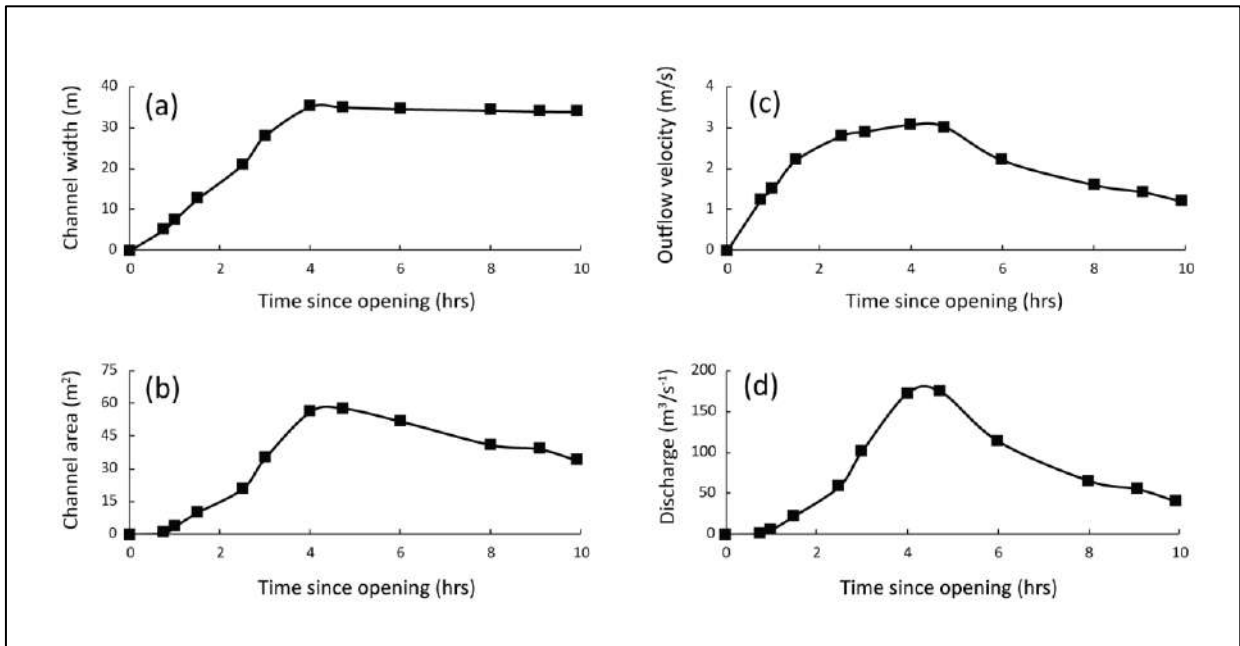


**Figure 16a-d.** Change in (a) channel width; (b) outflow velocity; (c) cross-sectional area; and (d) discharge during the artificial opening of Aire River 01/02/2019.

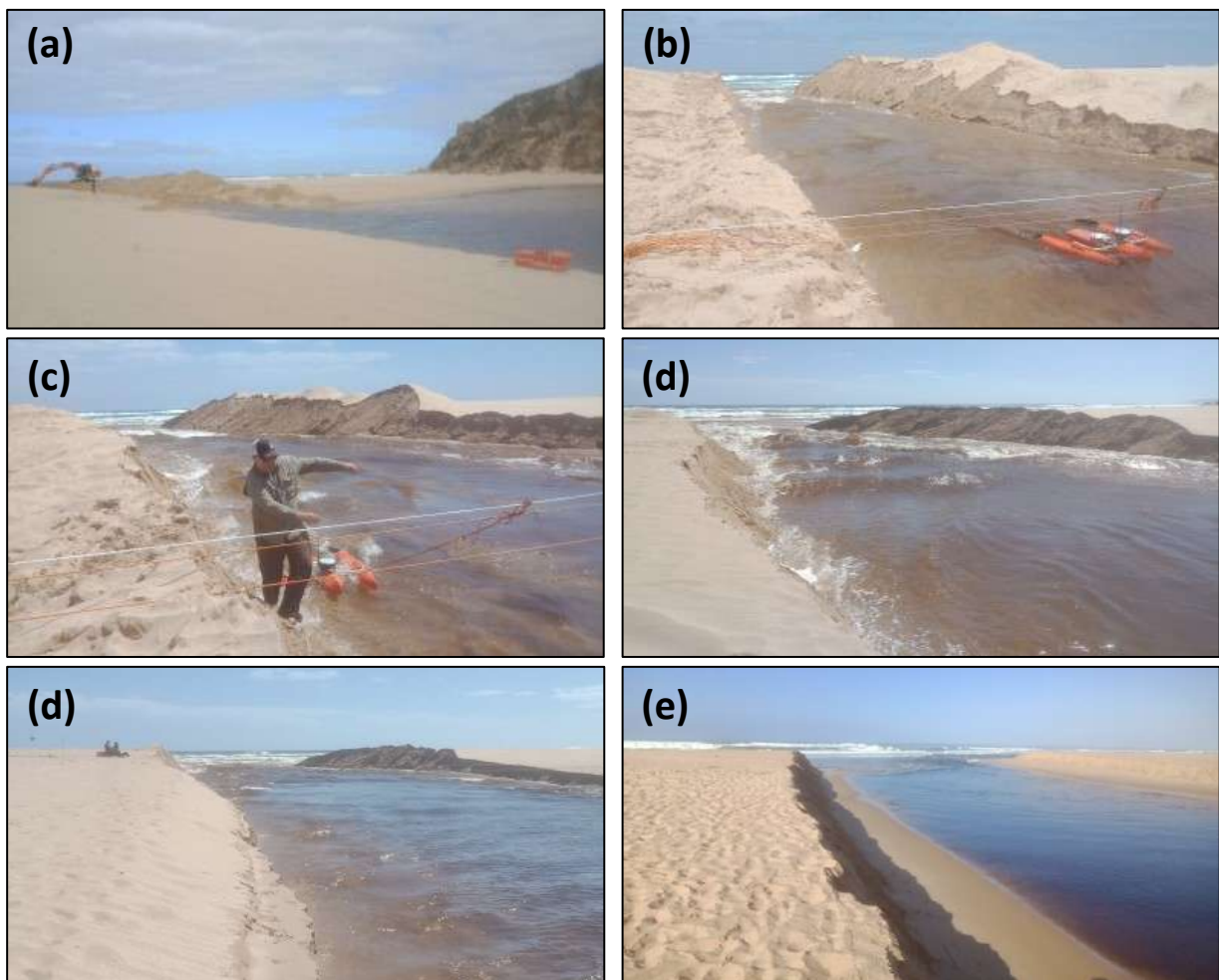


**Figure 17a-f.** (a) Opening 9 am 01/02/19; (b) 10.30 am 01/02; (c) 11 am 01/02; (d) 11.30 am 01/02; (e) peak outflow 1 pm 01/02; (f) 8 am 02/02 with a clear decrease in estuary water level and outflow velocity.

### 6.1.2 Gellibrand River: 09/03/19

**The Gellibrand was successfully opened but opening did not achieve its purpose of draining the basin.**

The opening occurred at 3 pm 09/03/19 on a falling high tide (0.90 m). At the time of excavation, the estuary water level was +1.52 m AHD and HG 0.016 m/m (grade: 1:61). The berm was 74 m long with a crest elevation of +1.82 m AHD. Offshore  $H_s$  (3.31 m) and  $Q$  (145.98 ML/day) were both moderate. During the opening, the ADCP was set up for use however the channel did not reach a sufficient depth (>0.50 m) to allow for measurements to be taken (Figure 20d). During the opening, geomorphic change was slow and for 20 hrs after opening outflow velocity remained below 1 m/s (Figure 19b). As a result, energy was expended in slowly widening the channel as opposed to incising it after the initial period of excavation. Because the channel did not reach a large size, discharge at the mouth was low overall, and the estuary water level only dropped by 0.13 m during the whole opening.

70 mins after excavation, outflow velocity had reached 0.93 m/s and the channel was 3.50 m wide and 0.48 m deep (Figure 19a-b; Figure 20a). Discharge at the mouth was  $1.56 \text{ m}^3/\text{s}^{-1}$  and the cross-sectional area was  $1.68 \text{ m}^2$  (Figure 19c-d). 3 hrs after opening, the outflow velocity had decreased to 0.85 m/s and the channel had become meandering and shallow at mouth (Figure 20b-d). The channel continued to decrease in outflow velocity, cross-sectional area, and discharge for the next 7 hrs - with outflow velocity reaching 0.61 m/s 10 hrs after opening. Throughout this time, the channel width fluctuated around an equilibrium value of 4.55 m and the estuary water level had not decreased at all (Figure 18; Figure 19a). 12 hrs after opening (3.30 am 10/03/19) outflow velocity started to increase again driving an increase in cross-sectional area and discharge (Figure 19a-d). The increase in velocity may be attributed to due to a slight increase in upstream fluvial discharge to 157.88 ML/day on 10/03. The peak outflow velocity of 1.12 m/s occurred 21 hrs after opening (12.17 pm 10/03) coinciding with the channel reaching its maximum depth (0.50 m), area ( $2.28 \text{ m}^2$ ), and discharge ( $2.55 \text{ m}^3/\text{s}^{-1}$ ) (Figure 19; Figure 20e). Outflow >1 m/s was sustained for another ~25 hrs until 4 pm 11/03 and during this time there was minimal change in morphology aside from a gradual decrease in water depth and cross-sectional area (Figure 19; Figure 20f). At the time of the last measurement (4 pm 11/03), the water level had only decreased by -0.03 m to +1.49 m AHD. The minimum water level of +1.39 m AHD was reached at 1 pm 12/03 representing a total decrease of -0.13 m. Drainage was slow overall at an average rate of -0.002 m/hr. The estuary remained open for five days until 13/03/19 (EstuaryWatch, 2019).

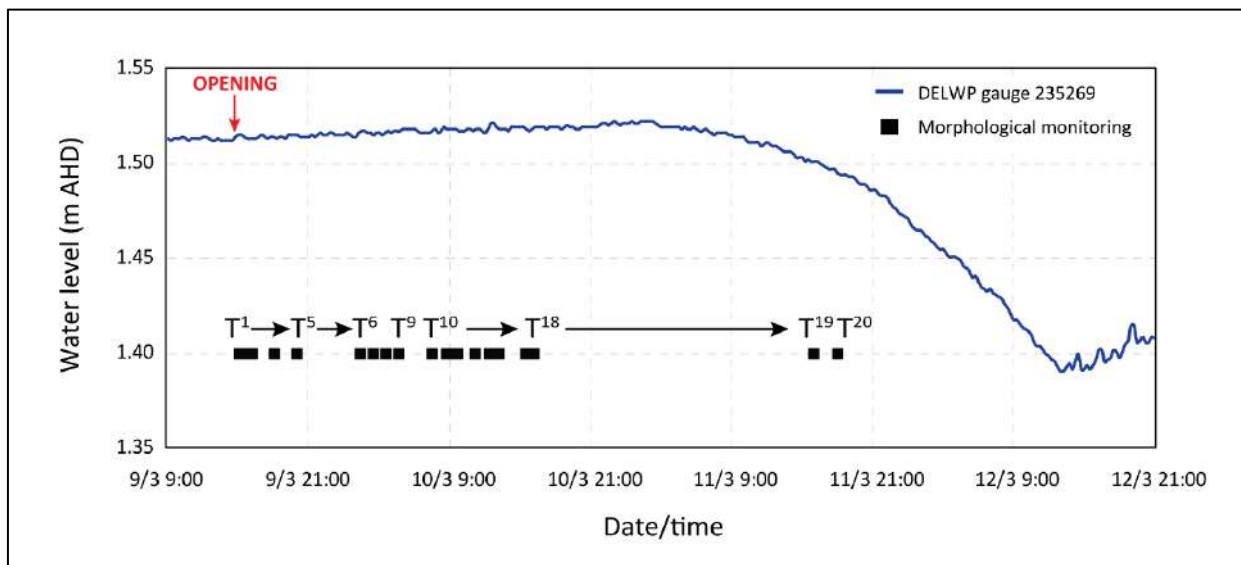


**Figure 18.** Basin water level drainage curve from DELWP gauge at Princetown (235269) (logging every 15 min) and the timing of morphological monitoring at Gellibrand River estuary mouth 09/03/19 - 12/03/19.



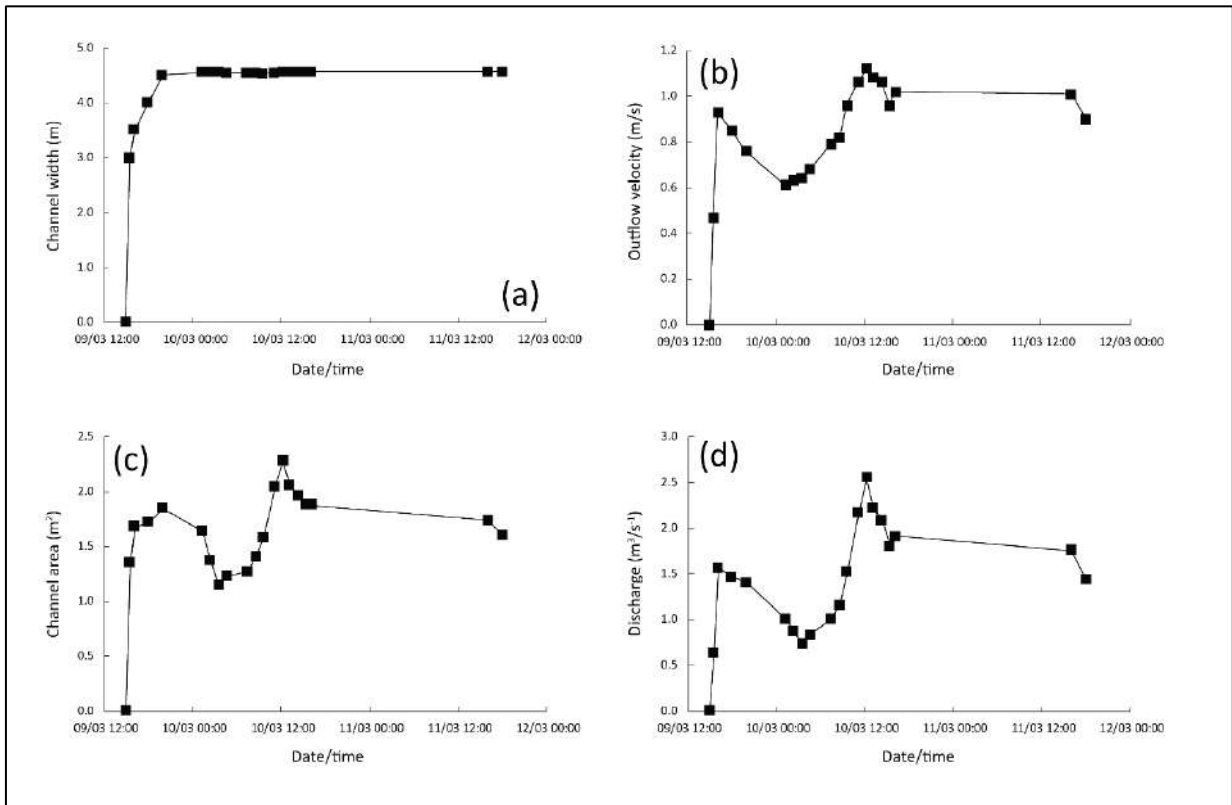


**Figure 19a-d.** Change in (a) channel width; (b) outflow velocity; (c) cross-sectional area; and (d) discharge during the artificial opening of Gellibrand River 09/03/2019 - 11/03/2019.

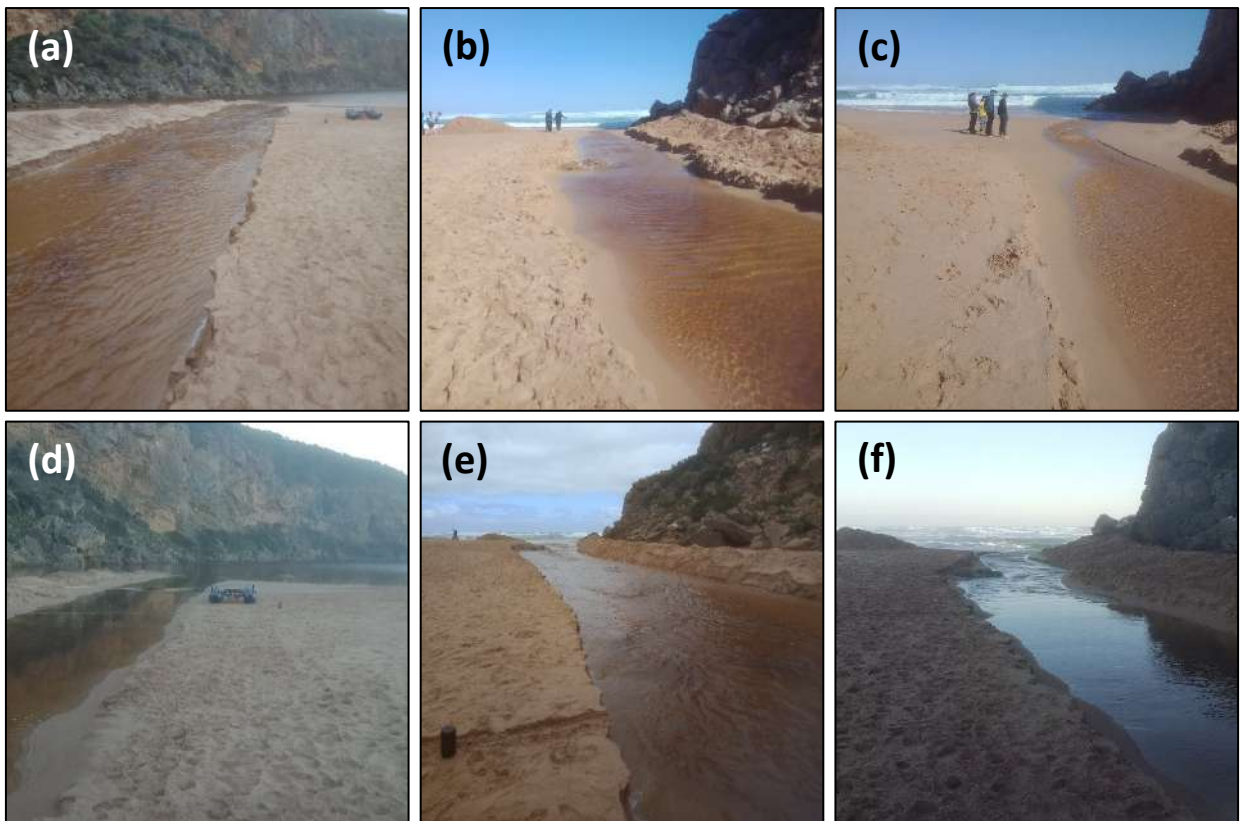


**Figure 20a-f.** (a) 4 pm 09/03 - 1 hr after excavation looking into lagoon; (b-c) 6 pm 09/03 shallow, low velocity outflow; (d) 8 pm 09/03 looking towards lagoon; (e) 12 pm 10/03 peak outflow; (f) 6 pm 11/03.

### 6.1.3 Aire River 2: 01/05/19

**Aire River was successfully opened but the opening did not achieve its purpose of draining the basin.**

Aire River was opened at 10 am 01/05/19 just after low tide (0.60 m). At the time of opening, the water level was +1.60 m AHD (Figure 21) and HG 0.010 m/m (grade: 1:97). The berm was long (190 m) with the crest +2.37 m AHD in elevation. On 01/05, offshore  $H_s$  was moderate (2 m) and  $Q$  (26 ML/day) very low. During the opening, outflow velocity remained below 0.75 m/s and morphological change was slow (Figure 22; Figure 23; Figure 24). The ADCP was set up but the channel did not reach a sufficient depth for measurements to be taken.

After excavation, the channel bed was lowered by >1.5 m (Figure 23; Figure 24). The minimum bed elevation (+0.79 m AHD), max water depth (0.77 m), discharge ( $0.70 \text{ m}^3/\text{s}^{-1}$ ), and cross-sectional area ( $1.48 \text{ m}^2$ ) were reached 3.6 hrs after excavation (Figure 24). At this time, outflow velocity was only 0.45 m/s. From then onwards, the channel began to slowly aggrade with a progressive decrease in area and discharge. During 01/05, outflow velocity remained below 0.60 m/s and energy was expended widening the channel as opposed to incising it. Peak outflow velocities of 0.70 m/s were reached 24 hrs after opening resulting in a slight lowering of the channel bed in the centre of the thalweg (T9 - 11; Figure 22). As the channel area had decreased, the increased velocity did not translate to an increase in discharge at the mouth (Figure 23). The channel then began to slowly aggrade as velocities decreased below 0.60 m/s (Figure 24d). A slight -0.02 m decrease in water level had occurred by 12 pm 01/05 (Figure 21). By 1 pm 02/05, the water level had increased to +1.62 m AHD - possibly due to increased fluvial inflow (78 ML/day on 02/05). Aire River remained open for four days closing on 04/05/19. The estuary was artificially opened again on 07/05/19.

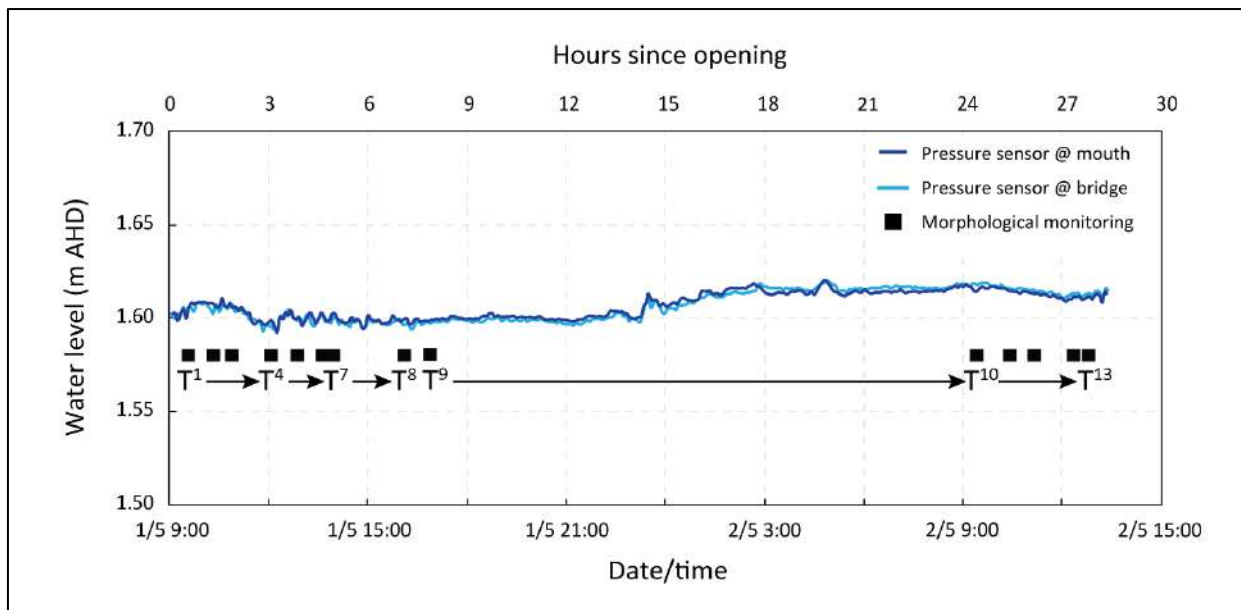


**Figure 21.** Basin water level (every 5 min) and the timing of morphological monitoring at the Aire River.



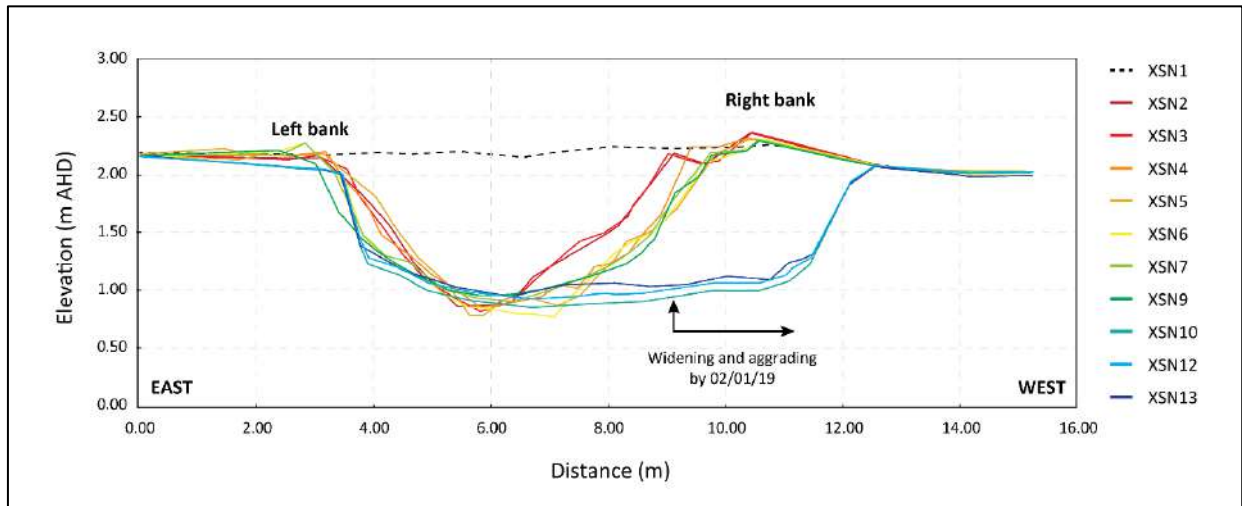


**Figure 22.** Surveyed entrance morphology at the mouth of Aire River 01/05 - 02/05 (XSN = cross-section).

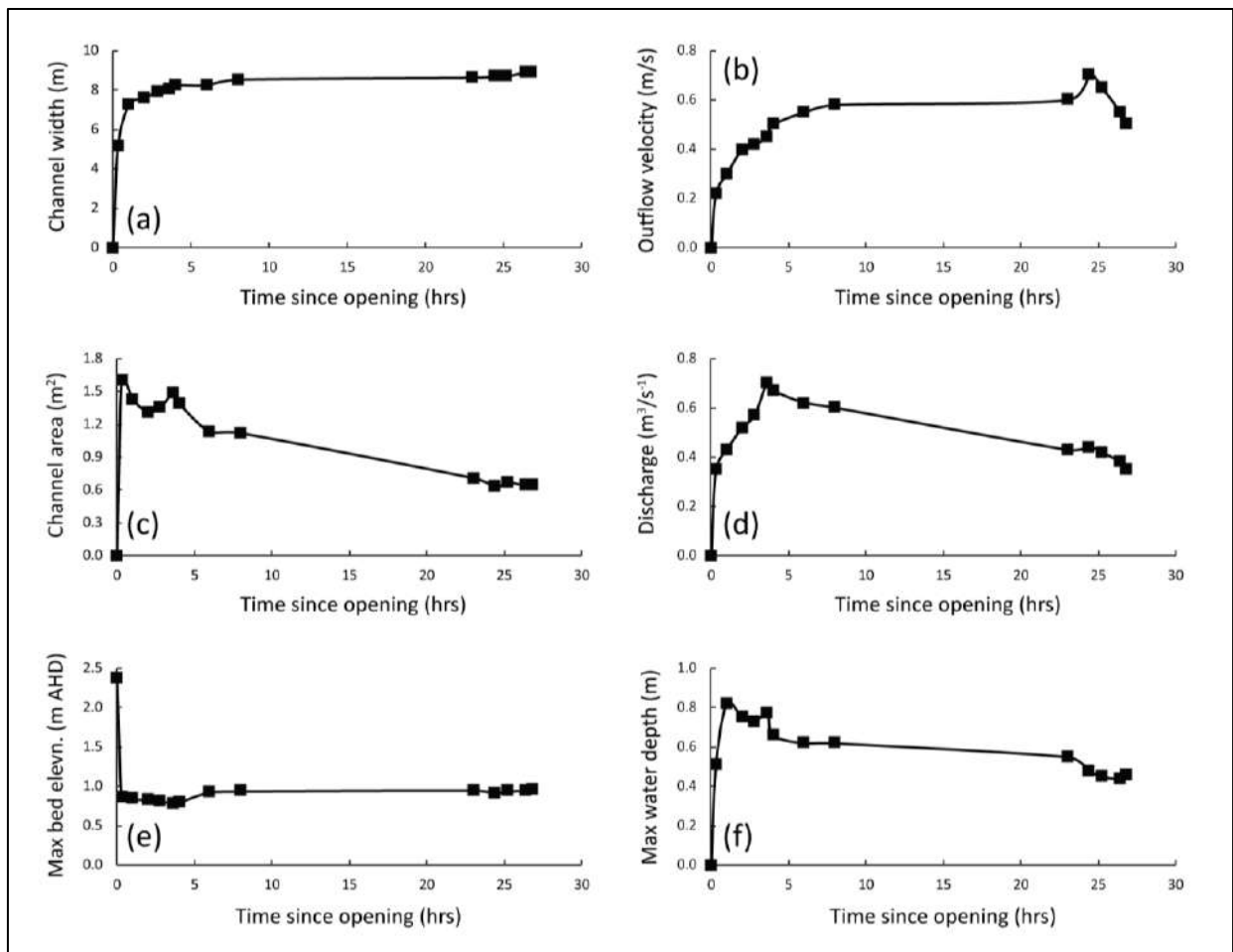


**Figure 23a-f.** Change in (a) channel width; (b) outflow velocity; (c) cross-sectional area; (d) discharge; (e) max bed elevation; (f) max water depth during artificial opening of Aire River 01/05/2019 - 02/05/2019.

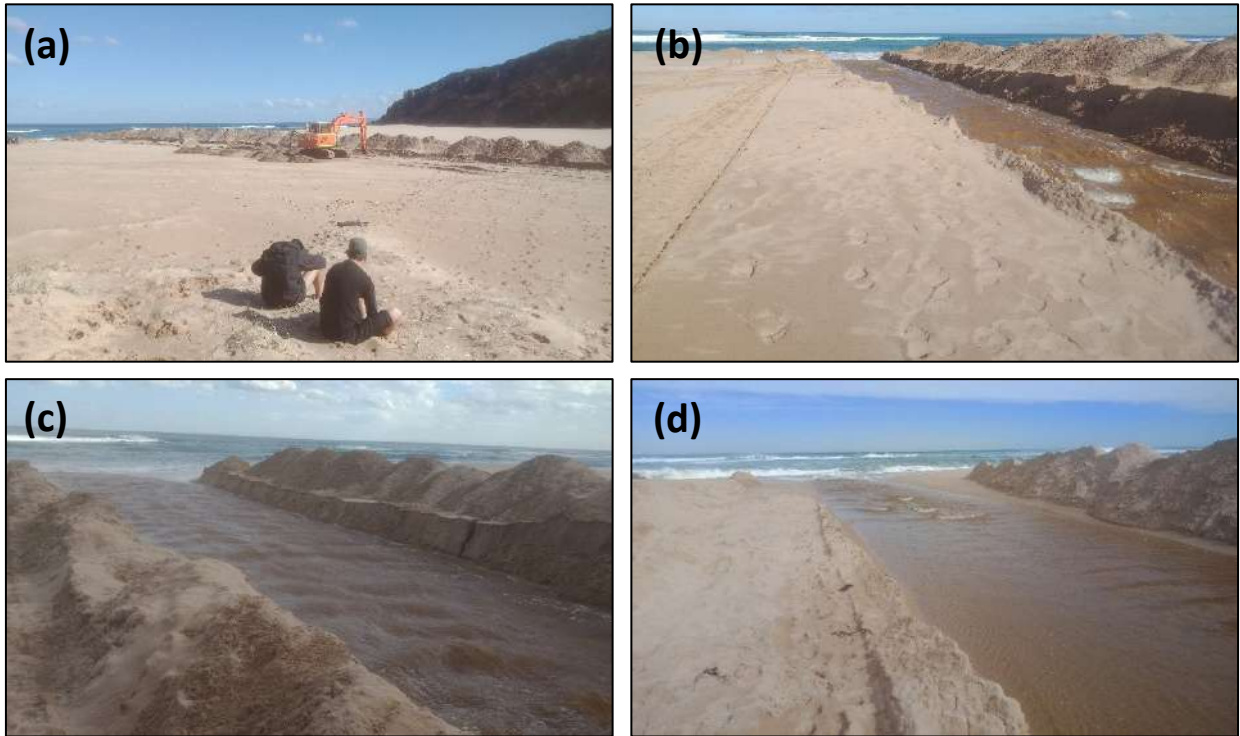


**Figure 24a-d.** (a-b) 10 am 01/05; (c) 2 pm 01/05 peak discharge; (d) 9 am 02/05 shallow, aggraded channel.

#### 6.1.4 Spring Creek: 31/05/19

**Spring Creek was successfully opened and the opening achieved its purpose of draining the basin.**

Excavation occurred at 2 pm 31/05/19 at low tide (0.90 m). At the time of opening, the basin water level was +1.90 m AHD (Figure 25) and HG 0.051 m/m (grade: 1:19). The berm was 38 m long and +1.96 m AHD high with offshore  $H_s$  being low (0.83 m). Because of the steep HG, morphological change at the mouth was very rapid (Figure 26; Figure 27; Figure 28; Figure 29).

Within 1.5 hrs of opening, outflow velocity had reached  $>1$  m/s and the channel was 5 m wide (Figure 27). 2 hrs after opening, the rates of channel expansion began to increase rapidly. A weir had formed at the seaward edge of the lagoon with standing waves moving back into the lagoon itself (Figure 28c). The peak outflow velocity of 2.70 m/s was reached 4.2 hrs after opening with the channel being 26 m wide and 1 m deep (Figure 27). 4.7 hrs after opening, the channel bed had incised to its lowest elevation (-0.26 m AHD) coinciding with peak discharge ( $44 \text{ m}^3/\text{s}^{-1}$ ) and area ( $17.44 \text{ m}^2$ ) at the mouth. At this time the estuary water level had decreased by -0.76 m to +1.14 m AHD (Figure 25). 5 hrs after opening, outflow velocity and discharge had started to decrease. By 9 am 01/06/19, outflow velocity had decreased to 0.40 m/s, the channel was 0.11 m deep, and the bed had aggraded to -0.19 m AHD (Figure 25; Figure 27; Figure 28f). The estuary reached a minimum water level of +0.80 m AHD at 7 am 01/06 having decreased by -1.10 m at an average drainage rate of -0.08 m/hr.

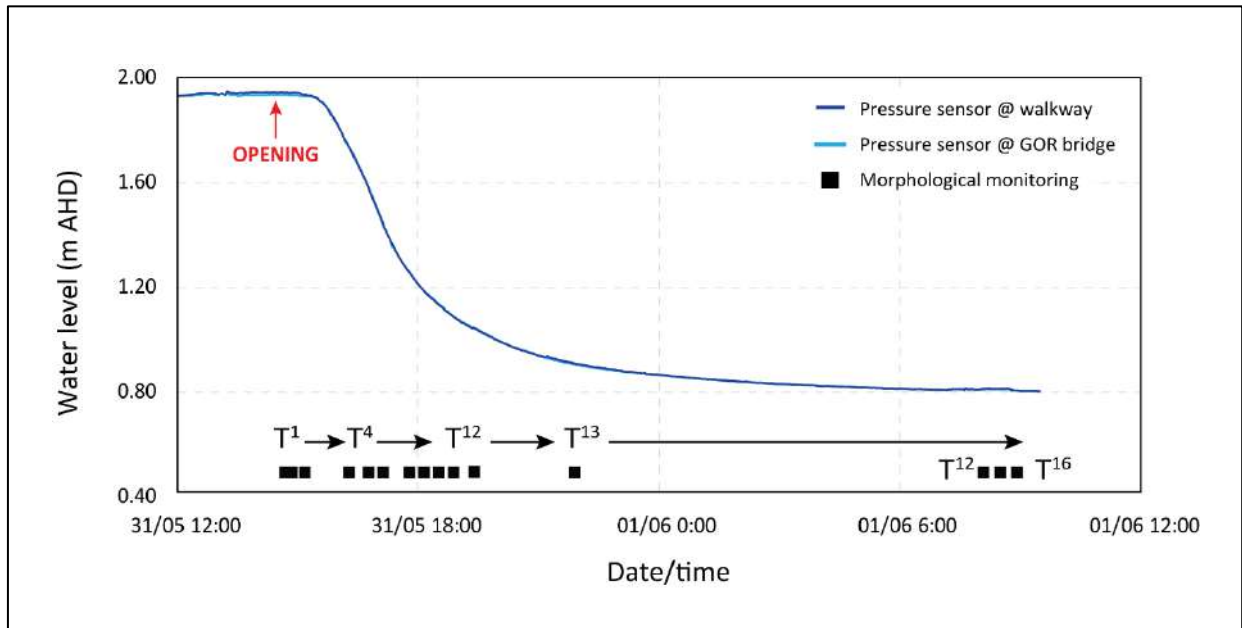


**Figure 25.** Spring Creek drainage curve from pressure sensors and timing of morphological monitoring.

Adjacent to the right bank (west side) of Spring Creek mouth is a calcarenite cliff with a rocky section which underlies the channel (this is on the Golf Course side of the mouth) (evident in Figure 28c). The rocky cliff provided a hard point where the channel could not expand further eastward. After the channel expanded to reach the lower section of this cliff, lateral expansion in a westward direction continued. Vertically, once the channel had incised to the base of the rock underlying the west side of the channel, incision occurred on the east side of the channel. This is evident in XSN's 8-14 where the channel is expanding and incising towards the east side only (Figure 26).

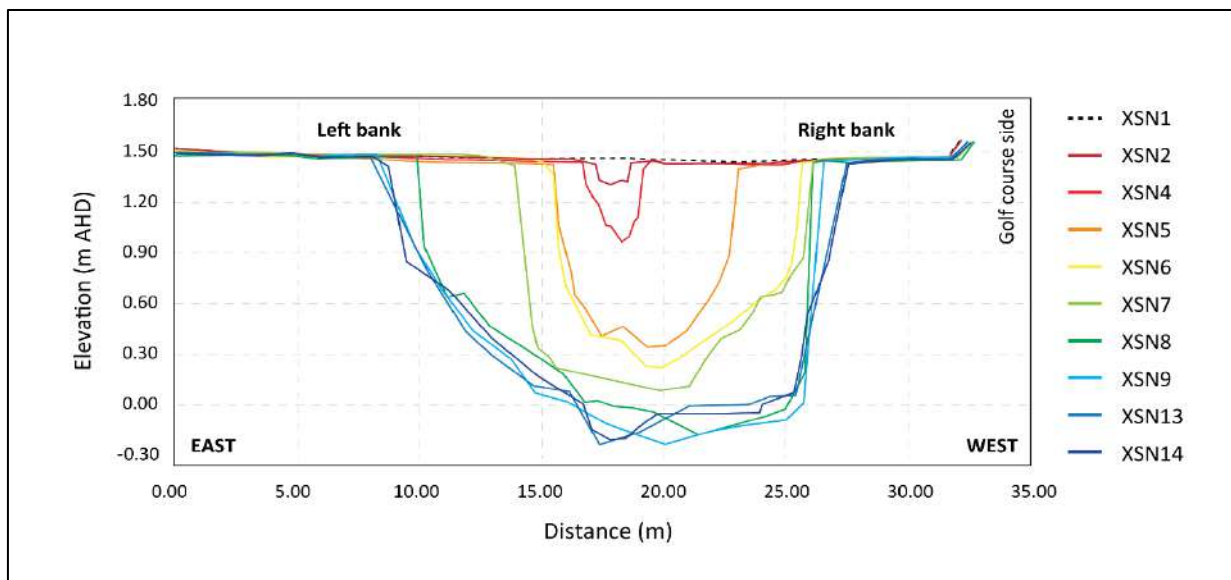


**Figure 26.** Select surveyed entrance channel cross-sections at the mouth of Spring Creek estuary during 31/05 - 01/06/19.

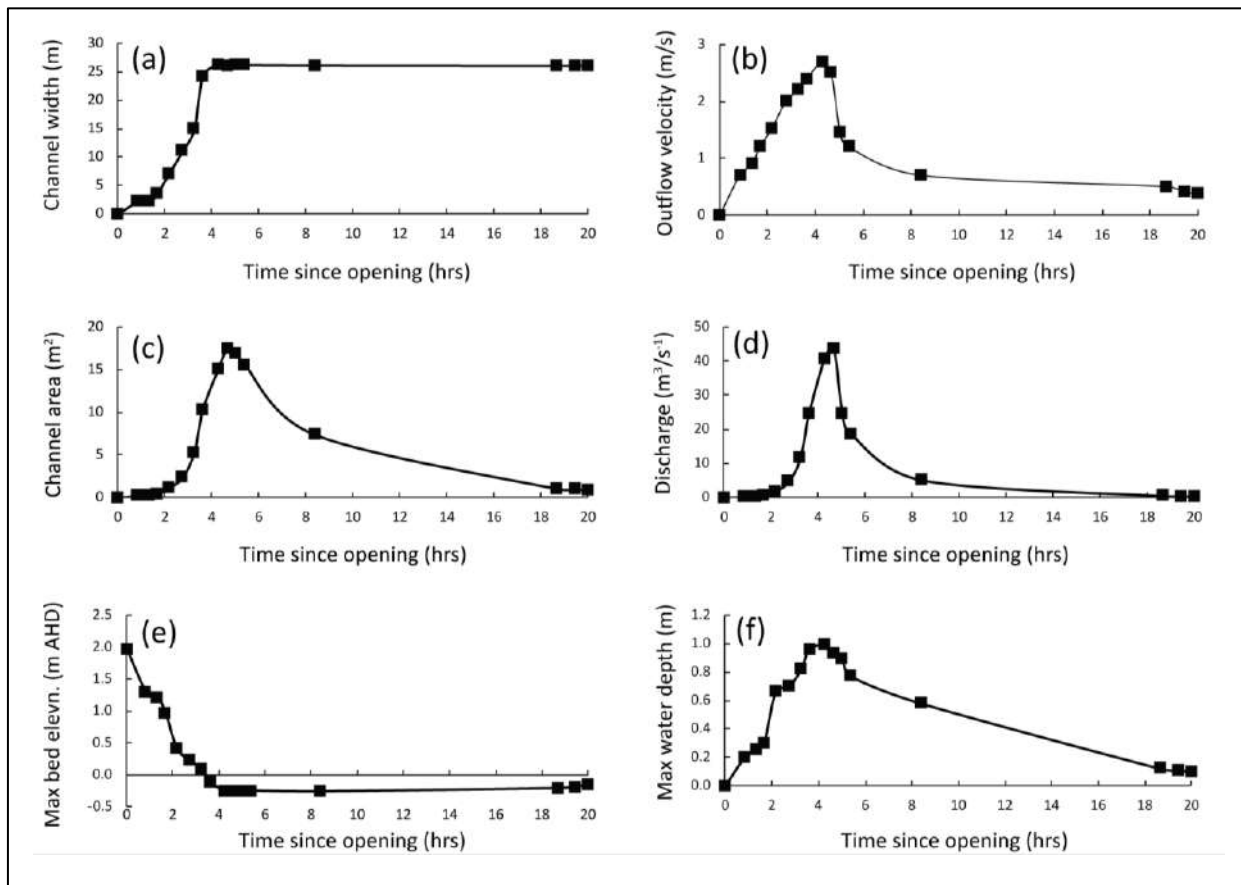


**Figure 27a-f.** Change in (a) channel width; (b) outflow velocity; (c) cross-sectional area; (d) discharge; (e) max bed elevation; (f) max water depth during Spring Creek artificial opening 31/05/2019 - 01/06/2019.

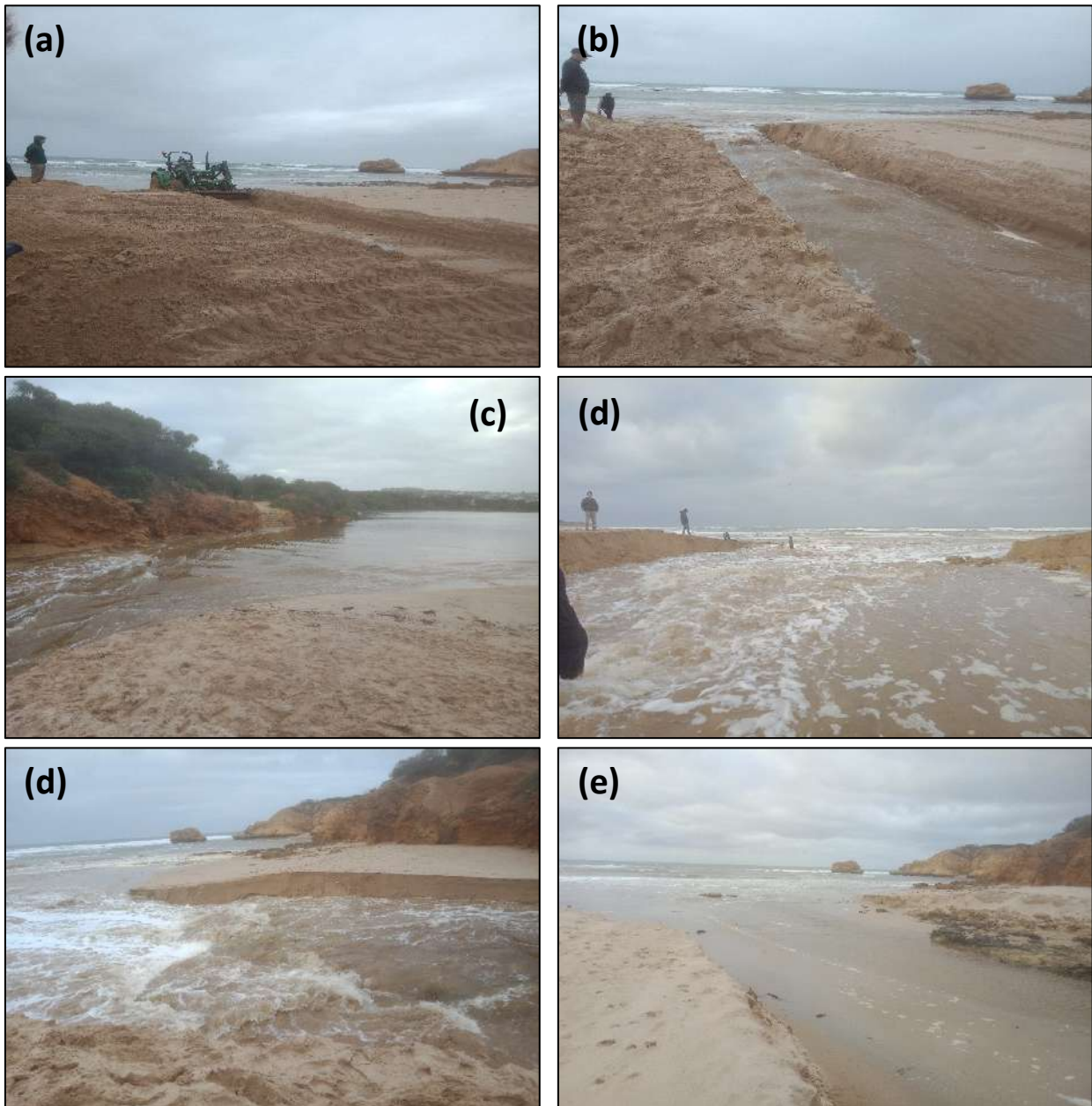


**Figure 28a-f.** Artificial opening at Spring Creek (a) 2 pm 31/05/19 excavation; (b) 3 pm 31/05; (c) 3 pm 31/05 weir at seaward edge of lagoon; (d) 4 pm 31/05; (e) 6 pm 31/05 peak outflow looking seaward; (f) 9 am 01/06 looking seaward at mouth after drainage with a now very shallow channel.

### 6.1.5 Curdies Inlet 1: 16/06/19

**Curdies Inlet was not successfully opened and opening did not achieve its purpose of draining the basin.**

Curdies Inlet was artificially opened at 10 am on 16/06/19 on a falling high tide (0.90 m). At the time of opening, the lagoon water level was +1.34 m AHD and HG 0.015 m/m (1:66). The berm was 68 m long and the crest was +2.32 m AHD in elevation (Figure 29). On 16/06, offshore  $H_s$  (2.86 m) and  $Q$  (276 ML/day) were moderate. After excavation, the berm crest was lowered to +1.48 m AHD. Within 1.2 hrs of excavation, the channel had infilled via deposition from waves as outflow did not reach a sufficient velocity (max = 0.30 m/s) to incise the channel and move sediment offshore (Figure 30). By 11.20 am, outflow had completely ceased and the channel at the former berm position had aggraded by +0.12 m. By 12.09 pm the berm had further aggraded by +0.10 m to +1.66 m AHD. As the basin water level did not



decrease at all during the opening, persistent flooding on Dorey Street resulted in road closure and emergency conditions which prompted a second opening the next day on 17/06 (Figure 31; Figure 32).

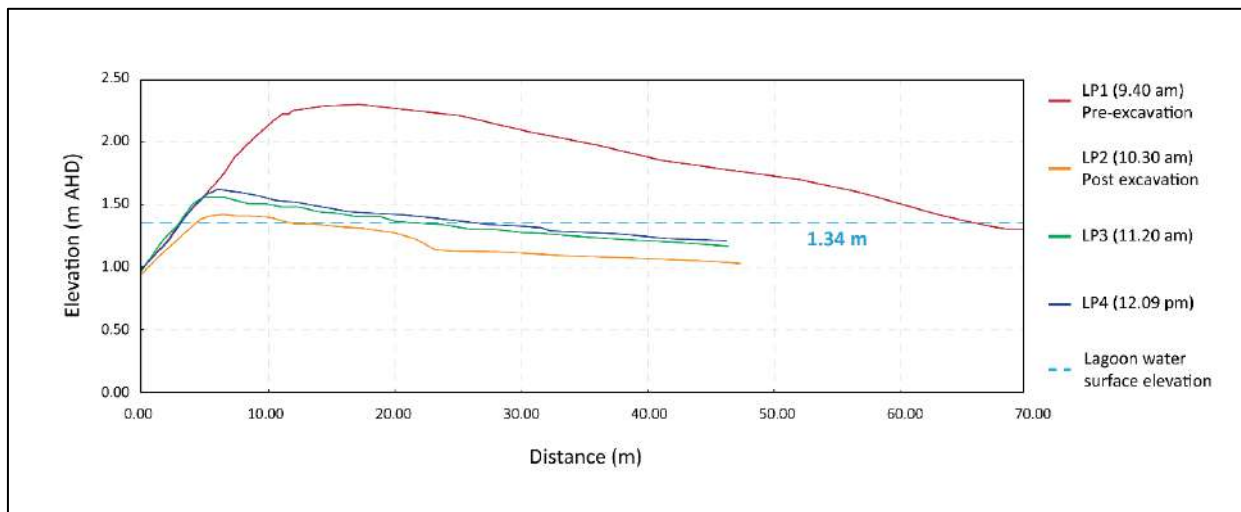


**Figure 29.** Surveyed long profiles from swash to seaward edge of the lagoon at Curdies Inlet on 16/06/19.



**Figure 30a-c.** (a) Curdies Inlet channel infill via waves 11.20 am 16/06/19; (b) looking towards the lagoon showing infill of the channel and a cessation of outflow 1 pm 16/06; (c) looking seaward at 2 pm 16/06.



**Figure 31a-b.** (a) Curdies Inlet 17/06/19 showing inundation of Dorey St (red square); (b) 23/06/19 after second opening showing drainage of floodwaters. Images from Planet Team (2019).

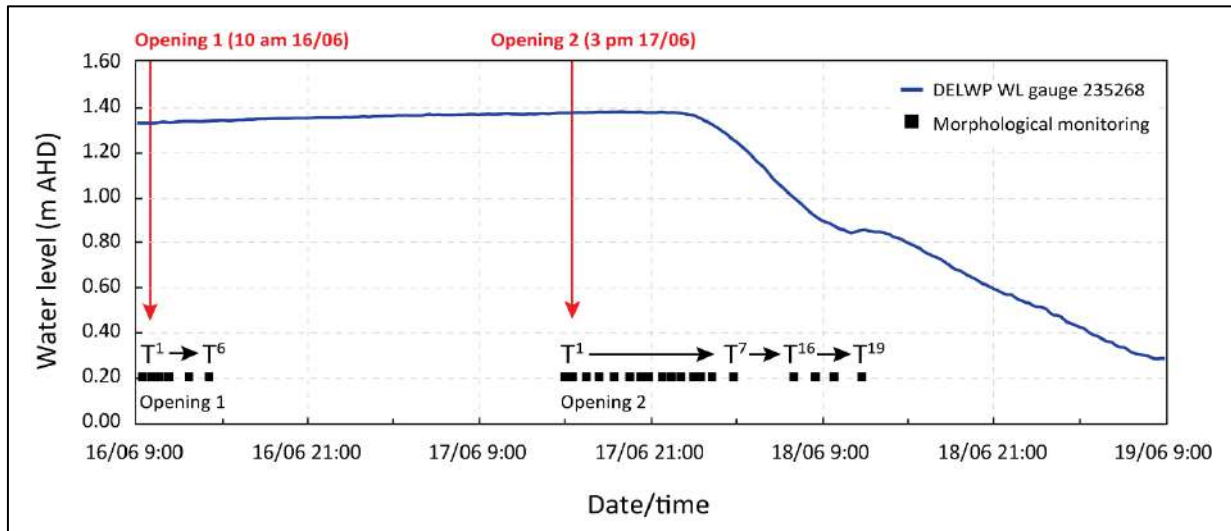


**Figure 32.** Curdies Inlet drainage curve from pressure sensors and timing of morphological monitoring.

### 6.1.6 Curdies Inlet 2: 17/01/19

**Curdies Inlet was successfully opened and the opening achieved its purpose of draining the basin.**

Opening occurred at 3 pm 17/06/19 on a falling high tide (0.80 m). The lagoon water level was +1.38 m AHD (Figure 32) and HG 0.025 m/m (1:41). The berm was 48 m long and +1.80 m AHD in elevation. On 17/06, offshore  $H_s$  was 2.17 m and  $Q$  210 ML/day. After excavation, outflow velocity reached 1.22 m/s 0.5 hrs after opening. Rates of incision and widening peaked 8-9 hrs after opening coinciding with velocity reaching  $>2$  m/s (Figure 33; Figure 34). Peak velocity (3.47 m/s) occurred 16 hrs after opening coinciding with the channel reaching its maximum width (62.50 m). Peak discharge ( $367 \text{ m}^3/\text{s}^{-1}$ ) and area ( $137 \text{ m}^2$ ) were reached 17 hrs after opening as velocity started to decrease (Figure 33). At the time of the last measurement (11.47 am 18/08), channel width had stabilised with outflow velocity decreasing to 1 m/s and discharge to  $138 \text{ m}^3/\text{s}^{-1}$ . By this time, the water level had decreased by -0.54 m to +0.85 m AHD. The water level temporarily increased with the flood tide but then continued to drain to reach a minimum of +0.28 m AHD  $\sim 42$  hrs after opening (9 am 19/06). This represents a -1.10 m decrease since opening at an average drainage rate of 0.03 m/hr. After opening, the estuary remained open for 16 days until 03/07/19.

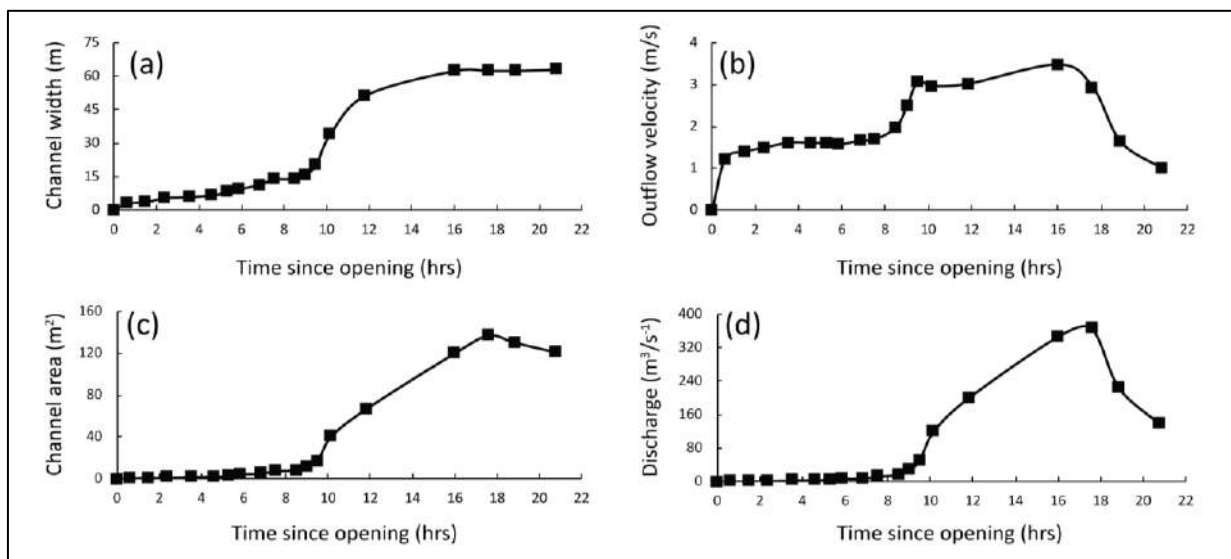


**Figure 33a-d.** Change in (a) channel width; (b) flow velocity; (c) cross-sectional area; and (d) discharge during artificial opening 2 of Curdies Inlet 17/06/2019 - 18/06/2019.





**Figure 34a-f.** Pictures from artificial opening 2 at Curdies Inlet. (a) 9 am 17/06/19 prior to opening; (b) 3 pm 17/06 excavation; (c) 5 pm 17/06 channel expansion; (d) 2.50 am 18/06 near peak outflow with standing waves (picture brightened); (e) 8 am 18/08 peak discharge; (f) 11 am 18/06 wave intrusion.

#### 6.1.7 Painkalac Creek: 08/08/19

**Painkalac Creek was successfully opened and opening achieved its purpose of draining the basin.**

Painkalac Creek was artificially opened at 9 am 08/08/19, one hour before low tide (0.70 m). The lagoon water level was +2.11 m AHD (Figure 35) and HG 0.045 m/m (1:22). The berm was 52 m long and +1.96 m AHD in elevation. Offshore  $H_s$  (2.44 m) was moderate. For 1 hr after opening, outflow velocity remained <2 m/s. 1.5 hrs after opening, velocity reached 2.34 m/s and the rates of channel incision and widening increased (Figure 36; Figure 37). A weir had also formed at the seaward edge of the lagoon (Figure 38a). The maximum outflow velocity (2.75 m/s) channel width (26 m), and discharge at the mouth ( $16.60 \text{ m}^3/\text{s}^{-1}$ ) were reached 3 hrs after opening (Figure 37). At this time, the basin water level was +1.79 m AHD, having decreased by -0.31 m since opening. 4 hrs after opening, outflow velocity had decreased to 1.86 m/s and discharge to  $10.53 \text{ m}^3/\text{s}^{-1}$  (Figure 36) with outflow gradually losing energy (Figure 39c). The channel had also stopped widening having reached an equilibrium width (Figure 37). 6 hrs after opening, the channel had incised to a bed elevation of +0.17 m AHD (Figure 36). Cross-sectional area ( $5.48 \text{ m}^2$ ), velocity (1.36 m/s), and discharge ( $7.43 \text{ m}^3/\text{s}^{-1}$ ) had decreased and ocean waves were observed to move up the channel (Figure 36; Figure 38d). By 3 pm, the estuary water level had decreased to +1.25 m AHD. This represents a decrease of -0.81 m over 6 hrs at an average drainage rate of -0.14 m/hr. The loggers had to be taken out at 3 pm 08/08/19, but it is expected that the basin would continue to slowly drain for another ~10 hrs as based on past openings. After opening, Painkalac Creek stayed open for 38 days until 15/09/19 (EstuaryWatch, 2019).

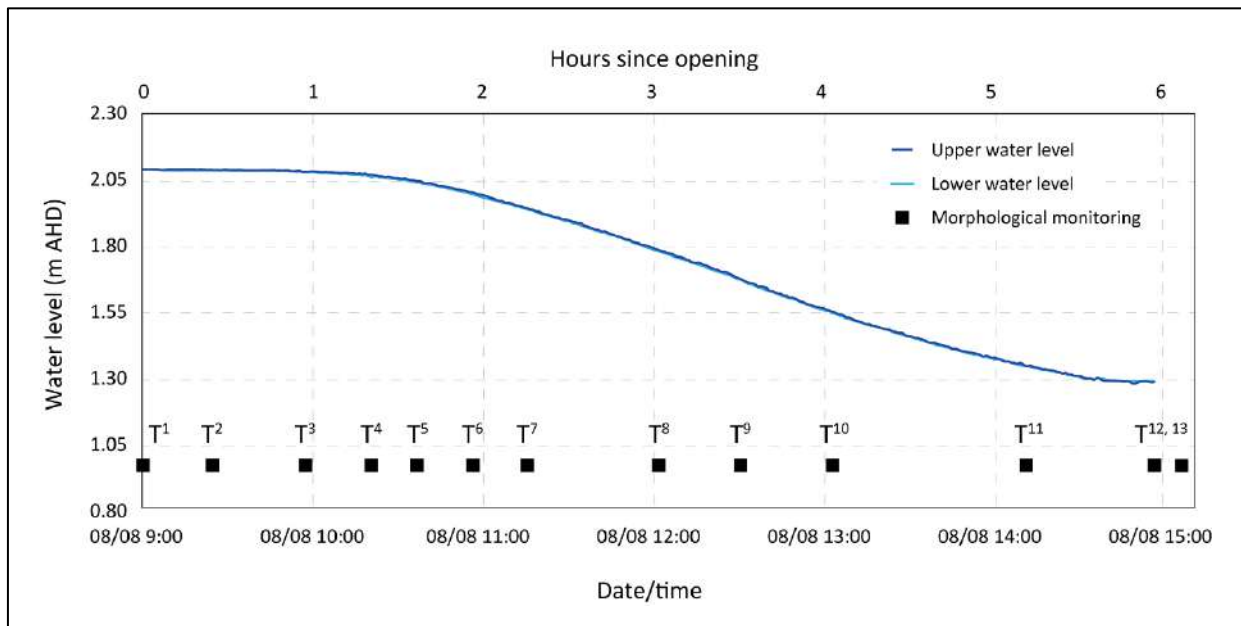


**Figure 35.** Painkalac Creek drainage curve from pressure sensors and timing of morphological monitoring.

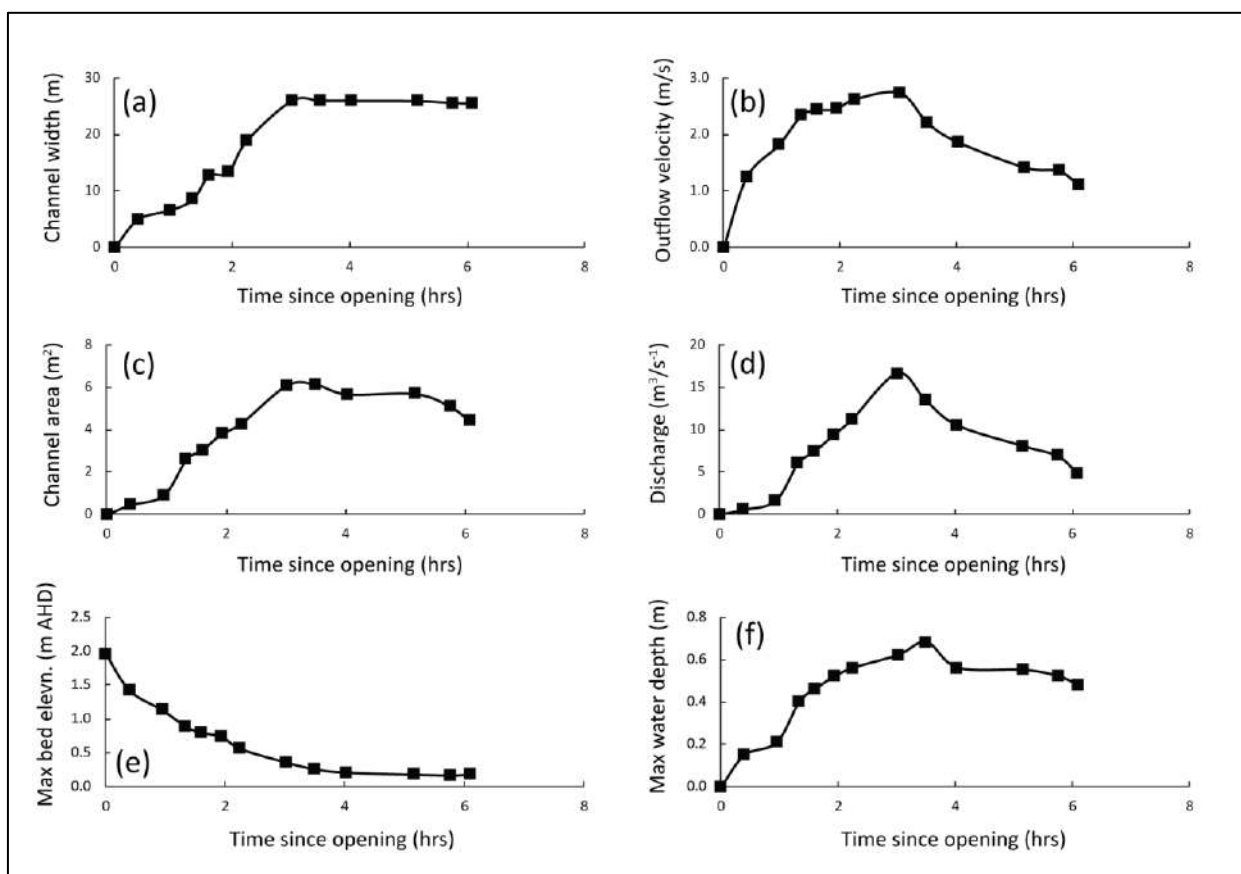


**Figure 36a-f.** Change in (a) channel width; (b) outflow velocity; (c) cross-sectional area; (d) discharge; (e) max bed elevation; (f) max water depth during Painkalac Creek artificial opening 08/08/2019.

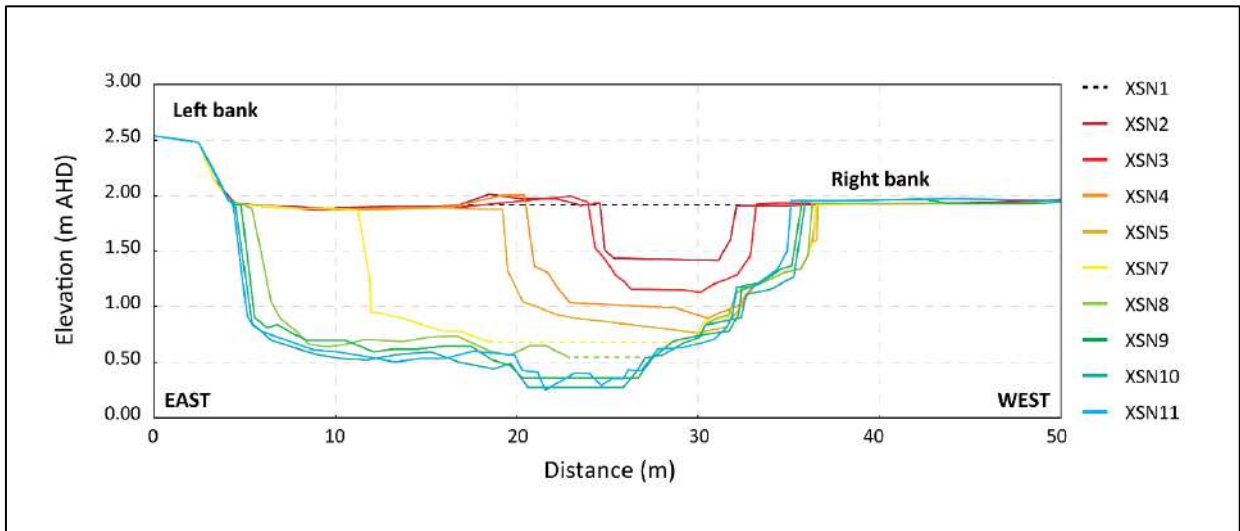


**Figure 37.** Select surveyed entrance channel cross-sections at the mouth at Painkalac Creek on 08/08/19.

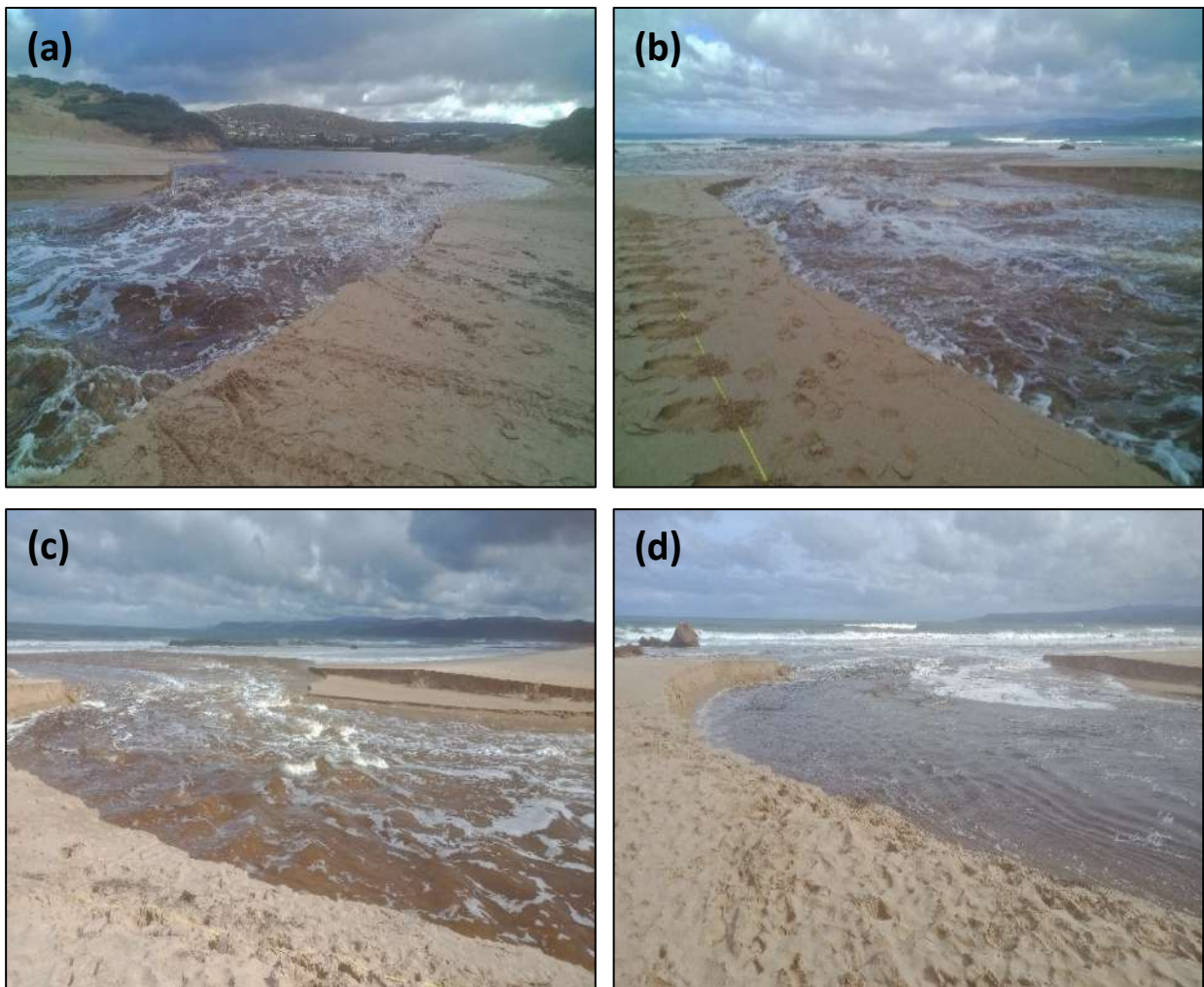


**Figure 38a-d.** (a-b) 1.5 hrs after opening weir forms at seaward edge of lagoon and peak outflow velocity with standing waves; (c) 4 hrs after opening max channel width; (d) wave intrusion 6 hrs after opening.



### 6.1.8 Anglesea River: 14/08/19

Anglesea River was successfully opened and the opening achieved its purpose of draining the basin.

Opening occurred at 11 am 14/08/19 on a falling high tide (1.50 m). The basin water level was +1.76 m AHD (Figure 40) and HG was 0.016 m/m (1:63). The berm was +2.25 m AHD in elevation, 76 m long, and offshore  $H_s$  was low (1.41 m). Geomorphic change was slow overall and the maximum velocity of 1.01 m/s occurred 3 hrs after opening (Figure 40; Figure 41; Figure 42). The maximum area (1.05 m<sup>2</sup>) and discharge (0.74 m<sup>3</sup>/s<sup>-1</sup>) were reached 7 hrs after opening despite velocity decreasing to 0.71 m/s (Figure 41). At this time, the water level had only decreased by 0.05 m to +1.71 m AHD. 11.2 hrs after opening, the channel had continued to widen and incise but velocity (0.62 m/s), area (0.68 m<sup>2</sup>), and discharge (0.42 m<sup>3</sup>/s<sup>-1</sup>) had decreased. At the mouth, the thalweg had started to meander indicating a loss of energy (Figure 42). 24 hrs after opening (11am 15/08), the channel had stopped widening and the bed had aggraded by +0.08 m to +0.51 m AHD. Velocity had decreased to 0.53 m/s and discharge to 0.13 m<sup>3</sup>/s<sup>-1</sup> with the channel water depth being only 0.11 m. At this time, the water level had decreased by -0.43 m to +1.33 m AHD at an average drainage rate of -0.02 m/hr. The estuary continued to drain slowly reaching a minimum level of +1.29 m AHD at 6 pm 18/08. Anglesea remained open for 7 days until 21/08/19.

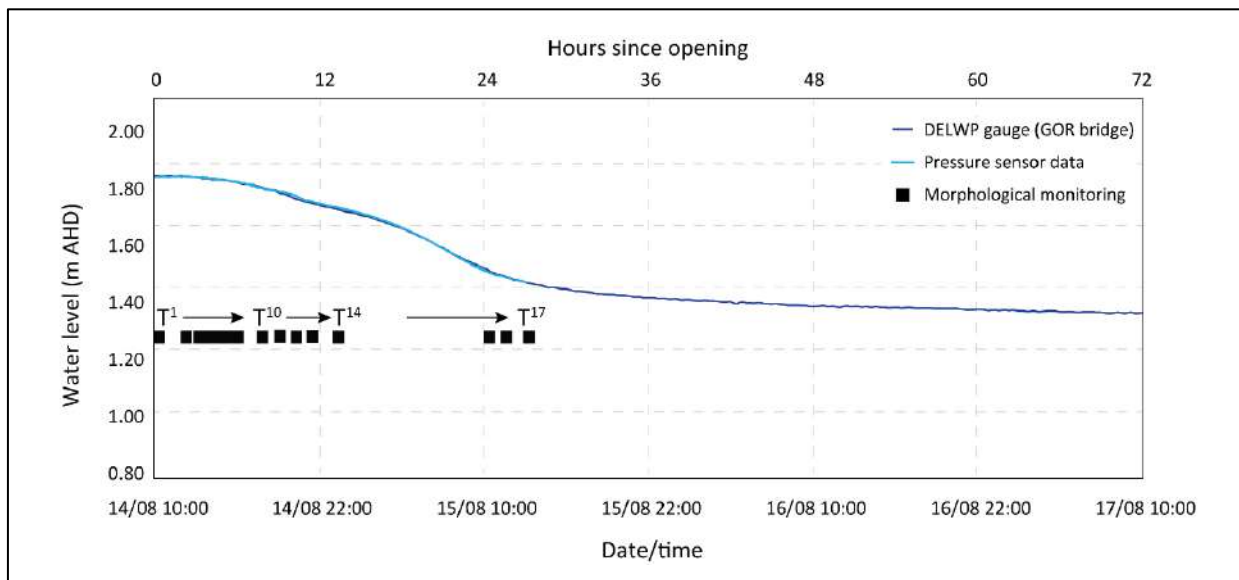


Figure 39 Anglesea drainage curve from pressure sensors + gauge and timing of morphological monitoring.

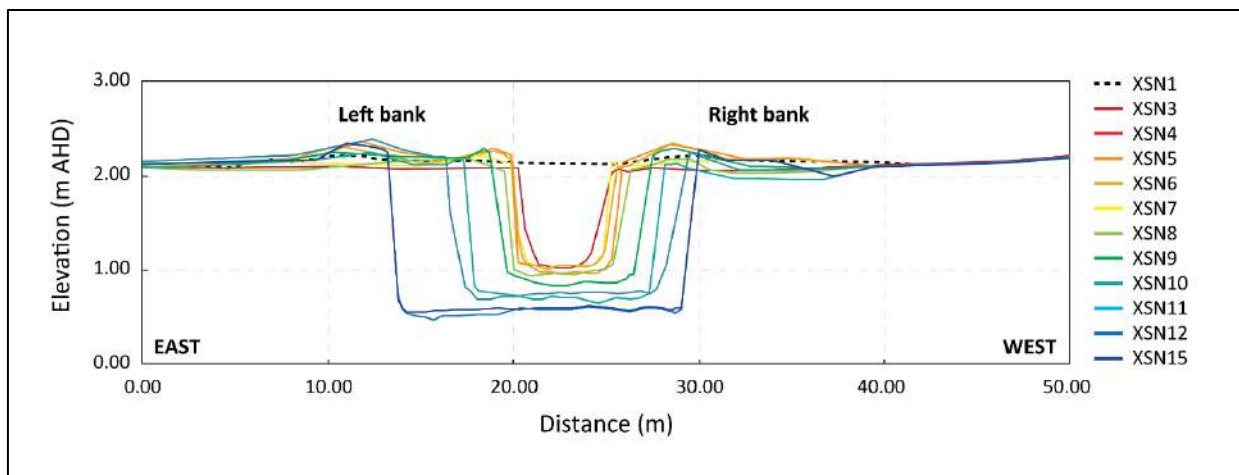
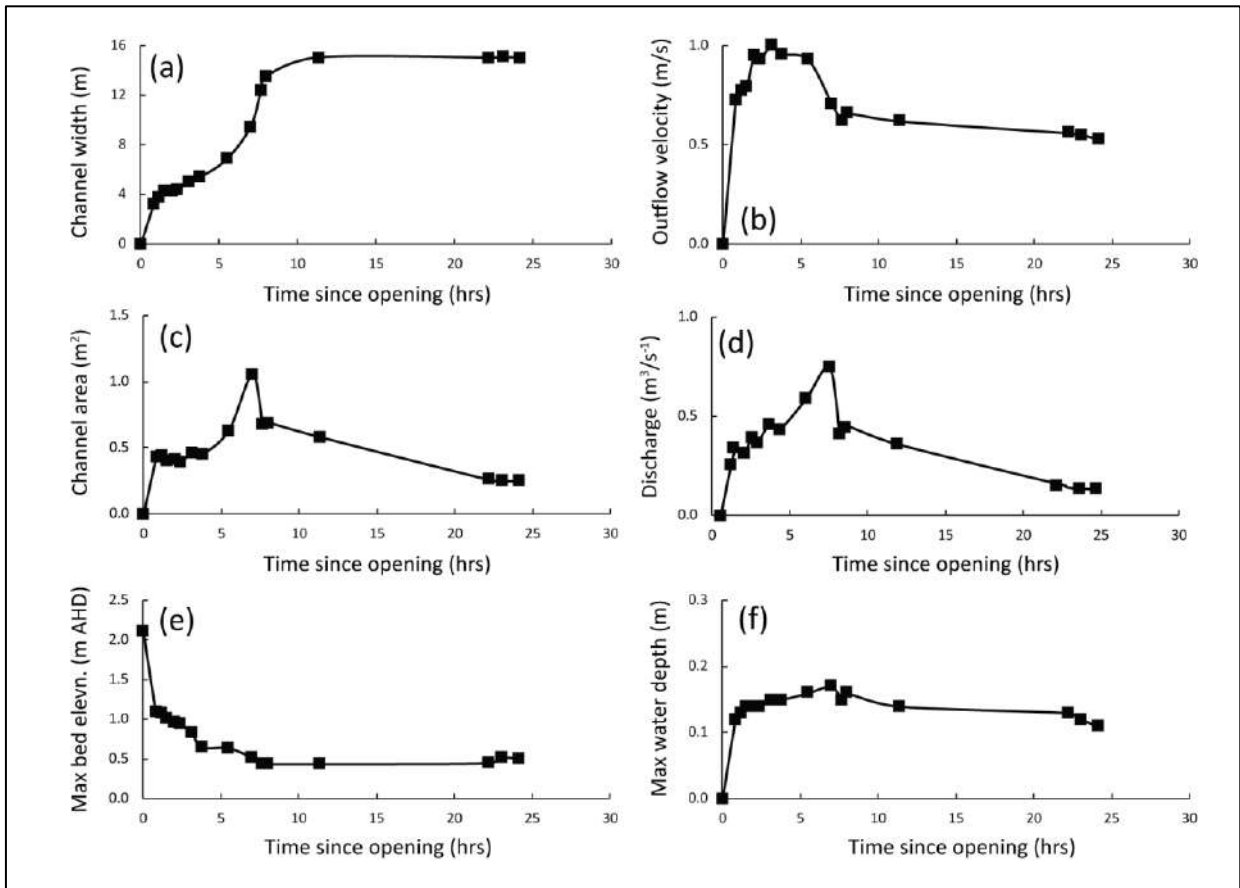
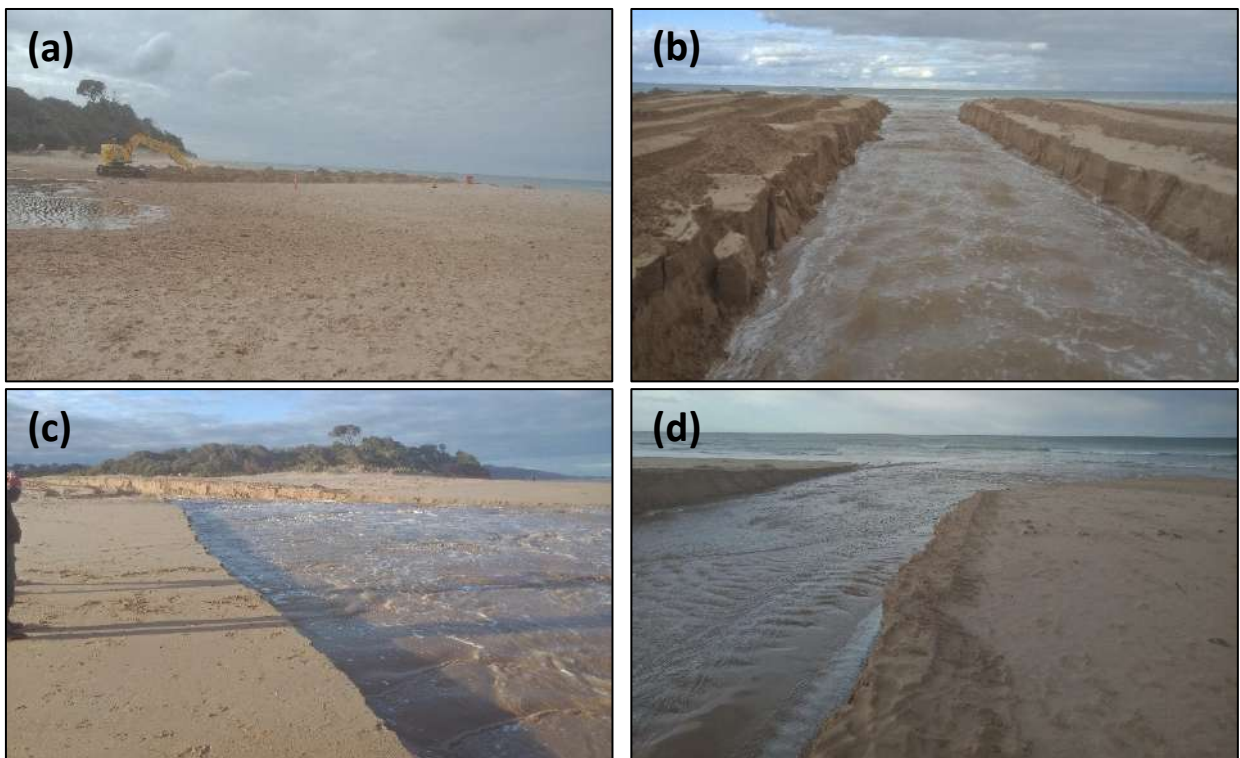


Figure 40. Select surveyed entrance cross-sections at Anglesea River mouth on 14/08/19 - 15/08/19.



**Figure 41a-f.** Change in (a) channel width; (b) outflow velocity; (c) cross-sectional area; (d) discharge; (e) max bed elevation; (f) max water depth during Anglesea artificial opening 14/08/2019 - 15/08/2019.



**Figure 42a-d.** (a) Anglesea artificial opening 10 am 14/08/19; (b) looking seaward during peak outflow velocity 1.30 pm 14/08/19; (c) channel at the mouth 4 pm 14/08; (d) shallow at mouth 10 am 15/08.



### 6.3 Timescales of geomorphic change during artificial openings

Field data was scaled and analysed to create a conceptual model to illustrate the timing of geomorphic change at the mouth vs basin drainage (Figure 43a-b). This allows us to understand the key parameters influencing the breach characteristics, the time taken for the channel to reach peak dimensions and discharge, and how these changes impact on basin drainage. From the field data, the main findings are:

- Temporal asymmetry exists in the rates of change in outflow velocity, cross-sectional area, and discharge during opening. These parameters increase rapidly on the rising limb of the hydrograph with a gradual decline after their peak value is reached. Changes in water level lag geomorphic change at the mouth.
- The maximum outflow velocity and channel width are reached before the maximum cross-sectional area and discharge. Peak discharge occurs only once the channel has reached a final equilibrium width.
- Peak outflow velocity is typically reached first. This occurs at 20-25 % of the total drainage time and when the basin water level is still within 20 % ( $\pm 5$  %) of its initial value. Velocity reaches its maximum value early on as available hydraulic head is greatest as water levels have not yet decreased substantially.
- The maximum channel width is reached at approximately the same time as velocity. In the field, the peak channel width was visually observed to occur just after peak velocity was reached but measurements were too infrequent to quantify this. Thus, the maximum channel width is likely reached at  $\sim 25$  % of the total drainage time, when the water level is still within 20-25 % ( $\pm 10$  %) of its initial value.
- The maximum cross-sectional area and discharge occur at similar times. Both peak at 25-40 % of the total drainage time and when the water level is still within 30-40 % ( $\pm 10$  %) of its initial value. Discharge decreases rapidly after the maximum value is reached. After this, basin drainage rates start to decrease.

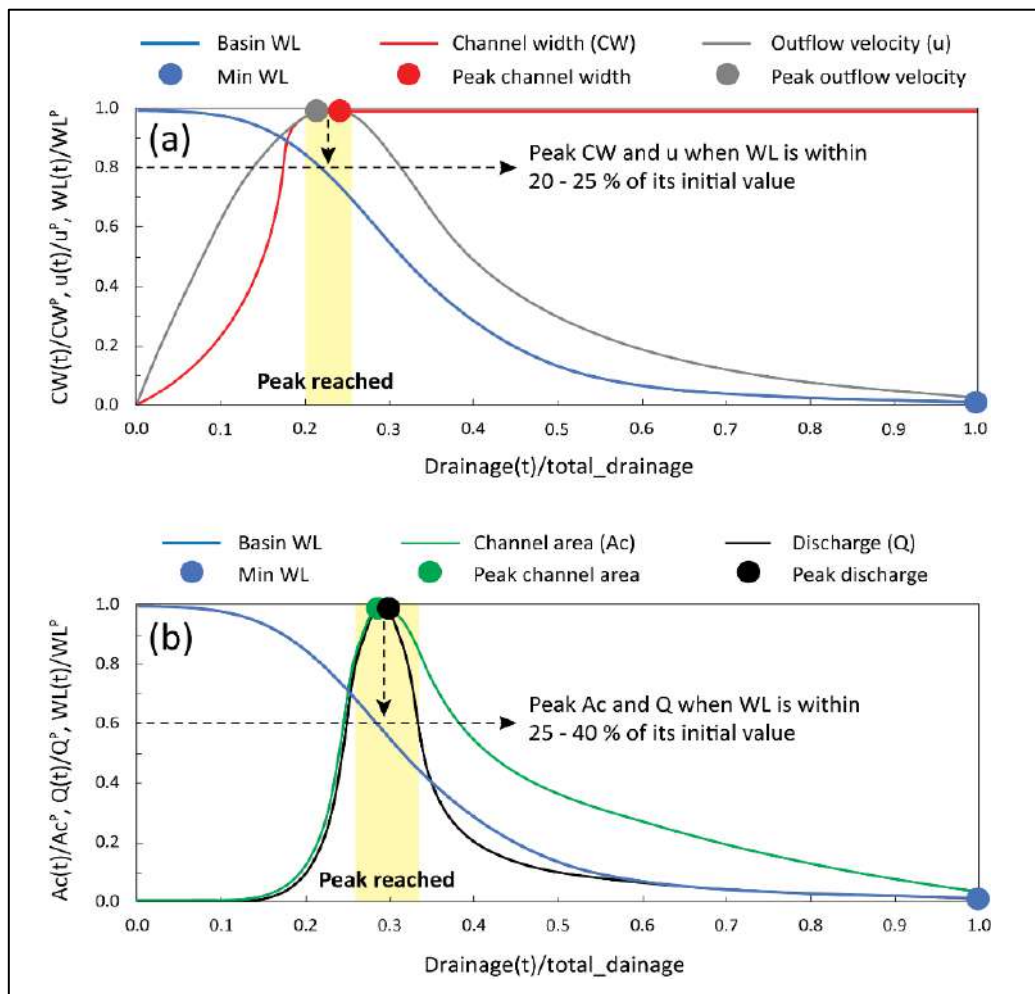


**Figure 43a-b.** Conceptual diagram showing (a) change in channel width and velocity vs water level, and (b) change in cross-sectional area and discharge vs water level.  $x(t) = x$  at that time;  $x^p$  is the peak value.

Figure 44a-h shows examples of the scaled field data used to create the conceptual model in Figure 43a-b. Data on the y-axis is scaled by the maximum value of that parameter during opening. The x-axis is the proportion of the total drainage time. This illustrates that these relationships scale well for artificial openings occurring at different sites with different basin volumes and morphologies. Here the maximum velocity and channel width are consistently reached before the maximum channel cross-sectional area and discharge across all openings. Peak discharge occurred once velocity had started to decrease (but was still within 10 % of its maximum value) due to the larger cross-sectional area at that time. These results agree with previous flume studies of Stretch and Parkinson(2006); Parkinson and Stretch (2007).

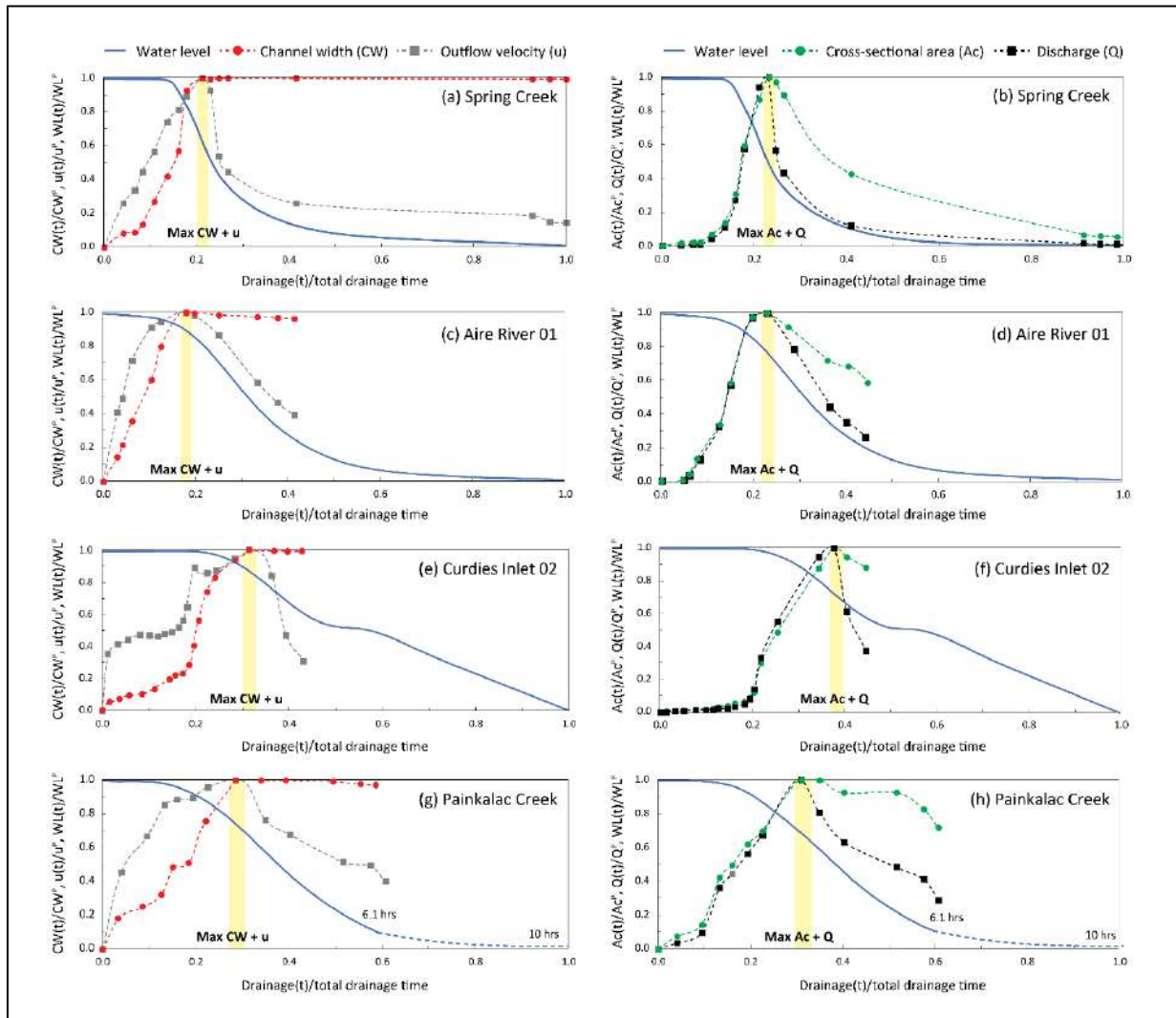


**Figure 44a-h.** Change in channel width (CW), outflow velocity (u), cross-sectional area (Ac), discharge (Q), and basin water level (WL) during select artificial openings including (a-b) Spring Creek; (c-d) Aire River 01; (e-f) Curdies Inlet 02; and (g-h) Painkalac Creek. Here CW, u, Ac, Q, and WL are scaled by their maximum value reached during the opening (y-axis) and the drainage time is scaled by the total duration of drainage (i.e. for the basin to cease decreasing in water level). Yellow bars indicate when the maximum value is reached. For Painkalac Creek, the drainage time was extended to 10 hrs based on prior openings.

#### 6.4 Thresholds for successful openings

The hydraulic gradient (HG) is a main factor controlling whether an artificial opening will be successful or not. The hydraulic gradient is calculated as the elevation (i.e. head) difference (in m) between the estuary water level and the ocean tidal elevation (both to AHD) divided by the berm length. Using just the elevation or head difference between the estuary and the ocean does not account for the distance water

has to travel from the estuary to the ocean. A higher HG equates to a steeper grade and energy slope between the estuary and the ocean (e.g. HG 0.05 m/m = 1:20 - a steeper grade vs HG 0.02 m/m = 1:50 - a less steep grade). HG values were calculated for 60 historic openings and an additional 5 EGCMA sites giving a dataset of n = 65 (Figure 45a-d).

- **Successful openings** had HG values of 0.016 (grade 1:68) to 0.126 (grade 1:8).
- **Unsuccessful openings** had HG values of 0.010 (grade 1:97) to 0.018 (grade 1:55).
- **Openings tend to be successful when the HG is >0.019.** This equates to a grade steeper than 1:53.
- **Openings tend to be unsuccessful when HG is <0.015.** This equates to grades more gradual than 1:67.
- **When the HG is between 0.015-0.019 (grade of 1:53-1:67), there is a risk of the opening not being successful.** The mixed success within this range of HG values likely depends on other factors such as the offshore wave height, excavation style, and the offshore tidal stage.

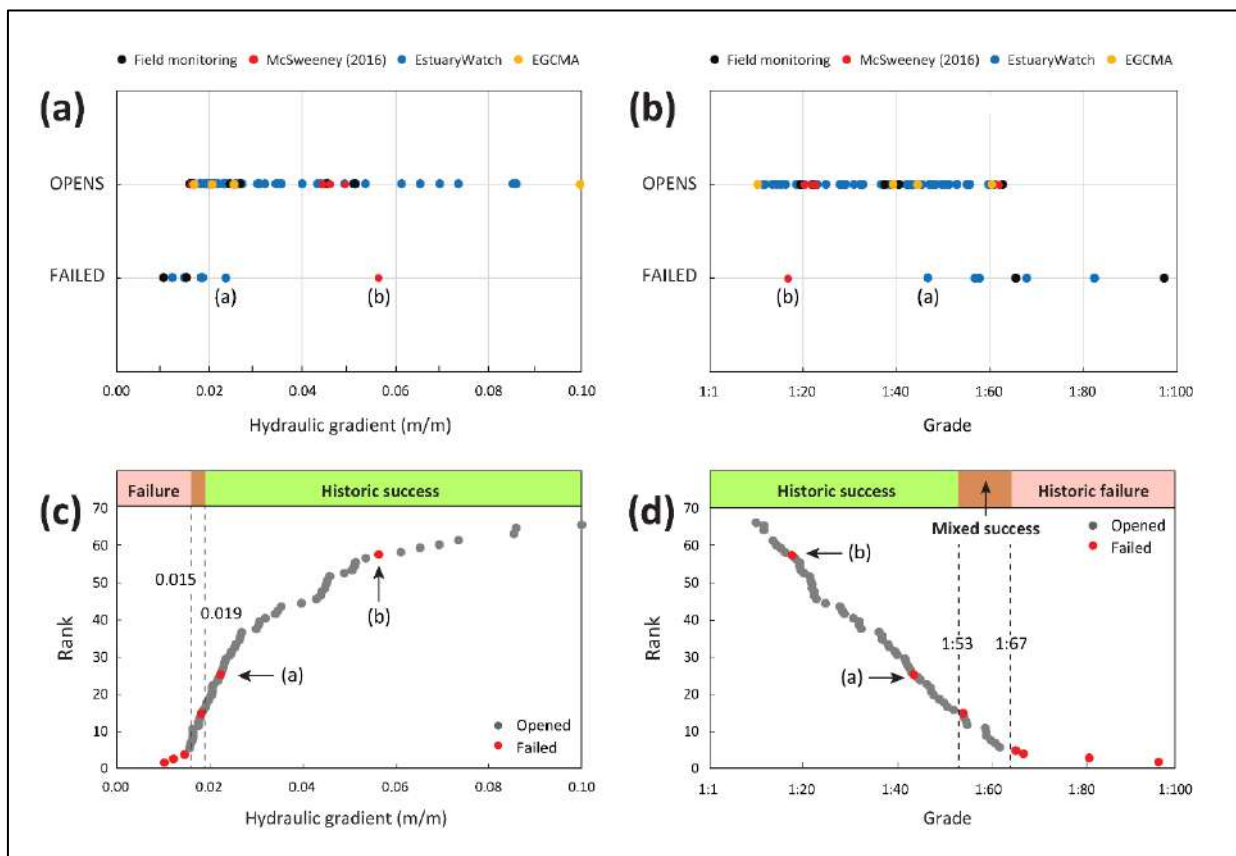


**Figure 45a-d.** (a) Hydraulic gradient and (b) grade for 60 estuary openings and 5x known gradients for successful openings at EGCMA estuaries. Openings that were successful are plotted as ‘opens’ and openings that were unsuccessful are plotted as ‘failed’. The dots marked (a) and (b) are openings which failed due to swell size ( $H_s > 4.5$  m) and not due to a low HG; (c) HG and (d) grade of all openings by rank.

Two openings in the dataset failed due to swell size (labelled a and b on Figure 46). These were at the Gellibrand River on 11/05/16 where  $H_s$  was 5.30 m and at the Aire River (01/05/2014) where offshore  $H_s$  was 4.80 m (Figure 46a-b). At the Aire River, the HG was very high at 0.056 (grade of 1:18) due to a high water level (+1.98 m AHD) and relatively short berm (40 m in length). At the Gellibrand, the HG was 0.023 (grade of 1:44) again due to a high water level (+1.78 m AHD) and short berm (56 m). For both openings, swells were extremely high and waves travelled up the excavated channel to deposit sediment at a rate faster than any outflow could remove it. This indicates that under extremely high waves, marine deposition can counter outflow regardless of a high HG. Both openings were reattempted in the following days with success once the swell size had decreased. No other openings were attempted with  $H_s > 4.2$  m.

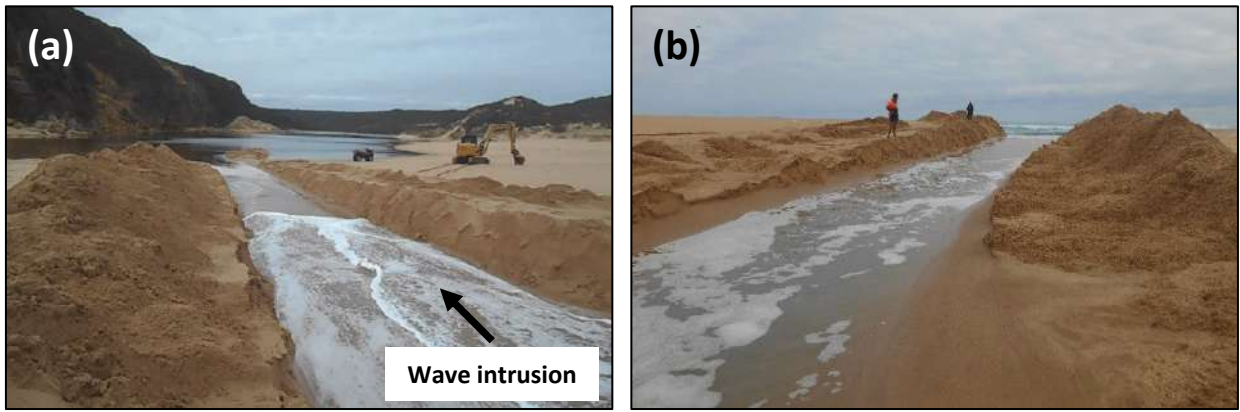


**Figure 46a-b.** Artificial opening of Aire River 01/05/14 that failed due to swell size despite a high HG. (a) waves moving up the channel despite a relatively high estuary water level and short berm; (b) looking seaward showing accretion at the berm position approximately 1 hour after excavation.

For estuaries that had data for >5 openings, the specific thresholds for opening success are listed in Table 4. These thresholds however would shift depending on the berm length (berm\_L). If this was to increase in length, a higher amount of head would be required to ensure a successful opening. Figure 47 shows the berm length vs hydraulic head (water level in estuary - tidal elevation) that openings are likely to be successful or unsuccessful based on all historic data. This illustrates that the minimum head needed to ensure a successful opening varies substantially under different berm lengths.

**Table 4.** Min and mean HG for a successful opening for estuaries that had >5 openings recorded.

Estuary	Min HG (m/m)	Min grade	Equivalent head (m)	Mean HG (m/m)	Mean grade	Equivalent head (m)
Gellibrand	0.016	1:61	1.22	0.035	1:35	1.22
Aire River	0.027	1:37	1.87	0.039	1:27	1.95
Curdies Inlet	0.025	1:41	1.18	0.032	1:34	1.83
Spring Creek	0.027	1:37	2.45	0.046	1:24	1.84
Wreck Creek	0.017	1:60	1.71	0.025	1:42	1.74

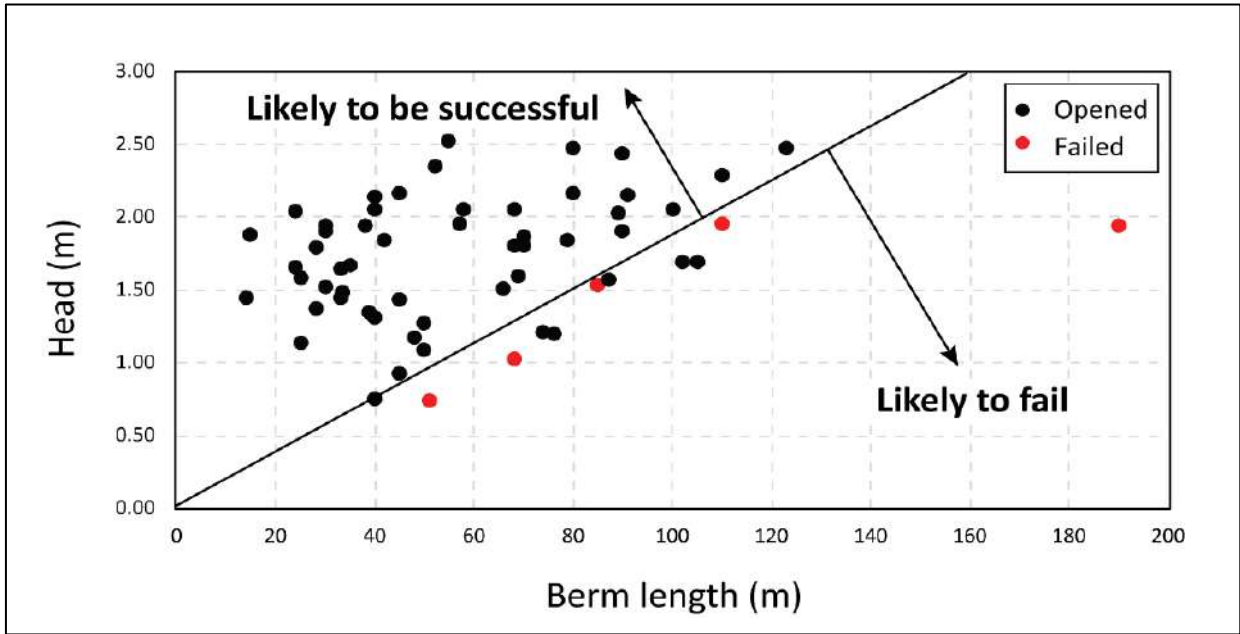


**Figure 47.** Berm length vs hydraulic head that openings are likely to be successful vs unsuccessful (n 60).



## 6.5 Predicting estuary drainage rates

Estuary drainage rates are assessed as an overall value (i.e. averaged during the whole drainage period) and during Stages 2 (Figure 5) as Stage 2 is when drainage rates are highest. Figure 48a-d shows that the main control on the both the overall and Stage 2 drainage rate is the HG at the time of opening (Figure 48a-b). The HG also controls the duration of the overall and Stage 2 drainage period (Figure 48c-d). Drainage rates and durations did not correlate well with the maximum channel dimensions, outflow velocity, or discharge during the opening. As the HG value adjusts during opening, rates of channel expansion are initially high but then reach an equilibrium value along with discharge. Drainage rates are also initially high during the first 20-40 % of the total drainage time and then decrease accordingly as the water level and head fall and discharge decreases. By this time, the channel has already reached its maximum dimensions (Figure 43a-b). This indicates that the drainage rate and duration is solely a function of the HG at the time of opening. The duration of Stage 1 (Figure 5) and the max outflow velocity reached during an opening also correlate strongly with the HG at the time of opening (Figure 48e-f). Once the estuary enters Stage 2, natural sediment transport processes have reached a physical threshold where the channel will continue to widen and incise. This point is where a rapid decrease in water level will occur. If slowing estuary drainage is a goal to reduce the risk of fish deaths, extending the duration of Stage 1 would effectively “drag out” the period of slower drainage. As, the HG also controls the max outflow velocity and Stage 1 duration (Figure 48e-f), the focus should shift to investigating strategies which may be able to sustain outflow velocities at a low value for longer to achieve slower drainage rates.

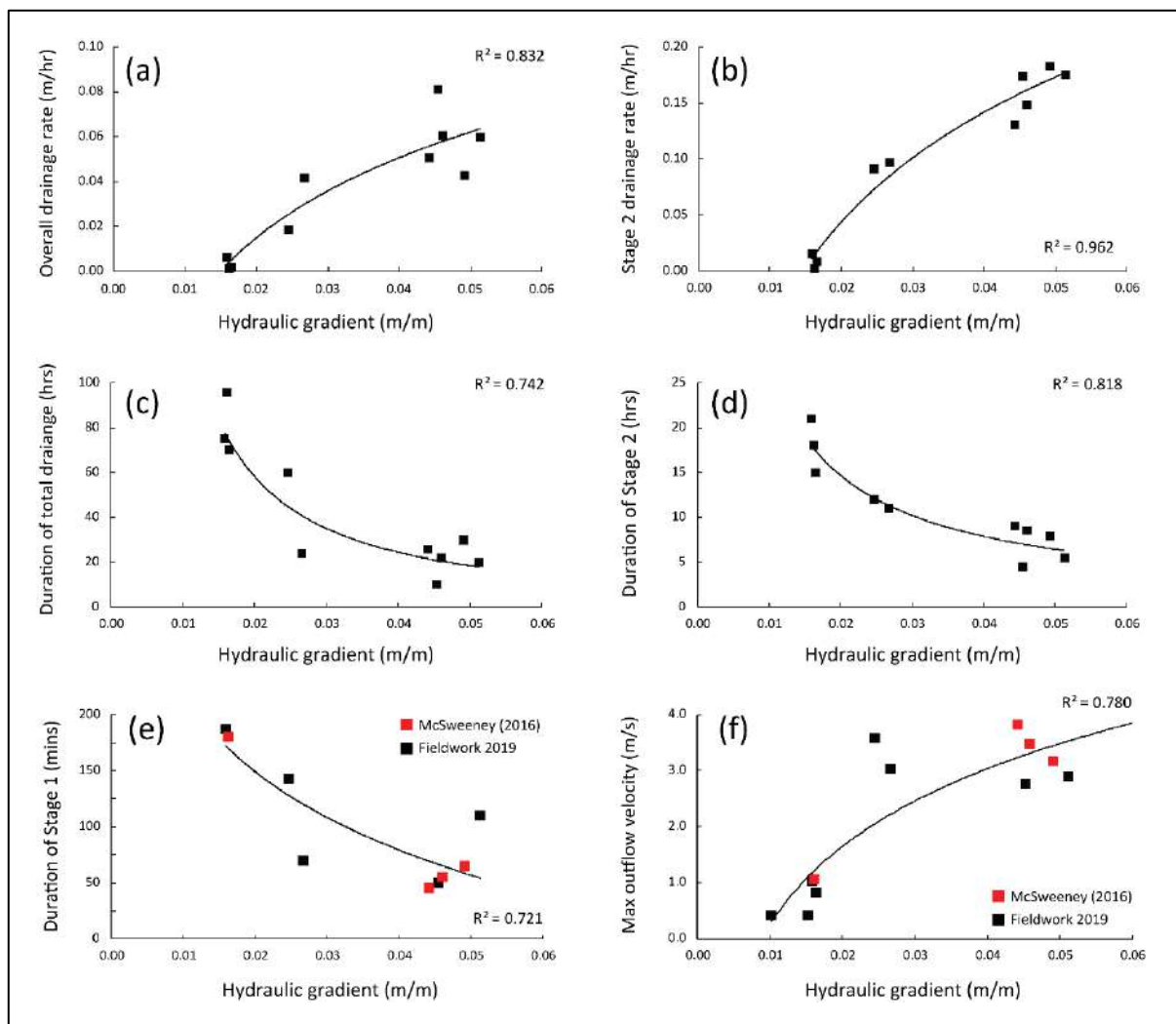


**Figure 48a-f.** Correlation between HG at time of opening and (a) overall drainage rate and (b) Stage 2 drainage rate; (c) overall drainage duration and (d) Stage 2 duration; (e) Stage 1 duration; (f) max velocity.



## 6.6 Physiochemical change during artificial openings

As physiochemical monitoring was a secondary focus of this study, a summary of physiochemical changes from during four artificial openings in 2019 and from historic data is presented in Appendix 4. No fish deaths occurred during the event-scale monitoring during fieldwork and the data provides information on conditions where fish deaths were avoided. Work to analyse drivers of change in physiochemistry is ongoing.

## 7.0 Discussion

### 7.1 Geomorphic controls on the success of artificial openings

Ensuring an estuary opening is successful is important as this means that openings do not need to be reimplemented. A “successful opening” is one where the estuary enters a period of rapid incision and widening then stays open after excavation. **Geomorphically, the hydraulic gradient (HG) at the time of opening is the main determinant of whether an estuary opening will be successful or not.** The HG is calculated as the total elevation head between the estuary water level (to m AHD) and the nearshore sea level (to m AHD) (best obtained by the tidal elevation at the time of opening) divided by the berm length. This represents the energy slope between the estuary and the ocean. The HG controls the maximum outflow velocity that water in the channel will attain where a higher HG equates to higher velocities and thus more energy to erode sediment offshore.

The geomorphic sequence occurring during an opening is summarised in Table 5. To achieve a successful opening, the estuary needs to transition into Stage 2 (Figure 49). This requires outflow to reach a critical velocity that will maintain offshore erosion. During Stage 1, a series of knickpoints migrate up the channel. Once these reach the upstream crest of the berm, the channel rapidly widens and incises, and the estuary enters Stage 2 of the opening sequence (Figure 49). From here on, the sequence of opening cannot be reversed as discharge through the mouth increases exponentially. This in turn causes the rates of estuary drainage to increase as a larger volume of water is exiting the basin. After discharge peaks, the estuary enters Stage 3 (Figure 49). Field observations show the estuary typically reaches maximum cross-sectional area and discharge (representing the end of Stage 2) at 30-40 % of the total drainage time.

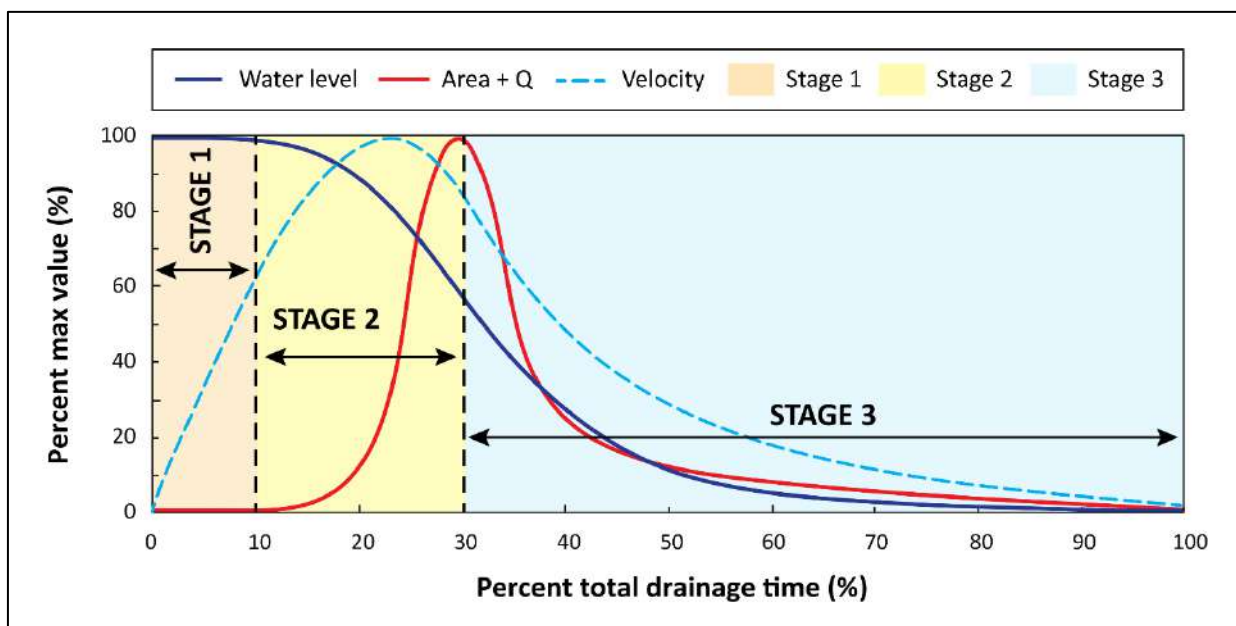


**Figure 49.** Sequence and stages of geomorphic change during an opening where Q is discharge. The Stages are as per the descriptions in Section 4.3 and the summary of Table 5 (next page). Stage durations

and geomorphic change are revised from the existing hypothesis (Figure 8) as based on the field observations for all openings monitored during this project.

**Table 5.** Summary of observed geomorphic stages during an artificial opening where WL is water level.

Stage	Stage description
1 (pilot channel)	WL high, drainage lags channel expansion, small channel, low velocity, HG controls rates of change.
2 (rapid expansion)	WL starts decreasing, channel area and discharge increase exponentially and then reach a maximum.
3 (river flow)	Area, velocity, and discharge decrease as HG adjusts to a falling water level, drainage rates decrease.

From a sample of 60 historic openings combined with the HG values at which five EGCMA estuaries are successfully opened, the minimum HG value to achieve a successful opening was obtained. Figure 50a-b shows the data plotted as the distribution of HG and grade values for all openings that have been successful and unsuccessful. The orange area of overlap shows a zone of risk where openings have historically gone either way. The mixed success within this range of HG values occurs as the HG is close to the threshold of not opening and likely depends on other factors such as the offshore wave height, excavation style, and the offshore tidal stage. Omitted from the dataset are two openings which failed due to swell size as failure was not a function of the HG or grade.

- **Successful openings** had HG values of 0.016 m/m (grade 1:68) and above.
- **Unsuccessful openings** had HG values of 0.018 m/m (grade 1:55) and below.
- **There is a risk of an opening being unsuccessful** when the HG is 0.015-0.019 m/m (grade of 1:53-1:67).

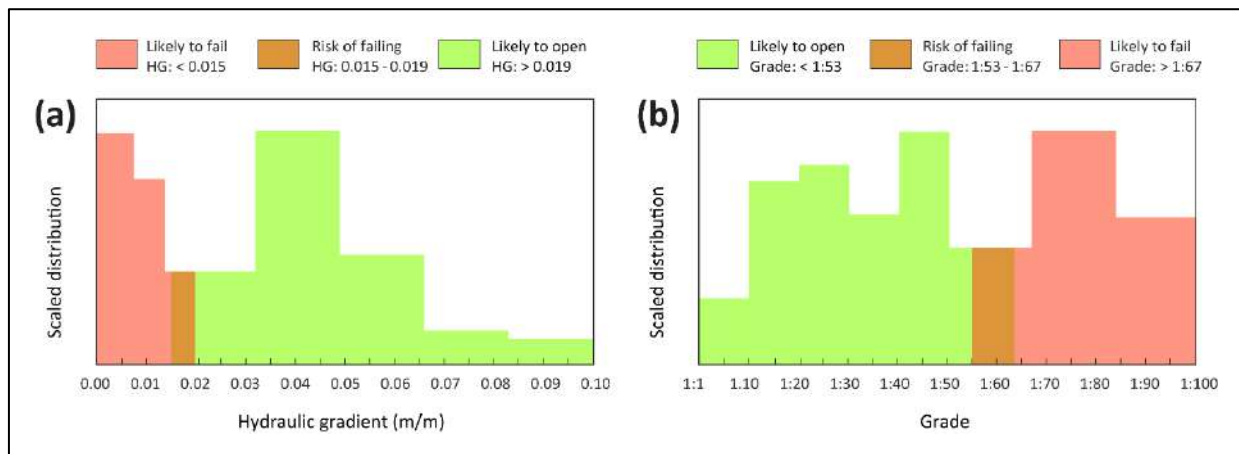


**Figure 50a-b.** (a) Hydraulic gradient and (b) grade at which estuary openings are likely to fail, are at risk of failing, and are likely to be successful as based on distributions from historic data (n = 63).

**The offshore wave height at the time of opening is also important.** When offshore wave heights are high, openings tend to be unsuccessful. This can even occur when the HG is above the minimum threshold for normal opening success (HG = >0.019 m/m). From the available data, when  $H_s$  is >4.20 m, openings tend to be unsuccessful despite a high HG. This is because onshore sediment transport via waves overwhelms outflow and rapidly infills the channel.

It is also important to note that if the purpose of an opening is simply to open the estuary successful to ensure basin drainage, considering the HG and offshore wave height is critical. If there is a concern about rapid drainage and/or fish deaths, then a method should be considered that will slow estuary outflow and 'drag out' the duration of Stage 1 (Figure 49). As the HG controls the max outflow velocity, opening with a high HG is likely to result in rapid channel expansion and thus drainage. Possible methods to achieve this will be discussed in Section 7.4.

## 7.2 Recommendations for ensuring a successful opening

The following recommendations are provided to maximise the success of artificial openings as based on the results of this study:

- To ensure an opening is successful, the HG at the time of opening should be  $>0.019$  m/m. This equates to a grade steeper than 1:53. Effectively this means openings should occur when the berm length is short and the head difference between the estuary and the ocean is high.
- The need for a successful opening must be carefully balanced with other concerns (i.e. fish deaths). For example, if draining the basin and maintaining a connection to the ocean after excavation is the sole aim of the opening, considering the HG and offshore swell conditions is sufficient. If a prolonged opening is a goal, the geomorphic conditions following lagoon drainage should be also considered.
- The HG can be easily calculated by estuary managers. This requires the following data:
  - (1) The estuary water level at the time of a proposed opening (in m AHD) (from a gauge);
  - (2) The nearshore sea level at the time of opening. This can be calculated by obtaining the offshore tidal elevation at the time of a proposed opening. This must then be converted from chart datum to m AHD (using the Victorian Tidal Planes regional tidal gauge conversion values).
  - (3) The berm length (i.e. distance from the nearshore water level to the seaward edge of the lagoon). This can be measured with a measuring wheel or approximated using m long steps.
- Opening with a HG of 0.015-0.019 m/m (grade of 1:53-1:67) delivers mixed success. If opening at this HG range is unavoidable (e.g. due to an emergency flooding situation), the opening should occur at a time during the day when offshore  $H_s$  is at a minimum and when the head difference between the estuary and nearshore sea level (i.e. as a function of the tidal elevation) is at a maximum. This requires checking offshore wave forecasts or tidal charts to time the opening to occur during these conditions.
- An opening should always occur when offshore  $H_s$  is low. The precise  $H_s$  thresholds where onshore deposition will overwhelm outflow vary between sites and openings. From the field data, openings were unsuccessful when  $H_s$  was  $>4.20$  m despite the HG being in the optimum range. The offshore wave height should be considered before implementing an opening. Recording offshore wave heights during openings (e.g. via EEMSS) would provide a record that could be used to determine thresholds for successful openings at individual sites relative to the HG at opening as more data is acquired.
- Recording the berm length and tidal elevation at the time of opening as part of the EEMSS process would mean that the HG dataset can be extended in future. This means that given sufficient data, HG thresholds for opening success can be calculated for individual sites. Physically these should not vary unless the berm grain size or local entrance morphology is vastly different (e.g. rocks at the entrance may impact on site specific HG values to achieve a successful opening). However, this has not yet been proving with real world data. This means that HG values would be more accurate instead of using the 0.019 m/m value which is currently calculated for all IOCE. An example of the variability in minimum HG values between sites is shown in Table 4.

**In light of these recommendations, a simple method of calculating HG and recording information that can be used in future is attached to this report as an Excel spreadsheet and summarised in Figure 51.** This sheet is modelled after EGCMA (2014: pp. 99) where HG and grade values for successful openings are known for five estuaries. The spreadsheet could be duplicated for different estuaries once sufficient HG data is collected as it is currently based on HG values for all IOCE in this study combined (i.e. min of 0.019 m/m for a successful opening). It is anticipated to be used alongside EEMSS as a method of assessing the success of openings and storing data (i.e. HG, head, and wave height) for future analysis.

Estuary name:	Curdies Inlet		
Tide height (m chart datum):	0.50		
Time/date of opening:	1/01/2020 11:30		
Datum to AHD:	0.597		
Tide height (converted to m AHD):	-0.097		
Estuary water level (m AHD):	1.65		
Berm length (m):	60		
Head (m):	1.75		
Hydraulic gradient:	0.029		
Grade:	1: 34.34		
Colour:	HG (m/m):	Grade:	Description
	> 0.025	> 1:40	Excellent - very high likelihood of successful opening
	> 0.019 - 0.025	> 1:40 - 1:53	Good - likely to be successful
	0.019 - 0.016	1: 53 - 1:67	Poor - risk of failure
	< 0.016	< 1:67	Bad - likely to fail
Offshore H <sub>s</sub> (m):	1.55		

**Figure 51.** Example recording sheet that could be used to calculate HG/grade at the time of opening and assess the risk of an opening being unsuccessful. HG values and their description relative to opening success are based on the results of this study.

**These parameters would need to be input into the spreadsheet by managers prior to an opening:**

- Estuary water level (to AHD) - simply measured from gauge boards or telemetry referenced to AHD;
- Tidal elevation at the time of opening (to chart datum) - this would be the tide height at the anticipated time of the opening occurring. Can be extracted from tide charts or a weather app. To chart datum is the number as you would read off a tide chart or weather app (e.g. 0.60 m);
- Berm length (in m) - this would be the length of the berm from the seaward edge of the lagoon to the ocean. This could be measured on the ground or even approximated by 1 m paces;
- Date/time of opening (for future record);
- Offshore H<sub>s</sub> (from a weather app or forecast).

**The spreadsheet then automatically:**

- (1) Converts chart tidal elevation to AHD using the local conversion value from the Victorian Tidal Planes;
- (2) Calculates the hydraulic head;
- (3) Calculates the HG and grade; and
- (4) Uses conditional formatting to colour code the risk of an opening being successful/unsuccessful.

### 7.3 Controls on basin drainage rates

The results of this study indicate that the HG at the time of opening is the main control on the both the rate and total duration of estuary basin drainage (Figure 48a-d). The HG at opening controls the maximum outflow velocity during an opening (Figure 48f) which then dictates how quickly the channel reaches peak dimensions and discharge. Peak outflow velocity is typically reached at 20-25 % of the total drainage time and discharge and cross-sectional area reach a maximum at 30-40 % of the total drainage time.

It is useful to think of these changes in relation to the sequence of geomorphic change during opening (Figure 49). The duration and rates of change during Stage 1 are a function of the initial HG (Figure 48e). A higher HG means the estuary will transition through Stage 1 quicker and reach peak velocity faster.

Once the estuary enters Stage 2, discharge and cross-sectional area increase exponentially and a physical threshold has been reached where drainage rates (as a result of increasing discharge) cannot be slowed. Drainage rates during Stage 2 remain a function of the HG at the time of opening. At the start of Stage 2, the water level has typically not decreased beyond 20 % of its initial value. Additionally, the bed has been lowered by erosion maintaining high head relative to the estuary. Once the channel reaches peak discharge and cross-sectional area, drainage rates start to decrease, and the estuary enters Stage 3. This represents the falling limb of the discharge hydrograph. The duration of Stage 3 is controlled by the volume of water remaining within the basin and the rate of discharge (a function of outflow velocity and area at the mouth). Upon entering Stage 3, the estuary has already drained by 50-60 % and the period of rapid drainage is over. This means that any intervention to decrease drainage rates to avoid fish strandings must occur before the estuary transitions into Stage 2 and well before peak outflow velocity is reached.

In summary, the HG is the primary control on drainage rates, and little can be done to slow estuary drainage aside from opening at a lower HG. The HG controls the rates of drainage during Stages 1 and 2 regardless of the volume of water in the basin. The volume of water within the basin may affect the duration of Stage 3, but by this time, the water level is already lowered by 50-60 % and drainage rates are decreasing rapidly on the falling limb of the hydrograph. Slowing the basin drainage rate can essentially only occur during Stage 1. As once the estuary enters Stage 2, physical processes take over and are effectively irreversible. The findings of this study indicate that basin drainage rates are a function of physical processes and therefore no easy way exists to decrease drainage rates.

#### **7.4 Can we slow estuary drainage rates to avoid fish strandings?**

The HG at the time of opening controls the basin drainage rate, maximum outflow velocity, and the duration of Stages 1 and 2. Essentially, we can do very little to slow drainage rates and we definitely cannot control drainage rates once peak outflow is reached or when the estuary enters Stage 2 (Figure 49). What can possibly be done is to consider ways to extend the duration of Stage 1 where outflow, channel expansion, and drainage rates are initially low. This may possibly be achieved by two methods:

##### **(1) Opening at a lower HG.**

If an estuary is opened at a HG just above the 0.019 m/m threshold required to achieve a successful opening, combined with low offshore  $H_s$ , drainage rates may be decreased and the duration of Stage 1 extended. Insufficient data exists to quantify the HG range at which this may be achieved, and further field observations are required. This option also needs to effectively balance the minimum HG for a successful opening at different sites with one which may achieve this goal.

##### **(2) Increasing or 'dragging out' the duration of Stage 1 where discharge and drainage rates are low.**

By extending the duration of Stage 1, the estuary is effectively held at a lower outflow velocity for a longer period of time. This means that the rates of increase in cross-sectional area and discharge would remain lower for longer thus extending the period of slower drainage. This is in a way similar to the geomorphic change anticipated to occur during 'shallow' openings. Field observations indicate that Stage 1 typically ends after a maximum of 3 hrs after opening. This is marked by a rapid increase in the rates of channel expansion as the series of knickpoints reach the upstream crest of the berm.

If we know that an estuary tends to favour erosion on a certain side of the channel, the majority of excavated sand or spoil could be strategically piled on that side of the channel. This means that as the channel expands, bank erosion would deliver this sand into the channel. This would slow the outflow meaning it may stay at a lower velocity for a longer duration. Additionally, the sand delivered to the channel must be eroded first before the channel can incise to a lower elevation and so incision may be slowed. This method of opening should be first trialled at estuaries where the preferential erosion path is known to assess the impact of the delivery of sand into the active channel.



## 7.5 Where this study fits within the current management procedure

This study has determined the HG values at which estuaries tend to be successfully opened or not. The parameters needed to calculate the HG at the time of opening (tidal elevation, berm length, and estuary water level) can be easily obtained by managers at a low cost and in minimum time. This information can be used to populate a spreadsheet (Figure 51 or similar) that can be used to assess the risk of an opening being unsuccessful. It is anticipated that this procedure would work well in conjunction with the current EEMSS process which assess the risks vs benefits of undertaking artificial openings or not. Alternatively, this could be included within the EEMSS assessment.

By continuing to record the berm length, water level, and tidal elevation at which different estuaries are artificially opened, along with whether openings are successful or not, sufficient HG data can be attained to begin to examine and extract specific HJG thresholds for individual sites. This is important as different estuaries likely have different HG thresholds at which artificial openings are successful. In order to refine the current HG thresholds, data for individual sites should be recorded. An example of this provided by EGCMA (EGCMA, 2014: pp.3). Here the Snowy River and Mallacoota Inlet are successfully opened at a minimum grade of 1:60 but Lake Tyers typically only requires 1:45. Establishing different HG thresholds for west Victorian estuaries would make the method highly accurate and site specific. A similar process should be undertaken for wave heights vs HG at which openings are successful or not.

The HG thresholds that determine opening success presented in this study could be used in conjunction with EEMSS and the Geomorphic Prediction Module (presented in Report 1 of this wider project) and amalgamated to provide Victoria with the most thorough management assessment of artificial estuary openings known globally (Figure 52). Here EEMSS assesses the site-specific socioeconomic and environmental risks vs benefits of undertaking an artificial opening. Physiochemical data is also included to assess the potential adverse environmental impacts of openings. The HG thresholds and spreadsheet presented with this report would work well alongside EEMSS to assess the likely success of openings. This would reduce the need for reimplementations and reduce the costs and time associated with this. Lastly, the Geomorphic Prediction Module (presented in the first report of this project) would assess the likely opening duration of an opening given the current and forecast geomorphic conditions. This becomes important when maintaining an open entrance for a longer duration is required past the initial drainage of the basin. By using these modes of assessment together prior to implementing an opening, multiple questions are answered and the opening process as a whole considers all aspects of management.

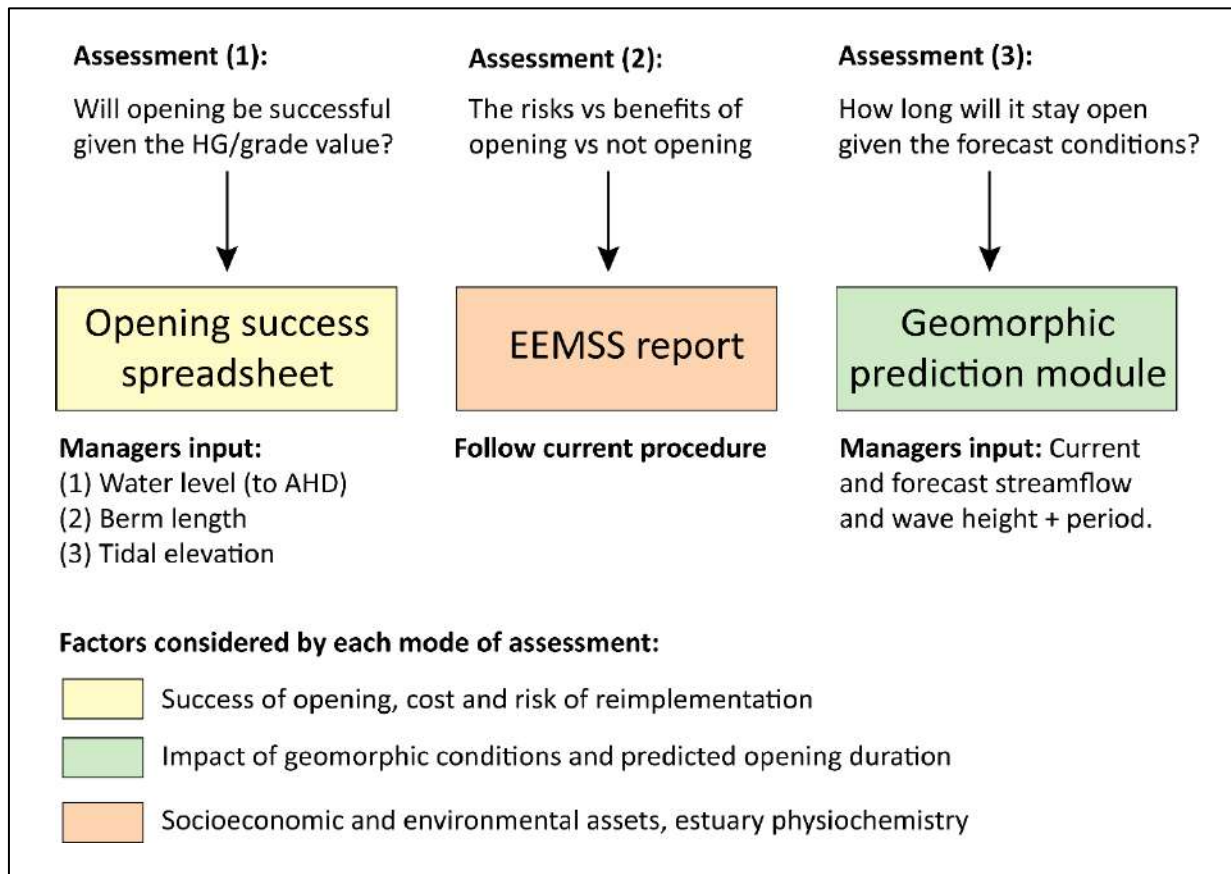


**Figure 52.** A potential method to incorporate (1) the pre-opening HG calculation to determine if an opening is likely to be successful and (3) the Geomorphic Prediction Module (part I of this project) alongside EEMSS in estuary entrance management decision making.

## 8.0 Conclusion

This report summarises the methods and results of an analysis of historic openings combined with fieldwork which comprises Part II of the project: *A geomorphic prediction module for intermittently open/closed estuaries (IOCE)*. The main findings of the report are as follows:

- **The water levels at which estuaries naturally open varies between sites.** The water level required to initiate a natural opening changes in accordance with the berm height and length and water level alone cannot be used to determine proximity to a natural opening. The hydraulic gradient (HG) is the main control on the likelihood of a natural opening occurring. This is a function of the head difference (in m) between the estuary and ocean and the berm length. The HG represents the energy slope between the estuary and the sea. Estuaries naturally open when the hydraulic gradient is at least 0.022 (minimum grade of: 1:46) and at an average HG of 0.052 (grade: 1:19).
- **The HG controls the success of an artificial opening.** Success is defined as when an estuary continues to maintain a connection to the ocean after excavation and enters a period of rapid channel expansion. Artificial openings as a whole tend to be successful when the HG at the time of opening is >0.019 m/m (grade of 1:53). High offshore waves should be avoided to ensure a successful opening as high, onshore sedimentation rates can overwhelm outflow, even when opened at high HG values.
- **The HG can be easily quantified at a low cost and should be included in current estuary opening assessments to gauge the likelihood of success and reduce the need for reimplementation of openings.** Data should be collected to quantify HG to refine thresholds for individual sites in future.

- **The rate and duration of basin drainage is a function of the hydraulic gradient at the time of opening.** Once an estuary reaches a critical outflow velocity, the drainage rate cannot be slowed down. This threshold is typically reached early in the opening (1-3 hrs) during Stage 1 of the opening sequence.
- **Temporal asymmetry exists in rates of change in outflow velocity, cross-sectional area, and discharge during opening.** These parameters increase rapidly on the rising limb of the hydrograph with a gradual decline after a max value is reached. Changes in water level lag geomorphic change at the mouth. The maximum outflow velocity and channel width are reached before the maximum cross-sectional area and discharge. Peak discharge occurs only once the channel has reached a final equilibrium width. Peak outflow velocity and channel width are typically reached at 20-25 % of the total drainage time and when the basin water level is still within 20 % ( $\pm 10$  %) of its initial value. The maximum cross-sectional area and discharge occur at similar times. Both peak at 25-40 % of the total drainage time and when the water level is still within 30-40 % ( $\pm 10$  %) of its initial value.
- The temporal variability in changes in channel morphology observed during the fieldwork of this study agree well with those described by Stretch and Parkinson (2006); Parkinson and Stretch (2007) for flume studies and Visser (1998); Morris (2009) for sand dikes.
- The risk of fish deaths occurring via the stranding of fish upon the floodplain may be linked to opening at a higher hydraulic gradient as the basin will drain faster (see Appendix 4). More analysis is needed to compare between sites over the event scale and so this work is ongoing.

## 9.0 References

- Aber, D., Downey, J., 1989. Scour mechanism at lake openings on sandy coasts. Presented at the Ninth Australasian Conference on Coastal and Ocean Engineering, pp. 93–97.
- Barton, J., Pope, A., Quinn, G. and Sherwood, J., 2008. Identifying threats to the ecological condition of Victorian estuaries. Department of Sustainability and the Environment Technical Report. <http://hdl.handle.net/10536/DRO/DU:30018691>
- Becker, A., Laurenson, L.J. and Bishop, K., 2009. Artificial mouth opening fosters anoxic conditions that kill small estuarine fish. *Estuarine, Coastal and Shelf Science*, 82(4), pp.566-572.
- Cooper, J.A.G., 2001. Geomorphological variability among microtidal estuaries from the wave-dominated South African coast. *Geomorphology*, 40(1-2), pp.99-122.
- East Gippsland Catchment Management Authority. 2014. Estuary Opening Protocols – Part B. Technical report. February 2014.
- Gordon, A.D., 1991. Coastal lagoon entrance dynamics. In *Coastal Engineering 1990* (pp. 2880-2893).
- Haines, P.E., 2006. Physical and chemical behaviour and management of Intermittently Closed and Open Lakes and Lagoons (ICOLLS) in NSW. Griffith University.
- Hoeksema, S.D., Chuwen, B.M., Potter, I.C., 2006. Massive mortalities of the black bream *Acanthopagrus butcheri* (Sparidae) in two normally-closed estuaries, following extreme increases in salinity. *Journal of the Marine Biological Association of the United Kingdom* 86, 893–897.
- McSweeney, S.L. 2016. The morphodynamics and evolution of intermittently closed and open coastal lakes and lagoons in Victoria, Australia. PhD thesis. The University of Melbourne. <http://hdl.handle.net/11343/116418>
- McSweeney, S.L., Kennedy, D.M. and Rutherford, I.D., 2018. The daily-scale entrance dynamics of intermittently open/closed estuaries. *Earth Surface Processes and Landforms*, 43(4), pp.791-807.
- Morris, M., 2009. Breaching processes: A state of the art review. T06-06-03.
- Morris, B.D. and Turner, I.L., 2010. Morphodynamics of intermittently open–closed coastal lagoon entrances: new insights and a conceptual model. *Marine Geology*, 271(1-2), pp.55-66.
- Odd, N.V.M., Roberts, W., Maddocks, J., 1995. Simulation of lagoon breakout. Presented at the 26th Congress of the International Association for Hydraulic Research, pp. 92–97.
- Parkinson, M. and Stretch, D., 2007. Breaching timescales and peak outflows for perched, temporary open estuaries. *Coastal engineering journal*, 49(03), pp.267-290.
- Perissinotto, R. 2010. Temporarily open/closed estuaries in South Africa. Nova Science Publishers.
- Russell I.A. 1994. Mass mortality of marine and estuarine fish in the Swartvlei and Wilderness lake systems, southern Cape. *Southern African Journal of Aquatic Sciences* 20: 93-96.
- Schallenberg, M., Larned, S.T., Hayward, S. and Arbuckle, C., 2010. Contrasting effects of managed opening regimes on water quality in two intermittently closed and open coastal lakes. *Estuarine, Coastal and Shelf Science*, 86(4), pp.587-597.



- Slinger, J.H., 2017. Hydro-morphological modelling of small, wave-dominated estuaries. *Estuarine, Coastal and Shelf Science*, 198, pp.583-596.
- Sloan, R., Kamer, K., 2005. Investigations of a fish kill in a central coast California lagoon. In: 18th Biennial Conference of the Estuarine Research Federation, Norfolk, Virginia.
- Stretch, D. and Parkinson, M., 2006. The breaching of sand barriers at perched, temporary open/closed estuaries—A model study. *Coastal Engineering Journal*, 48(01), pp.13-30.
- Suara, K., Mardani, N., Fairweather, H., McCallum, A., Allan, C., Sidle, R. and Brown, R., 2018. Observation of the dynamics and horizontal dispersion in a shallow intermittently closed and open lake and lagoon (ICOLL). *Water*, 10(6), p.776.
- Visser, P.J., 1998. Breach growth in sand-dikes. Delft University of Technology. Pp. 172.
- Wainwright, D.J. and Baldock, T.E., 2015. Measurement and modelling of an artificial coastal lagoon breach. *Coastal Engineering*, 101, pp.1-16.
- Whitfield, A.K., 1995. Mass mortalities of fish in South African estuaries. *South African Journal of Aquatic Science* 21, 29–34.
- Whitfield, A.K. and Cowley, P.D., 2018. A mass mortality of fishes caused by receding water levels in the vegetated littoral zone of the West Kleinemonde Estuary, South Africa. *African journal of aquatic science*, 43(2), pp.179-186.

## Appendix 1: Natural opening historic water levels

**Table 1.** List of all known historic natural openings and water levels at the time of opening.

Estuary	Date of opening	WL (m AHD)	Estuary	Date of opening	WL (m AHD)
Glenelg River	07/05/12	1.43	Aire River	29/08/09	2.50
	08/05/14	1.22		30/11/09	1.60
	17/06/15	1.32		15/12/09	1.45
	20/07/15	1.54		19/12/09	1.60
	24/06/16	1.04		25/06/14	1.64
Fitzroy River	15/02/10	1.07	Barham River	05/11/19	1.75
	23/04/10	1.11		15/03/09	1.72
	01/04/12	1.10		26/04/09	2.30
	11/04/13	1.07		16/03/12	1.46
	24/04/14	0.98		20/01/13	1.28
	02/01/15	0.93		06/03/13	1.46
	26/02/15	0.63		22/04/13	1.68
	04/06/15	1.15		15/05/13	1.79
	14/07/15	1.06		09/03/14	1.20
	20/01/16	0.86		22/03/14	1.77
	28/06/16	1.46		09/04/14	1.68
	21/02/17	0.98		22/04/14	1.68
	21/04/17	1.38		16/06/14	1.66
	03/05/18	1.25		30/12/14	1.46
Surrey River	09/06/09	1.62	Barham River	06/03/15	1.70
	29/01/10	1.49		20/03/15	1.62
	09/07/10	1.00		30/03/15	1.91
	08/11/10	0.96		24/06/15	1.60
	13/01/11	1.32		03/02/16	1.64
	09/05/11	1.44		26/02/16	1.64
	15/06/12	1.70		18/03/16	1.44
	27/11/12	0.84		10/05/16	1.66
	13/06/13	1.55		03/02/17	1.24
	16/12/13	0.56		20/02/17	1.60
	09/04/14	1.08		11/03/17	1.34
	08/05/14	1.40		22/03/17	1.48
	01/10/14	0.80		27/01/18	1.10
	15/10/14	0.93		15/04/18	1.98
	19/06/15	1.71		08/11/18	1.20
	16/07/15	1.39		24/11/18	1.20
	10/10/15	0.78		04/12/18	1.25
	24/06/16	1.69		12/12/18	1.20
	25/12/16	0.84		08/02/19	1.58
	01/11/17	1.44	20/02/19	1.82	
11/11/17	1.00	02/03/19	1.30		
17/06/18	0.67	23/03/19	1.92		
20/09/18	1.70	10/04/19	1.64		
06/10/18	0.85	01/05/19	1.90		
14/10/18	0.89	Painkalac Creek	23/08/14	1.66	
19/10/18	0.55		29/07/16	1.43	

Eumeralla River	23/06/09	0.63	Anglesea River	22/07/17	1.65
	13/01/11	1.36		24/07/17	1.55
	09/05/11	1.56		01/02/05	2.00
	26/02/14	0.50		25/04/09	1.60
	30/06/14	1.79		04/08/09	1.60
	01/09/15	0.65		05/12/11	1.23
	10/09/15	0.75		07/05/12	1.35
	28/09/15	0.64		12/08/12	1.38
	11/11/16	1.06		13/06/13	1.72
	19/08/17	1.69		09/04/14	1.69
	18/11/17	1.09		23/04/14	1.52
	Merri River	12/08/10		1.08	Spring Creek
25/06/14		1.40	12/05/15	1.84	
10/09/16		1.70	28/06/08	1.65	
07/09/17		2.00	01/09/09	1.95	
Hopkins River	16/06/13	1.50	Powlett River	12/05/16	1.90
	05/08/13	1.50		22/07/18	2.05
	25/06/14	1.40		11/07/18	2.21
	23/07/15	1.59	Gellibrand River	14/06/13	2.35
	28/07/15	1.30		29/04/09	1.53
	01/09/15	1.30		20/05/09	1.70
	11/09/15	1.40		12/06/10	1.33
	14/06/16	1.50		02/05/13	1.24
	26/06/16	1.90		04/02/15	1.25
	07/04/17	1.24		01/05/15	1.46
	27/04/17	0.82		14/05/15	2.02
	13/07/17	1.24		12/06/15	1.39
	16/02/18	0.74		08/03/17	1.41
	12/04/18	1.17		31/05/17	1.79
	21/10/18	1.21		14/05/18	1.45
	14/11/18	1.40		18/06/18	1.23
10/12/18	1.00	06/01/19	1.01		
Curdies Inlet	18/06/18	1.98			

## Appendix 2: Field data for 2019 artificial openings

**Table 1.** Aire River artificial opening 01: 01/02/2019 where T is time since opening, u is outflow velocity, CW is channel width, WD is water depth in channel, Ac is cross-sectional area, Q is discharge. Measurement number corresponds with XSN's.

Measurement	Date/time	T (min)	T (hr)	u (m/s)	CW (m)	WD (m)	Ac (m <sup>2</sup> )	Q (m <sup>3</sup> /s <sup>-1</sup> )	Percent total drainage time
1	1/02/2019 09:00	0	0.00	0.00	0.00	0.00	0.00	0.00	0 %
2	1/02/2019 09:45	45	0.75	1.25	5.00	0.15	0.75	0.94	3 %
3	1/02/2019 10:05	60	1.00	1.50	7.50	0.50	3.75	5.63	4 %
4	1/02/2019 10:30	90	1.50	2.20	12.55	0.80	10.04	22.09	6 %
5	1/02/2019 11:30	150	2.50	2.80	21.00	1.00	21.00	58.80	10 %
6	1/02/2019 12:00	180	3.00	2.90	28.00	1.25	35.00	101.50	13 %
7	1/02/2019 13:00	240	4.00	3.07	35.11	1.60	56.18	172.46	17 %
8	1/02/2019 13:44	284	4.73	3.02	35.00	1.65	57.75	174.41	20 %
9	1/02/2019 15:00	360	6.00	2.20	34.55	1.50	51.83	114.02	25 %
10	1/02/2019 17:00	480	8.00	1.60	34.21	1.20	41.05	65.68	33 %
11	1/02/2019 18:05	545	9.08	1.42	33.96	1.15	39.05	55.46	38 %
11	1/02/2019 18:55	595	9.92	1.20	33.90	1.00	33.90	40.68	41 %

**Table 2.** Gellibrand artificial opening: 09/03/2019 - 11/03/2019 where T is time since opening, u is outflow velocity, CW is channel width, WD is water depth in channel, Ac is cross-sectional area, and Q is discharge. Measurement number corresponds with XSN's.

Measurement	Date/time	T (min)	T (hr)	u (m/s)	CW (m)	WD (m)	Ac (m2)	Q (m3/s-1)
1	09/03/2019 15:00	0	0.00	0.00	0.00	0.00	0.00	0.00
2	09/03/2019 15:30	30	0.50	0.47	3.00	0.45	1.35	0.63
3	09/03/2019 16:09	69	1.10	0.93	3.50	0.48	1.68	1.56
4	09/03/2019 18:00	180	3.00	0.85	4.00	0.43	1.72	1.46
5	09/03/2019 20:00	300	5.00	0.76	4.50	0.41	1.845	1.40
6	10/03/2019 01:19	619	10.00	0.61	4.55	0.36	1.64	1.00
7	10/03/2019 02:24	684	11.00	0.63	4.56	0.30	1.37	0.86
8	10/03/2019 03:35	755	12.00	0.64	4.57	0.25	1.14	0.73
9	10/03/2019 04:36	816	13.00	0.68	4.54	0.27	1.23	0.83
10	10/03/2019 07:29	989	16.00	0.79	4.54	0.28	1.27	1.00
11	10/03/2019 08:37	1057	17.00	0.82	4.54	0.31	1.41	1.15
12	10/03/2019 09:36	1136	18.00	0.96	4.52	0.35	1.58	1.52
13	10/03/2019 11:08	1208	20.00	1.06	4.54	0.45	2.04	2.17
14	10/03/2019 12:17	1277	21.00	1.12	4.55	0.50	2.28	2.55
15	10/03/2019 13:06	1326	22.00	1.08	4.56	0.45	2.05	2.22
16	10/03/2019 14:22	1402	23.00	1.06	4.57	0.43	1.97	2.08
17	10/03/2019 15:25	1475	24.00	0.96	4.57	0.41	1.87	1.80
18	10/03/2019 16:10	1510	25.00	1.02	4.57	0.41	1.87	1.91
19	11/03/2019 16:00	2940	49.00	1.01	4.57	0.38	1.74	1.75
20	11/03/2019 18:00	3060	51.00	0.90	4.57	0.35	1.60	1.44



**Table 3.** Aire River artificial opening 02: 01/05/2019 - 02/05/2019 where T is time since opening, u is outflow velocity, CW is channel width, WD is water depth in channel, Ac is cross-sectional area, Q is discharge, and BE is bed elevation at berm/former berm position. Measurement number corresponds with XSN's.

Measurement	Date/time	T (min)	T (hr)	u (m/s)	CW (m)	WD (m)	Ac (m <sup>2</sup> )	Q (m <sup>3</sup> /s <sup>-1</sup> )	BE (m AHD)
1	1/05/2019 09:40	0	0.00	0.00	0.00	0.00	0.00	0.00	2.37
2	1/05/2019 10:19	19	0.30	0.22	5.14	0.51	1.60	0.35	0.86
3	1/05/2019 10:54	54	1.00	0.30	7.27	0.82	1.43	0.43	0.84
4	1/05/2019 12:03	123	2.00	0.40	7.62	0.75	1.31	0.52	0.83
5	1/05/2019 12:53	173	2.80	0.42	7.94	0.73	1.36	0.57	0.81
6	1/05/2019 13:38	218	3.60	0.45	8.07	0.77	1.48	0.70	0.79
7	1/05/2019 13:57	237	4.00	0.50	8.26	0.66	1.39	0.67	0.80
8	1/05/2019 16:06	366	6.00	0.55	8.27	0.62	1.13	0.62	0.93
9	1/05/2019 18:06	486	8.00	0.58	8.55	0.62	1.12	0.60	0.94
10	2/05/2019 09:00	1380	23.00	0.60	8.65	0.55	0.71	0.43	0.95
11	2/05/2019 10:24	1464	24.40	0.70	8.69	0.48	0.63	0.44	0.92
12	2/05/2019 11:09	1509	25.20	0.65	8.71	0.45	0.67	0.42	0.94
13	2/05/2019 12:21	1581	26.40	0.55	8.91	0.44	0.64	0.38	0.95
14	2/05/2019 12:48	1608	26.80	0.50	8.91	0.46	0.64	0.35	0.96

**Table 4.** Spring Creek artificial opening: 31/05/2019 - 01/06/2019 where T is time since opening, u is outflow velocity, CW is channel width, WD is water depth in channel, Ac is cross-sectional area, Q is discharge, and BE is bed elevation at berm/former berm position. Measurement number corresponds with XSN's.

Measurement	Date/time	T (min)	T (hr)	u (m/s)	CW (m)	WD (m)	Ac (m <sup>2</sup> )	Q (m <sup>3</sup> /s <sup>-1</sup> )	BE (m AHD)	Percent total drainage time
1	31/05/2019 13:30	0	0.00	0.00	0.00	0.00	0.00	0.00	1.96	0 %
2	31/05/2019 14:40	50	0.83	0.70	2.10	0.20	0.21	0.15	1.29	4 %
3	31/05/2019 14:51	81	1.35	0.90	2.25	0.25	0.29	0.26	1.20	7 %
4	31/05/2019 15:10	100	1.67	1.20	3.50	0.30	0.35	0.42	0.97	8 %
5	31/05/2019 15:40	130	2.17	1.52	7.00	0.66	1.13	1.72	0.41	11 %
6	31/05/2019 16:15	165	2.75	2.00	11.00	0.70	2.35	4.70	0.22	14 %
7	31/05/2019 16:45	195	3.25	2.20	14.94	0.82	5.31	11.68	0.09	16 %
8	31/05/2019 17:07	217	3.62	2.40	24.19	0.96	10.30	24.72	-0.12	18 %
9	31/05/2019 17:47	257	4.28	2.70	26.15	0.99	15.10	40.77	-0.26	21 %
10	31/05/2019 18:09	279	4.65	2.50	26.00	0.93	17.44	43.60	-0.26	23 %
11	31/05/2019 18:31	301	5.02	1.45	26.10	0.89	16.88	24.48	-0.26	25 %
12	31/05/2019 18:53	323	5.38	1.20	26.15	0.77	15.54	18.65	-0.25	27 %
13	31/05/2019 21:53	503	8.38	0.70	26.08	0.58	7.35	5.15	-0.26	42 %
14	01/06/2019 08:11	1121	18.68	0.50	26.02	0.12	1.02	0.51	-0.21	93 %
15	01/06/2019 08:56	1166	19.43	0.40	26.03	0.11	0.98	0.39	-0.19	96 %
16	01/06/2019 09:30	1210	20.00	0.38	26.02	0.10	0.85	0.32	-0.15	1.00 %

**Table 5.** Curdies Inlet artificial opening 2: 17/06/2019 - 18/06/2019 where T is time since opening, u is outflow velocity, CW is channel width, WD is water depth in channel, Ac is cross-sectional area, Q is discharge, and BE is bed elevation at berm/former berm position. Measurement number corresponds with XSN's.

Measurement	Date/time	T (min)	T (hr)	u (m/s)	CW (m)	WD (m)	Ac (m <sup>2</sup> )	Q (m <sup>3</sup> /s <sup>-1</sup> )	Percent total drainage time
1	17/06/2019 15:00	0	0.00	0.00	0.00	0.00	0.00	0.00	0 %
2	17/06/2019 15:36	36	0.60	1.22	3.00	0.25	0.75	0.92	1 %
3	17/06/2019 16:30	90	1.50	1.40	3.80	0.30	1.14	1.60	3 %
4	17/06/2019 17:23	143	2.38	1.49	5.50	0.26	1.43	2.13	5 %
5	17/06/2019 18:32	212	3.53	1.61	6.00	0.35	2.10	3.38	8 %
6	17/06/2019 19:36	276	4.60	1.61	6.75	0.35	2.36	3.80	10 %
7	17/06/2019 20:18	318	5.30	1.60	8.05	0.35	2.82	4.51	11 %
8	17/06/2019 20:52	352	5.87	1.57	9.50	0.50	4.75	7.46	13 %
9	17/06/2019 21:50	410	6.83	1.66	11.45	0.45	5.15	7.52	15 %
10	17/06/2019 22:30	450	7.50	1.69	13.80	0.55	7.59	12.83	16 %
11	17/06/2019 23:10	510	8.50	1.98	14.20	0.60	8.52	16.87	18 %
12	18/06/2019 00:00	540	9.00	2.50	15.80	0.75	11.85	29.63	19 %
13	18/06/2019 00:30	570	9.50	3.06	20.50	0.80	16.40	50.18	20 %
14	18/06/2019 01:10	610	10.17	2.96	34.00	1.20	40.80	120.77	22 %
15	18/06/2019 02:50	710	11.83	3.01	51.50	1.30	66.95	201.52	25 %
16	18/06/2019 07:00	960	16.00	3.47	62.50	1.80	120.00	347.00	34 %
17	18/06/2019 08:35	1055	17.58	2.93	62.50	2.00	137.00	366.57	38 %
18	18/06/2019 09:52	1132	18.87	1.64	62.50	2.20	130.00	225.41	40 %
19	18/06/2019 11:47	1247	20.78	1.00	62.50	2.10	121.00	137.78	45 %

**Table 6.** Painkalac Creek artificial opening: 08/08/2019 where T is time since opening, u is outflow velocity, CW is channel width, WD is water depth in channel, Ac is cross-sectional area, Q is discharge, and BE is bed elevation at berm/former berm position. Measurement number corresponds with XSN's.

Measurement	Date/time	T (min)	T (hr)	u (m/s)	CW (m)	WD (m)	Ac (m <sup>2</sup> )	Q (m <sup>3</sup> /s <sup>-1</sup> )	BE (m AHD)	Percent total drainage time
1	8/08/2019 09:00	0	0.00	0.00	0.00	0.00	0.00	0.00	1.96	0 %
2	8/08/2019 09:24	24	0.40	1.25	5.00	0.15	0.45	0.56	1.42	4 %
3	8/08/2019 09:57	57	0.95	1.82	6.62	0.21	0.89	1.62	1.13	10 %
4	8/08/2019 10:20	80	1.33	2.34	8.53	0.40	2.58	6.04	0.89	13 %
5	8/08/2019 10:36	96	1.60	2.43	12.67	0.46	3.03	7.36	0.80	16 %
6	8/08/2019 10:56	116	1.93	2.46	13.32	0.52	3.81	9.37	0.74	19 %
7	8/08/2019 11:15	135	2.25	2.63	18.94	0.56	4.27	11.23	0.56	23 %
8	8/08/2019 12:01	181	3.02	2.74	26.00	0.62	6.07	16.63	0.36	30 %
9	8/08/2019 12:30	210	3.50	2.20	26.00	0.68	6.12	13.46	0.26	35 %
10	8/08/2019 13:02	242	4.03	1.86	25.99	0.56	5.66	10.53	0.21	40 %
11	8/08/2019 14:10	310	5.17	1.42	25.93	0.55	5.68	8.06	0.18	52 %
12	8/08/2019 14:45	345	5.75	1.36	25.62	0.52	5.08	6.88	0.17	58 %
13	8/08/2019 15:15	365	6.08	1.10	25.52	0.48	4.40	4.84	0.18	61 %

**Table 7.** Anglesea artificial opening: 14/08/2019 - 15/05/2019 where T is time since opening, u is outflow velocity, CW is channel width, WD is water depth in channel, Ac is cross-sectional area, Q is discharge, and BE is bed elevation at berm/former berm position. Measurement number corresponds with XSN's.

Measurement	Date/time	T (min)	T (hr)	u (m/s)	CW (m)	WD (m)	Ac (m <sup>2</sup> )	Q (m <sup>3</sup> /s <sup>-1</sup> )	BE (m AHD)	Percent total drainage time
1	14/08/2019 10:00	0	0.00	0.00	0.00	0.00	0.00	0.00	2.11	0 %
2	14/08/2019 11:00	0	0.00	0.00	0.00	0.00	0.00	0.00	2.11	0 %
3	14/08/2019 11:50	50	0.83	0.73	3.20	0.12	0.43	0.31	1.09	3 %
4	14/08/2019 12:10	70	1.17	0.77	3.69	0.13	0.44	0.34	1.08	4 %
5	14/08/2019 12:31	91	1.52	0.79	4.25	0.14	0.40	0.32	1.01	5 %
6	14/08/2019 12:59	119	1.98	0.95	4.31	0.14	0.41	0.39	0.96	6 %
7	14/08/2019 13:20	140	2.33	0.93	4.35	0.14	0.39	0.36	0.94	8 %
8	14/08/2019 14:07	187	3.12	1.01	5.05	0.15	0.46	0.46	0.83	10 %
9	14/08/2019 14:45	225	3.75	0.96	5.39	0.15	0.45	0.43	0.65	13 %
10	14/08/2019 16:28	328	5.47	0.93	6.85	0.16	0.63	0.59	0.64	18 %
11	14/08/2019 18:59	419	6.98	0.71	9.47	0.17	1.05	0.75	0.52	23 %
12	14/08/2019 19:39	459	7.65	0.62	12.37	0.15	0.68	0.42	0.43	26 %
13	14/08/2019 20:29	479	7.98	0.66	13.55	0.16	0.69	0.46	0.44	27 %
14	14/08/2019 22:06	681	11.35	0.62	15.04	0.14	0.58	0.36	0.44	38 %
15	15/08/2019 09:06	1331	22.18	0.56	15.03	0.13	0.26	0.15	0.45	74 %
16	15/08/2019 10:00	1385	23.08	0.55	15.05	0.12	0.25	0.14	0.52	77 %
17	15/08/2019 11:04	1449	24.15	0.53	15.04	0.11	0.25	0.13	0.51	81 %



### Appendix 3: Historic hydraulic gradients, water levels, and drainage details for known openings

**Table 1.** Records of all openings where HG could be calculated prior to opening. Berm\_L is berm length, Berm\_H is berm height, Tide\_H is tidal elevation, HG is hydraulic gradient. % drain is the percentage reduction in water level. ‘Opens’ is a successful opening and ‘Drains’ is one that reduced the basin water level by >10 % and/or alleviated flooding. \* is a natural opening. Sites in **red** are those monitored during this study, sites in **blue** are from McSweeney (2016), and sites in **black** are from EstuaryWatch historic data.

#	Opening	Date	Berm_L (m)	Berm_H (m AHD)	WL start (m AHD)	Tide_H (m AHD)	Head (m)	HG (m/m)	Grade	H <sub>s</sub> (m)	WL end (m AHD)	Drainage (m)	Time to drain (hr)	Drain rate (m/hr)	Opens	Drains
1	<b>Aireys</b>	08/08/19	52	1.96	2.11	-0.25	2.36	0.045	1: 22	2.44	1.30	0.81	16	0.051	Y	Y
2	<b>Anglesea</b>	14/08/19	76	2.25	1.76	0.55	1.21	0.016	1: 63	1.41	1.29	0.47	100	0.005	Y	Y
3	<b>Gellibrand</b>	09/03/19	74	1.82	1.52	0.30	1.22	0.016	1:61	3.31	1.39	0.13	70	0.002	Y	<b>N</b>
4	<b>Aire_01</b>	01/02/19	70	-	1.52	-0.35	1.87	0.027	1:37	2.59	0.52	1.00	24	0.042	Y	Y
5	<b>Aire_02</b>	01/05/19	190	2.37	1.60	-0.35	1.95	0.010	1:97	2.02	1.60	0.00	-	0.000	<b>N</b>	<b>N</b>
6	<b>Spring</b>	31/05/19	38	1.96	1.90	-0.05	1.95	0.051	1:19	0.83	0.70	1.20	16	0.075	Y	Y
7	<b>Curdies_01</b>	16/06/19	68	2.32	1.34	0.30	1.04	0.015	1:66	2.86	1.34	0.00	-	0.000	<b>N</b>	Y
8	<b>Curdies_02</b>	17/06/19	48	1.88	1.38	0.20	1.18	0.025	1:41	2.17	0.28	1.10	42	0.026	Y	Y
9	<b>Anglesea</b>	14/02/14	105	2.37	1.65	-0.05	1.70	0.016	1:62	2.10	1.54	0.11	96	0.001	Y	<b>N</b>
10	<b>Aire_01</b>	20/03/14	55	2.49	1.98	-0.55	2.53	0.046	1:22	2.90	0.65	1.33	22	0.060	Y	Y
11	<b>Aire_02</b>	01/05/14	40	2.45	1.99	-0.25	2.24	0.056	1:18	4.80	1.99	0.00	-	0.000	<b>N</b>	<b>N</b>
12	<b>Aire_03</b>	10/05/14	33	3.27	2.11	0.65	1.46	0.044	1:23	2.08	0.80	1.31	26	0.050	Y	Y
13	<b>Gellibrand</b>	11/04/14	28	3.79	1.48	0.10	1.38	0.049	1:20	2.75	0.20	1.28	36	0.036	Y	Y
14	<b>Anglesea_01</b>	18/06/15	66	1.74	1.69	0.17	1.52	0.023	1:43	2.03	1.40	0.29	48	0.006	Y	Y
15	<b>Anglesea_02</b>	06/07/16	87	2.01	1.73	0.15	1.58	0.018	1:55	2.61	1.40	0.33	96	0.003	Y	Y
16	<b>Curdies_01</b>	30/06/14	69	3.31	1.61	0.00	1.61	0.023	1:43	3.60	0.27	1.34	72	0.019	Y	Y
17	<b>Curdies_02*</b>	18/06/18	80	2.00	1.98	-0.50	2.48	0.031	1:32	2.27	0.30	1.68	36	0.047	Y	Y
18	<b>Curdies_03</b>	05/07/17	85	2.25	1.45	-0.10	1.55	0.018	1:55	3.00	1.45	0.00	0	0.000	<b>N</b>	<b>1</b>
19	<b>Curdies_04</b>	11/07/17	60	1.86	1.62	-0.20	1.82	0.030	1:33	2.80	0.40	1.22	30	0.041	Y	Y
20	<b>Painkalac</b>	22/07/16	40	3.90	2.20	0.14	2.06	0.052	1:19	3.80	1.20	1.00	24	0.042	Y	Y
21	<b>Spring_01</b>	26/06/14	30	2.22	1.82	0.29	1.53	0.051	1:20	3.40	1.00	0.82	24	0.034	Y	Y

22	Spring_02	15/06/18	51	2.20	1.60	0.85	0.75	0.015	1:68	4.20	1.60	0.00	25	0.000	N	N
23	Spring_03	23/06/16	25	-	1.89	0.75	1.14	0.046	1:22	2.80	1.20	0.69	48	0.014	Y	Y
24	Spring_04	05/06/16	40	2.10	2.00	-0.15	2.15	0.054	1:19	1.61	1.20	0.80	20	0.040	Y	Y
25	Spring_05	05/06/15	90	2.40	2.00	-0.45	2.45	0.027	1:37	2.02	1.20	0.80	24	0.033	Y	Y
26	Powlett_01	04/06/19	100	3.00	2.42	0.36	2.06	0.021	1:49	0.90	1.27	1.15	48	0.024	Y	Y
27	Powlett_02	07/07/17	68	2.81	2.61	0.54	2.07	0.030	1:33	0.95	1.20	1.41	40	0.035	Y	Y
28	Powlett_03	13/05/16	110	2.16	2.01	0.04	1.97	0.018	1:56	3.00	2.01	0.00	0	0.000	N	N
29	Powlett_04	19/06/18	123	2.92	2.42	-0.06	2.48	0.020	1:50	1.23	1.30	1.12	26	0.043	Y	Y
30	Bourne	03/05/17	33	2.00	1.80	0.14	1.66	0.050	1:20	1.79	1.40	0.40	24	0.017	Y	Y
31	Erskine	13/04/16	24	1.70	1.60	-0.45	2.05	0.085	1:12	1.78	0.70	0.90	24	0.038	Y	Y
32	Wreck_01*	08/11/19	79	2.15	2.10	0.24	1.86	0.024	1:43	3.10	1.40	0.70	30	0.023	Y	Y
33	Wreck_02	16/06/18	57	2.40	2.10	0.14	1.96	0.034	1:29	0.58	1.40	0.70	24	0.029	Y	Y
34	Wreck_03	22/05/18	45	2.48	2.18	1.24	0.94	0.021	1:48	2.80	1.45	0.73	24	0.030	Y	Y
35	Wreck_04	11/05/18	102	2.70	1.95	0.24	1.71	0.017	1:60	1.81	1.80	0.15	48	0.003	Y	N
36	Wreck_05*	01/12/17	89	2.10	1.98	-0.06	2.04	0.023	1:44	1.40	1.40	0.58	49	0.012	Y	Y
37	Wreck_06	25/07/17	90	2.55	2.05	0.14	1.91	0.021	1:47	2.05	1.50	0.55	24	0.023	Y	Y
38	Wreck_07	26/04/17	40	2.30	1.90	1.14	0.76	0.019	1:53	1.30	1.75	0.15	24	0.006	Y	N
39	Thompsons	08/09/16	110	3.00	1.65	-0.65	2.30	0.021	1:48	1.06	0.60	1.05	120	0.009	Y	Y
40	Merricks_01*	21/06/19	91	2.10	2.01	-0.15	2.16	0.024	1:42	1.05	0.70	1.31	48	0.027	Y	Y
41	Merricks_02*	09/07/18	30	2.07	1.96	0.05	1.91	0.064	1:16	1.20	1.10	0.86	24	0.036	Y	Y
42	Merricks_03	19/07/17	42	1.82	1.50	-0.35	1.85	0.044	1:23	0.80	0.90	0.60	24	0.025	Y	Y
43	Merricks_04	02/11/16	24	2.02	1.72	0.05	1.67	0.070	1:14	0.50	0.66	1.06	24	0.044	Y	Y
44	Gellibrand_01	28/03/19	50	1.89	1.69	0.40	1.29	0.026	1:39	1.70	0.30	1.39	72	0.019	Y	Y
45	Gellibrand_02*	06/01/19	50	-	1.10	0.00	1.10	0.022	1:46	2.74	0.70	0.40	24	0.017	Y	Y
46	Gellibrand_03	19/04/18	58	1.94	1.74	-0.33	2.07	0.036	1:28	1.90	0.20	1.54	50	0.031	Y	Y
47	Gellibrand_04	10/03/18	45	1.87	1.55	0.10	1.45	0.032	1:31	1.25	0.31	1.24	48	0.026	Y	Y
48	Gellibrand_05*	31/05/17	15	1.89	1.79	0.50	1.29	0.086	1:12	3.63	0.30	1.49	24	0.062	Y	Y
49	Gellibrand_06	13/04/17	80	1.87	1.78	0.20	1.58	0.020	1:51	1.90	0.36	1.42	72	0.020	Y	Y
50	Gellibrand_07*	08/03/17	68	1.81	1.42	0.20	1.22	0.018	1:56	1.60	0.49	0.93	96	0.010	Y	Y

51	Gellibrand_08	11/05/16	56	1.83	1.78	1.10	0.68	0.012	1:82	5.30	1.78	0.00	-	0.000	N	N
52	Gellibrand_09	12/05/16	45	2.07	1.87	0.30	1.57	0.035	1:29	4.50	0.54	1.33	96	0.014	Y	Y
53	Gellibrand_10	12/03/16	39	1.76	1.46	0.70	0.76	0.019	1:51	2.10	0.18	1.28	48	0.027	Y	Y
54	Gellibrand_11	26/12/15	34	1.73	1.43	0.53	0.90	0.027	1:37	1.01	0.18	1.25	75	0.017	Y	Y
55	Gellibrand_12*	01/05/15	35	1.60	1.60	0.52	1.08	0.031	1:32	2.05	0.31	1.29	72	0.018	Y	Y
56	Gellibrand_13*	06/02/15	14	1.60	1.25	0.39	0.86	0.061	1:16	3.05	0.28	0.97	70	0.014	Y	Y
57	Gellibrand_14	12/01/15	40	1.82	1.42	0.70	0.72	0.018	1:56	1.80	0.43	0.99	74	0.013	Y	Y
58	Gellibrand_15	23/02/13	28	2.11	1.51	0.30	1.21	0.043	1:23	2.10	0.15	1.36	30	0.045	Y	Y
59	Gellibrand_16	16/02/12	25	1.70	1.20	0.20	1.00	0.040	1:25	3.10	0.34	0.86	92	0.009	Y	Y
60	Gellibrand_17	17/03/09	30	2.70	1.55	0.20	1.35	0.045	1:22	2.20	0.27	1.28	100	0.013	Y	Y

**EGCMA estuaries: known thresholds for successful openings (from EGCM, 2014).**

#	Estuary	HG (m:m)	Grade
61	Snowy River	0.017	1:60
62	Mallacoota Inlet	0.017	1:60
63	Lake Tyers	0.025	1:40
64	Sydenham Inlet (upper)	0.100	1:10
65	Sydenham Inlet (lower)	0.022	1: 45

## Appendix 4: Physiochemical change vs morphological change at the mouth

### Section 1: FIELD OBSERVATIONS:

Field observations during artificial openings undertaken in 2019 will be analysed in more detail as part of a Melbourne University honours project and with collaborators from Griffith University. The analysis below provides a brief summary of the main changes observed in physiochemical conditions in conjunction with changes in basin water level and mouth morphology as detailed in Appendix 2. During all monitored openings, no fish deaths occurred. Here natural diurnal fluctuations in physiochemical parameters are not accounted for due to limited data.

#### (a) Spring Creek 31/05/19

Spring Creek data is presented for the Great Ocean Road bridge at Torquay (-38.34, 144.31°). The boardwalk near the mouth was also monitored but drained to a depth of 0.30 m allowing only minimal depth profiling to be undertaken. Results at the boardwalk were consistent with upstream while the depth was high enough to monitor.

**Table 1.** Timing of depth profiles compared to change in mouth morphology and total depth profile water depth.

Depth profile #	Date/time	Hrs since opening	Mouth area (m <sup>2</sup> )	Discharge (m <sup>3</sup> /s <sup>-1</sup> )	Profile water depth (m)
1 (pre-opening)	31/05/19 13:58	0.0	0.0	0.0	1.78
2	31/05/19 15:28	1.5	1.13	1.72	1.77
3	31/05/19 17:00	2.5	10.30	24.72	1.36
4	31/05/19 18:40	3.6	16.88	24.48	1.01
5	31/05/19 20:54	5.0	15.54	18.65	0.84
6	31/05/19 22:48	7.0	7.35	5.15	0.78
7	01/06/19 07:54	18.60	1.02	0.51	0.71
8	01/06/19 09:08	19.80	0.39	0.39	0.70

- Prior to opening, depth profile #1 shows that Spring Creek was slightly stratified for both salinity and dissolved oxygen (DO) (Figure 1a-d). DO was lower and salinity was higher at the bottom of the profile (Figure 1a-d).
- At the time of depth profile #2, the channel was 1.13 m<sup>2</sup> in cross-sectional area and discharge was 1.72 m<sup>3</sup>/s<sup>-1</sup> (Table 1). Minimal change in water level had occurred since opening (Table 1). Depth profile #2 showed bottom and top velocity had both increased to 0.01 m/s (Figure 1i). DO had slightly increased throughout the profile - increasing most markedly at 0.9 m depth from 18 % to 27 % (Figure 1c) and turbidity had also slightly increased at 0.90 m depth (Figure 1f). All other parameters remained similar to profile #1.
- During profile #3, the cross-sectional area was 10.30 m<sup>2</sup> and discharge 24.72 m<sup>3</sup>/s<sup>-1</sup> (Table 1). The profile had decreased in total depth to 1.36 m. Top velocity had increased to a max of 0.08 m/s with bottom velocity being 0.02 m/s (Figure 1i). pH had decreased and turbidity was more even (Figure 1f-g). Conductivity had decreased from 30 to 18 ms/cm at the bottom of the water column (Figure 1e). The salinity profile remained similar to profiles #1 and #2 but DO had increased to >30 % saturation in the top 0.60 m of the water column (Figure 1c).
- At the time of profile #4, the estuary had entered the falling limb of the hydrograph and the profile water depth had decreased to 1.01 m (Table 1). Top velocity had decreased slightly to 0.07 m/s with bottom velocity increasing to 0.05 m/s (Figure 1i). DO had further increased and pH had decreased (Figure 1b-c; g).
- At the time of Profile #5, the channel area and discharge had further decreased (Table 1). Top (0.02 m/s) and bottom (0.01 m/s) velocity had decreased, pH had further increased, and DO had increased (Figure 1b-i).
- At the time of the last depth profile, #8, top and bottom velocity had reached 0 m/s and the total depth was 0.70 m (Figure 1i; Table 1). Conductivity and pH had progressively decreased from their pre-opening value with pH reaching a minimum of 7.5 (at 0.6 m depth) (Figure 1e-g). Salinity and conductivity showed little change indicating that saltwater intrusion from the mouth had not reached the upstream location (Figure 1d-e). DO and turbidity had progressively increased (Figure 1b-c; f) indicating mixing of the water column.

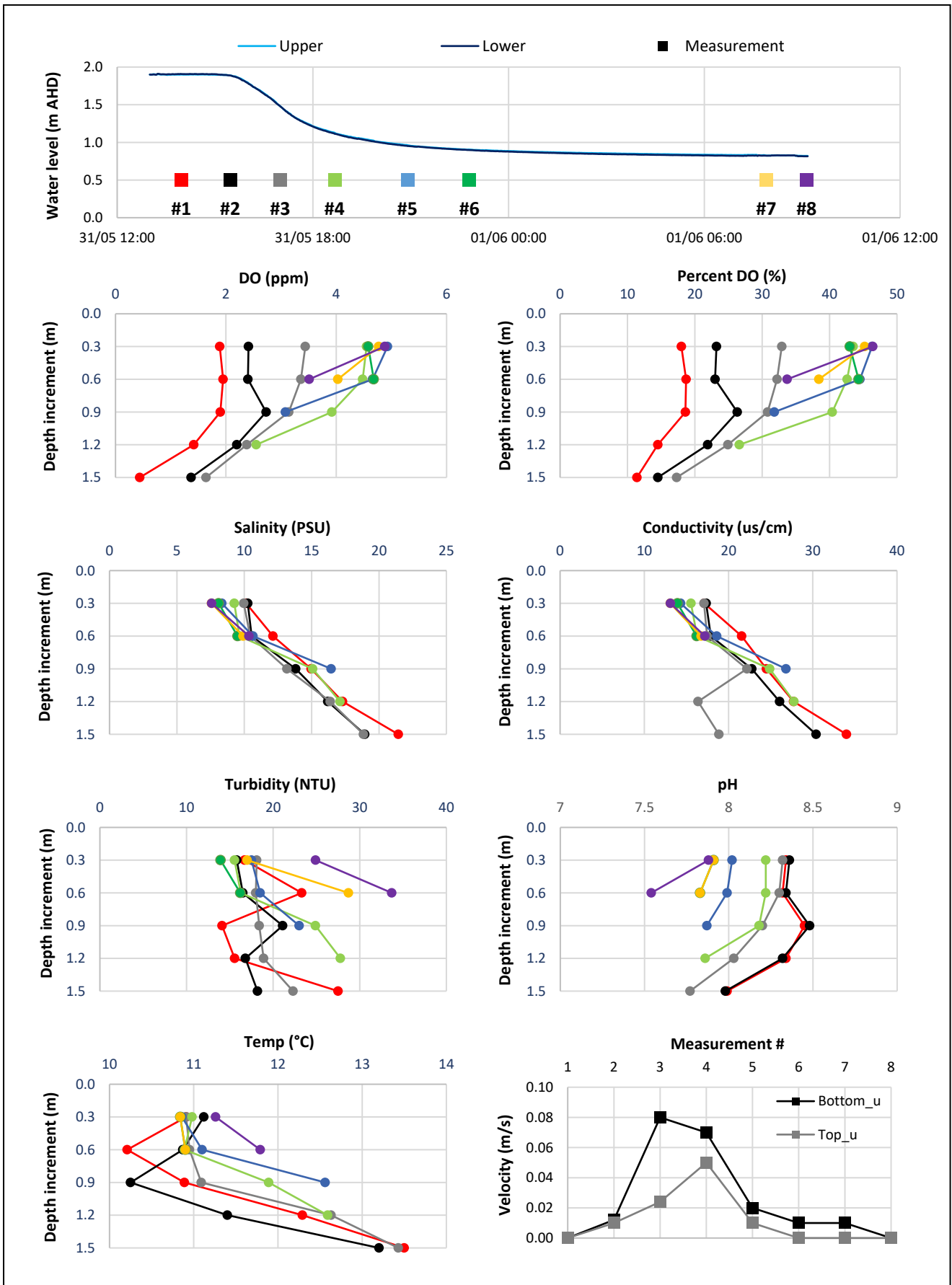


**Figure 1a-i.** (TOP) Estuary water level (to AHD) and the timing of physiochemical measurements - the colours used in this image match the depth profile # and colour used in all other graphs; DO (% saturation and ppm); salinity; conductivity; turbidity; pH; (h) temperature; and top and bottom velocity at Anglesea River.



### (b) Anglesea River 14/08/2019

Physiochemical change at Anglesea was measured at the fishing platform upstream of the Great Ocean Road Bridge (-38.41°, 144.19°). The corresponding morphodynamic change at the mouth is presented in Appendix 2 for Anglesea. During the opening, there was minimal change in estuary physiochemistry measured at the Great Ocean Road bridge (Table 2). Prior to opening, the estuary was non-stratified for both salinity and DO, with a relatively well-mixed water column (Table 1 depth profile #1). The estuary pH was slightly lower on the bottom of the water column at 1 m depth (Table 1). During the opening, the max outflow velocity at the mouth of 1.01 m/s was reached at 2.07 pm on 14/08 (Appendix 2). Top (0.014 m/s) and bottom (0.024 m/s) velocity at the physiochemical monitoring site reached a maximum at this time and then decreased to 0 m/s for the remainder of the opening (Table 2). The estuary maintained a small cross-sectional area with a max discharge of 0.75 m<sup>3</sup>/s<sup>-1</sup> at 5 pm on 14/08/19. Despite this, minimal change in estuary physiochemistry had occurred (Table 1). By the end of the monitoring period (depth profile #6), the estuary had decreased by -0.27 m in water depth. Depth profile #6 showed a slight increase in salinity and DO, but all other parameters remained similar to before the opening (Table 1).

**Table 2.** Physiochemical measurements taken during the artificial opening of Anglesea River on 14/08/2019. Profile #1 is pre-opening. \* is EstuaryWatch data taken at the same location several days after the artificial opening.

#	Depth (m)	Date time	Temp (°C)	PH	Turbidity (NTU)	Conductivity (us/cm)	Salinity (PSU)	DO (%)	DO (ppm)	u (m/s)	Depth (m)
1	0.00	14/08	10.02	4.84	8.30	8718	4.89	19.70	2.18	0 (top)	1.08
1	0.50	09:30	10.51	4.84	19.60	9285	5.23	19.00	2.07		
1	1.00		9.97	4.68	20.18	8586	4.81	19.60	2.17	0 (bot)	
2	0.00	14/08	10.69	4.46	9.10	8851	4.97	19.90	1.25	0 (top)	1.08
2	0.50	13:41	10.75	4.41	23.10	9116	5.13	19.60	2.13		
2	1.00		10.90	4.39	22.60	9523	5.38	20.00	2.15	0 (bot)	
3	0.00	14/08	10.83	4.23	8.40	8857	4.97	22.00	2.38	0.014	0.95
3	0.50	16:15	10.87	4.25	8.90	8888	5.01	22.60	2.38		
3	0.80		10.85	4.46	9.30	8944	5.03	22.00	2.43	0.024	
4	0.00	14/08	10.80	4.34	9.10	9230	5.20	20.40	2.21	0 (top)	0.93
4	0.50	19:29	10.84	4.34	15.10	9256	5.22	20.60	2.21		
4	0.80		10.83	4.35	9.00	9238	5.20	19.90	2.15	0 (bot)	
5	0.00	14/08	10.63	4.36	9.60	9136	5.20	21.60	2.34	0 (top)	0.88
5	0.50	22:36	10.63	4.36	10.80	9220	5.20	21.20	2.33		
5	0.80		10.63	4.38	13.80	9185	5.17	21.60	2.31	0 (bot)	
6	0.00	15/08	9.81	4.44	10.00	9185	5.17	24.20	2.66	0 (top)	0.81
6	0.50	09:31	9.89	4.40	10.70	9278	5.23	24.20	2.66		
6	0.80		9.87	4.49	22.00	9255	5.21	25.00	2.70	0 (bot)	
7*	0.10	21/08	11.60	3.90	9.00	9660	5.40	98.60	-	-	0.50
7*	0.40	09:14	11.60	4.30	9.00	9660	5.50	98.60	-	-	

### (c) Curdies Inlet openings 1 and 2 16/06/2019 and 17/06/2019

Prior to opening, a depth profile taken at the Dorey Street fishing platform at 8 am on 16/06/19 showed a well-mixed water column for all parameters. This was consistent with EstuaryWatch observations taken on the 04/06/19. As only two people were able to attend this opening, depth profiles were not able to be taken as the focus was on gaining morphodynamic data at the mouth. As such, 15 min interval observations from the DELWP automated Curdies River gauge @ Peterborough (-38.56°, 142.86°) were used to analyse physiochemical change in conjunction with changes in entrance morphology. The gauge is located 3.5 km upstream of the mouth and does not include depth profiles. Artificial opening 1 was unsuccessful but artificial opening 2 was successful at Curdies Inlet.

- Prior to opening 1 (10 am 16/06), DO was 2.45 ppm conductivity 9597  $\mu\text{S}/\text{cm}$ , and temperature 12.80 °C (Table 3). Opening 1 did not change the estuary water level but after the opening, conductivity dropped sharply then increased and DO increased slightly (Table 3; Figure 2). The influence on estuary physiochemistry during artificial opening 1 was minimal as the mouth rapidly infilled and the estuary did not commence draining.
- Prior to opening 2 (3 pm 17/06), DO was 3.73 ppm conductivity 7045  $\mu\text{S}/\text{cm}$ , and temperature 12.80 °C (Table 3). Immediately after opening, conductivity increased - reaching 11286  $\mu\text{S}/\text{cm}$  by 6 pm 17/06 coinciding with the cross-sectional area at the mouth reaching 2.10  $\text{m}^2$ . DO also increased sharply to 5.86 ppm by 8 pm 17/06 coinciding with the cross-sectional area increasing to 2.82  $\text{m}^2$  and discharge to 4.51  $\text{m}^3/\text{s}^{-1}$  (Table 3). This may be due to freshwater being drawn into the basin. This event is shown by a green arrow on Figure 2.
- By 12.00 am 18/06, DO had declined to 2.67 ppm as the estuary entered a stage of rapid expansion and basin drainage with discharge being 29.63  $\text{m}^3/\text{s}^{-1}$  (Table 3). By 2 am 18/06, conductivity had decreased to 5898  $\mu\text{S}/\text{cm}$  further indicating freshwater being drawn into the basin. This event is shown by a pink arrow on Figure 2.
- When the mouth had reached its peak discharge of 366.57  $\text{m}^3/\text{s}^{-1}$  at 8 am 18/06, DO had increased again to 4.49 ppm and conductivity remained lower at 5932  $\mu\text{S}/\text{cm}$ . From here on, the estuary entered the falling limb of the hydrograph and the basin drained steadily. Conductivity continued to gradually decrease and DO fluctuated. On 22/06, an increase in fluvial discharge upstream to 322 ML/day (from previously <275 ML/day). Throughout the opening, temperature fluctuated corresponding with diurnal cycles and tidal oscillations.

**Table 3.** Change in estuary water level, change in entrance morphology, and estuary physiochemistry during two artificial openings at Curdies Inlet. The timing of opening 1 is in blue and the timing of opening 2 is in red.

Date/time	WL (m AHD)	DO (ppm)	Temp (°C)	Conductivity ( $\mu\text{S}/\text{cm}$ )	Mouth area ( $\text{m}^2$ )	Discharge ( $\text{m}^3/\text{s}^{-1}$ )
16/06/19 08:00	1.34	2.94	12.70	9737	0.00	0.00
16/06/19 10:00	1.34	2.45	12.80	9597	0.00	0.00
16/06/19 12:00	1.34	3.40	12.70	10396	0.00	0.00
16/06/19 12:00	1.34	3.40	12.70	10396	0.00	0.00
16/06/19 14:00	1.35	4.10	12.80	8172	0.00	0.00
16/06/19 16:00	1.35	5.04	12.80	10365	0.00	0.00
16/06/19 18:00	1.35	5.32	12.80	10389	0.00	0.00
17/06/19 12:00	1.37	4.67	12.80	11448	0.00	0.00
17/06/19 14:00	1.38	3.73	12.80	7045	0.00	0.00
17/06/19 16:00	1.38	3.98	12.80	9160	1.14	1.60
17/06/19 18:00	1.38	3.94	12.80	11286	2.10	3.38
17/06/19 20:00	1.38	5.86	12.80	10521	2.82	4.51
17/06/19 22:00	1.37	3.27	12.90	10732	7.59	12.83
18/06/19 00:00	1.36	2.67	12.50	7827	11.85	29.63
18/06/19 02:00	1.33	4.08	12.20	5898	40.80	120.77
18/06/19 04:00	1.23	3.98	12.10	6343	66.95	201.52
18/06/19 06:00	1.11	4.74	12.00	6069	120.00	347.00
18/06/19 08:00	0.99	4.49	12.00	5932	137.00	366.57
18/06/19 10:00	0.90	4.24	11.90	5877	130.00	225.41
18/06/19 12:00	0.85	3.55	11.90	5799	121.00	137.78
18/06/19 14:00	0.85	4.07	12.10	5745	-	-
18/06/19 16:00	0.80	4.40	12.10	5617	-	-
18/06/19 18:00	0.70	4.41	12.00	5553	-	-
18/06/19 20:00	0.55	3.92	11.90	5593	-	-

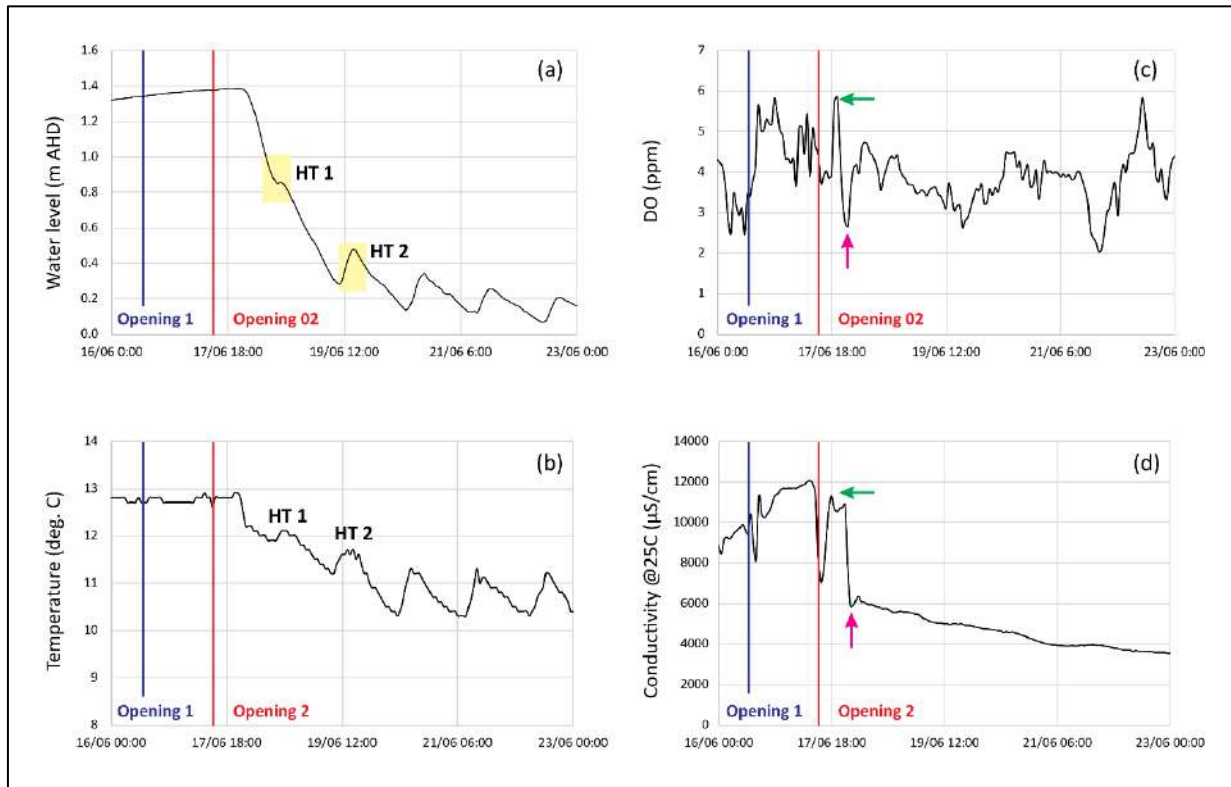


**Figure 3a-d.** (a) Estuary water level (to AHD) with HT showing high tide peaks; (b) DO ppm); (d) temperature; (e) conductivity. Data is taken from the DELWP Curdies @ Peterborough gauge. Openings are annotated on the graphs.

#### **(d) Gellibrand River artificial opening 09/03/2019**

At the Gellibrand River, depth profiles were taken at two locations:

- (1) Downstream - Princetown Bridge (-38.70°, 143.16°)
- (2) Upstream - Coxon's Bridge (-38.71°, 143.18°).

This data was supplemented with EstuaryWatch data taken at the same locations.

Prior to opening, both locations showed a highly stratified water column both for DO and salinity (Figure 5; Figure 6). Estuary drainage and channel expansion and discharge at the mouth was minimal during the opening and no drastic change in estuary physiochemistry was observed.

During the opening, velocity was higher at the Coxon's Bridge site - possible due to the influence of freshwater inflow as this location was higher in the basin and near the influence of freshwater inflow (Figure 5g; Figure 6g). Estuary drainage and channel expansion and discharge at the mouth was minimal during the opening and no drastic change in estuary physiochemistry was observed.

At the Coxon's Bridge site, DO decreased during the opening (Figure 5 a-c) while at the Princetown bridge site it increased slightly (Figure 6a-c). Salinity showed little change at both sites (Figure 5d; Figure 6d).

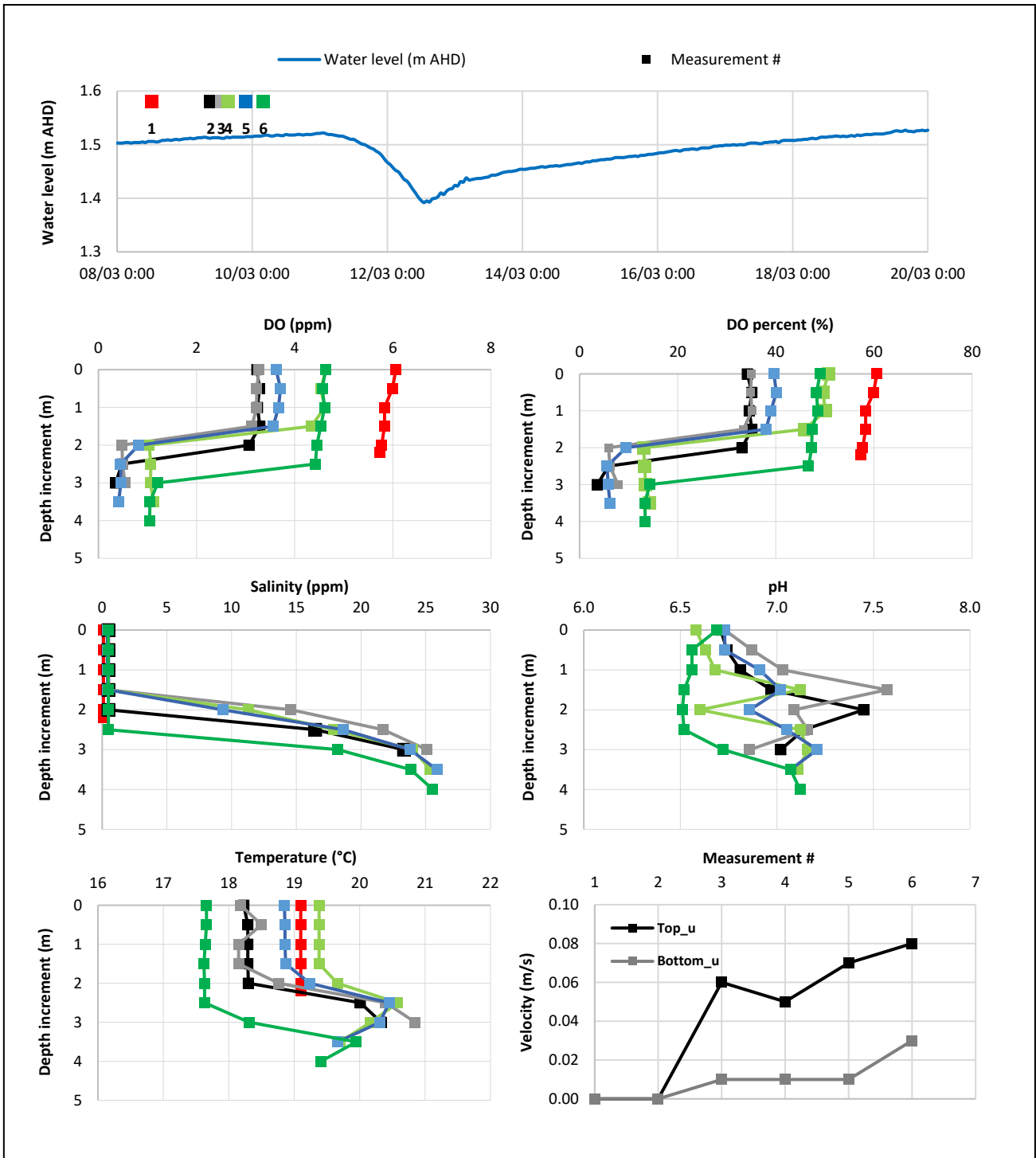


**Figure 5a-g.** (TOP) Estuary water level (to AHD) and the timing of physiochemical measurements - the colours used in this image match the depth profile # and colour used in all other graphs; DO (% saturation and ppm); salinity; pH; temperature; and top and bottom velocity at Gellibrand River Coxon's Bridge site (upstream).

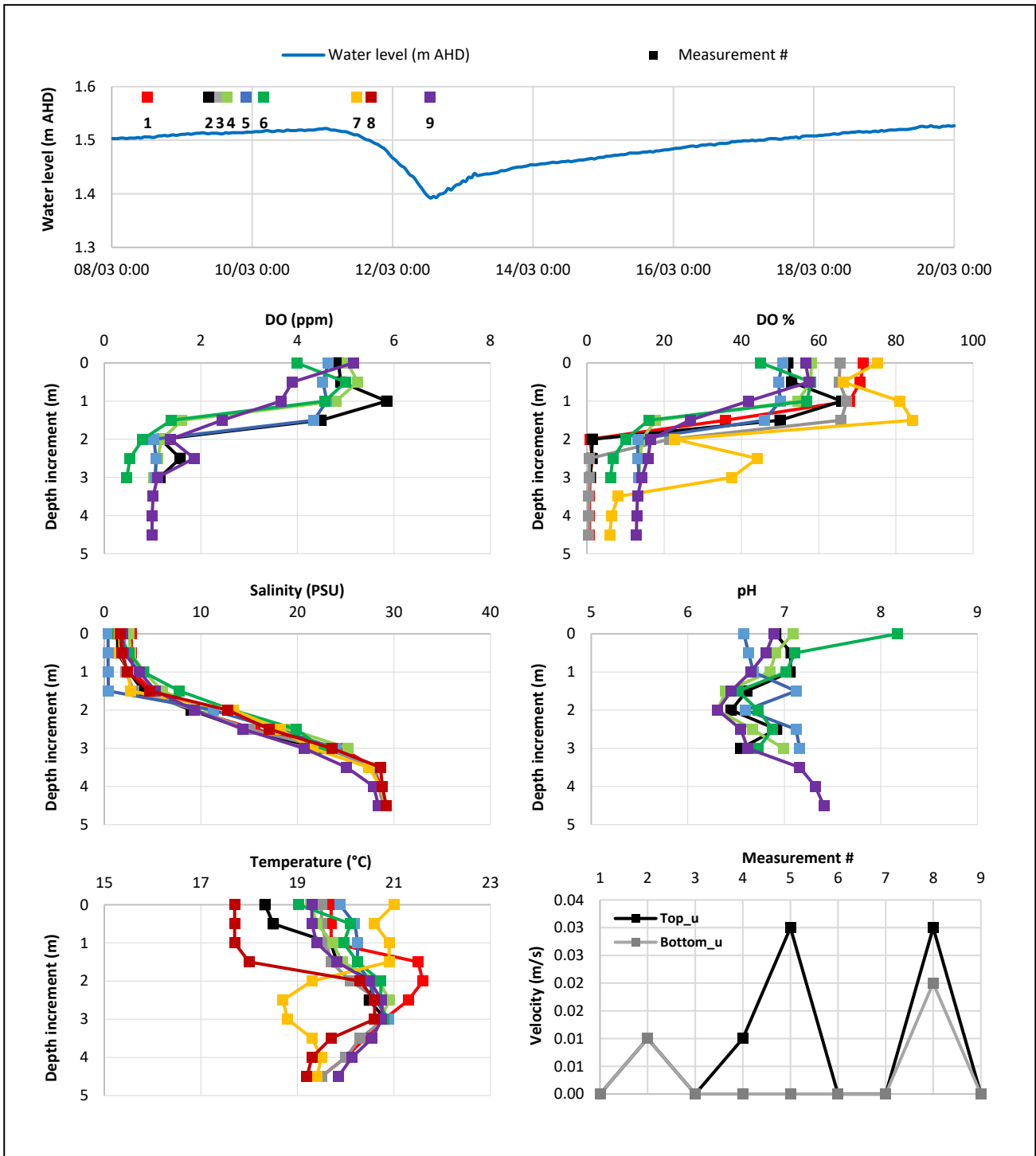


**Figure 6a-g.** (TOP) Estuary water level (to AHD) and the timing of physiochemical measurements - the colours used in this image match the depth profile # and colour used in all other graphs; DO (% saturation and ppm); salinity; pH; temperature; and top and bottom velocity at Gellibrand River Princetown Bridge site (downstream).



**Table 4.** Change in physiochemistry depth profiles at Gellibrand River Coxon’s Bridge site (upstream). \* is EstuaryWatch data.

UPSTREAM	Depth (m)	Date/time	Temp (°C)	PH	Salinity (PSU)	DO %	DO (ppm)	u (m/s)
1 (PRE)*	0.00	06/03/19 10:30	19.10		0.10	60.60	6.06	0.00
1	0.50		19.10		0.10	59.90	5.99	
1	1.00		19.10		0.10	58.30	5.83	
1	1.50		19.10		0.10	58.30	5.83	
1	2.00		19.10		0.10	57.70	5.77	
1	2.20		19.10		0.10	57.30	5.73	0.00
2 (PRE)	0.00	09/03/19 9:55	18.23	6.71	0.48	34.20	3.23	0.060
2	0.50		18.29	6.74	0.48	35.10	3.28	
2	1.00		18.29	6.81	0.48	34.60	3.24	
2	1.50		18.29	6.97	0.48	35.10	3.29	
2	2.00		18.30	7.45	0.48	33.10	3.07	
2	2.50		20.01	7.14	16.47	5.90	0.48	
2	3.00		20.33	7.02	23.31	3.63	0.35	0.000
3	0.00	09/03/19 15:25	18.18	6.73	0.49	35.00	3.27	0.040
3	0.50		18.50	6.87	0.49	34.90	3.23	
3	1.00		18.15	7.03	0.49	35.10	3.22	
3	1.50		18.15	7.57	0.50	33.40	3.13	
3	2.00		18.76	7.09	14.60	5.90	0.48	
3	2.50		20.40	7.16	21.71	6.20	0.49	
3	3.00		20.85	6.86	25.09	7.80	0.54	0.010
4	0.00	09/03/19 21:17	19.38	6.58	0.39	50.70	4.64	0.050
4	0.50		19.38	6.63	0.39	49.60	4.53	
4	1.00		19.38	6.68	0.40	50.10	4.61	
4	1.50		19.38	7.12	0.43	45.90	4.34	
4	2.00		19.66	6.60	11.29	13.10	1.03	
4	2.50		20.58	7.12	17.88	13.20	1.07	
4	3.00		20.17	7.16	24.00	13.50	1.06	
4	3.50		19.70	7.11	25.36	14.30	1.12	0.010
5	0.00	10/03/19 3:25	18.85	6.73	0.41	39.60	3.62	0.070
5	0.50		18.86	6.73	0.40	40.10	3.71	
5	1.00		18.86	6.91	0.41	39.00	3.67	
5	1.50		18.87	7.02	0.43	38.00	3.56	
5	2.00		19.24	6.86	9.33	9.50	0.82	
5	2.50		20.45	7.05	18.62	5.60	0.45	
5	3.00		20.31	7.21	23.77	5.80	0.46	
5	3.50		19.67	7.07	25.86	6.20	0.41	0.010
6	0.00	11/03/19 16:30	17.66	6.69	0.47	49.00	4.63	0.080
6	0.50		17.66	6.56	0.47	48.30	4.56	
6	1.00		17.64	6.56	0.47	48.50	4.61	
6	1.50		17.62	6.52	0.47	47.40	4.53	
6	2.00		17.63	6.51	0.48	47.30	4.45	
6	2.50		17.63	6.52	0.49	46.70	4.42	
6	3.00		18.31	6.72	18.20	14.30	1.21	
6	3.50		19.95	7.07	23.83	13.30	1.05	
6	4.00		19.41	7.12	25.55	13.40	1.04	0.030

**Table 5.** Change in physiochemistry depth profiles at Gellibrand River Princetown Bridge site (downstream). \* is EstuaryWatch data.

Profile #	Depth (m)	Date/time	Temp (°C)	PH	Salinity (PSU)	DO %	DO (ppm)	u (m/s)
1 (PRE)*	0.0	6/03/19 12:20	19.70		2.80	71.60		0.00
	0.5		19.70		2.80	70.80		
	1.0		19.70		3.00	68.00		
	1.5		21.50		5.00	35.90		
	2.0		21.60		9.20	0.80		
	2.5		21.30		15.60	1.40		
	3.0		20.80		24.60	0.80		
	3.5		20.40		27.90	0.70		
	4.0		20.00		28.60	0.70		
4.5	19.50		29.10	0.70		0.00		
2 (PRE)	0.0	09/03/19 9:17	18.33	6.91	1.36	52.00	4.85	0.01
	0.5		18.50	7.07	1.40	53.00	4.90	
	1.0		19.69	7.06	2.58	66.00	5.85	
	1.5		19.82	6.61	4.03	50.00	4.49	
	2.0		20.57	6.45	9.01	1.38	1.17	
	2.5		20.49	6.92	14.62	1.20	1.57	
	3.0		20.82	6.55	22.31	0.90	1.15	
3*	0.0	09/03/19 13:05	19.50		2.10	65.50		0.00
	0.5		19.50		2.10	65.30		
	1.0		19.60		2.20	67.30		
	1.5		19.70		3.10	65.80		
	2.0		20.10		9.50	21.50		
	2.5		20.70		15.10	0.70		
	3.0		20.80		23.00	0.60		
	3.5		20.30		27.90	0.50		
	4.0		20.00		28.40	0.50		
4.5	19.50		28.90	0.50		0.00		
4	0.0	09/03/19 15:30	19.27	7.09	2.58	58.10	5.04	0.00
	0.5		19.41	6.91	2.71	58.00	5.25	
	1.0		19.73	6.85	4.16	54.60	4.80	
	1.5		19.93	6.39	6.01	17.80	1.61	
	2.0		20.68	6.31	10.90	14.30	1.19	
	2.5		20.91	6.67	19.20	13.80	1.10	
	3.0		20.71	6.99	25.24	13.40	1.03	
5	0.0	09/03/19 21:50	19.88	6.58	0.39	50.70	4.64	0.03
	0.5		20.19	6.63	0.39	49.60	4.53	
	1.0		20.25	6.68	0.40	50.10	4.61	
	1.5		20.24	7.12	0.43	45.90	4.34	
	2.0		20.48	6.60	11.29	13.10	1.03	
	2.5		20.62	7.12	17.88	13.20	1.07	
	3.0		20.89	7.16	24.00	13.50	1.06	
6	0.0	10/03/2019 3:58	19.03	8.17	1.43	45.00	3.99	0.00
	0.5		20.10	7.11	2.59	58.00	5.00	
	1.0		19.96	7.02	4.05	57.00	4.57	
	1.5		20.24	6.52	7.80	16.00	1.39	
	2.0		20.73	6.73	13.30	10.01	0.8	

	2.5		20.73	6.88	19.90	6.70	0.53	
	3.0		20.80	6.73	22.57	6.10	0.47	0.00
7*	0.0	11/03/19 11:45	21.00		1.60	75.30		0.00
	0.5		20.60		1.60	66.30		
	1.0		20.90		2.50	81.10		
	1.5		20.90		2.70	84.30		
	2.0		19.30		13.40	22.70		
	2.5		18.70		18.20	44.10		
	3.0		18.80		21.60	37.60		
	3.5		19.30		27.40	8.10		
	4.0		19.50		28.60	6.40		
	4.5		19.40		29.20	5.90		0.00
8	0.0	11/03/19 16:43	19.30	6.89	1.88	56.60	5.16	0.03
	0.5		19.30	6.81	2.02	57.50	3.90	
	1.0		19.40	6.65	3.64	41.80	3.66	
	1.5		19.82	6.45	5.32	26.70	2.44	
	2.0		20.50	6.31	9.36	16.50	1.37	
	2.5		20.75	6.55	14.39	15.80	1.86	
	3.0		20.75	6.62	20.71	14.20	1.10	
	3.5		20.55	7.16	25.11	13.10	1.01	
	4.0		20.13	7.32	27.90	12.90	0.99	
	4.5		19.85	7.41	28.40	12.80	0.99	0.02
9*	0.0	12/03/19 12:50	17.70		1.70	46.90		0.00
	0.5		17.70		1.80	44.80		
	1.0		17.70		2.40	33.30		
	1.5		18.00		4.70	17.50		
	2.0		20.30		12.80	1.90		
	2.5		20.60		17.10	0.60		
	3.0		20.60		23.60	0.50		
	3.5		19.70		28.60	0.50		
	4.0		19.30		28.80	0.50		
	4.5		19.20		29.20	0.40		0.00

## **Section 2: DESKTOP ANALYSIS**

Water level and physiochemical data was compared for historic openings at two sites: the Gellibrand and Curdies River estuaries to compare conditions which resulted in fish deaths vs when fish deaths did not occur. The fish death in focus at Curdies Inlet was one in 2017 where fish were stranded on the floodplain after a period of rapid drainage. Three fish deaths at the Gellibrand were compared to openings which suffered no fish deaths. The fish deaths at the Gellibrand resulted from a loss of oxygenated water as openings occurred when the estuary was stratified. Work to analyse this data is ongoing and will be further analysed as part of a Melbourne University honours project in 2020 in conjunction with existing and further field data.

### **(a) HISTORIC DATA: Fish death via rapid drainage and stranding - Curdies Inlet**

Curdies Inlet suffered a fish death after an artificial opening on 11/07/2017 where fish were stranded on the floodplain. Table 5 and Figure 5a-i show the conditions prior to opening and during openings for this event compared to four historic artificial openings where no fish deaths occurred. The fish death event had a higher HG at the time of opening (0.030 m/m) compared to all other historic events where data was available for (Table 5). While the opening was not undertaken at the highest water level relative to prior openings, the short berm length and tidal stage here would have increased the relative HG. This caused the estuary to drain quickly (~40 hrs

compared to 60 - 72 hrs for other openings). The drainage rate was higher (-0.039 m/hr) compared to other openings and the drainage rate during Stage 2 were also higher (Table 5). During Stage 2, the estuary drained at 0.10 m/hr (Table 5). While a drop in DO during the fish death event was not the primary cause of fish deaths, it did also show a clear decrease corresponding with the period of rapid drainage (Figure 5a-b). Given the limited available data, the high HG at the time of opening seems to be the primary cause for the rapid drainage and fish deaths occurring on 11/07/17.

**Table 5.** Data for historic artificial openings at Curdies Inlet compared to opening on 11/07/17 that left fish stranded on the floodplain at Curdies Inlet. The opening associated with the fish death is in red text. T is the duration of drainage, Q\_d1 is discharge on the day of opening and Q\_d2 is discharge the day after opening, drain rate is drainage rate, and DO is dissolved oxygen concentration (ppm). Stg. 2 refers to the period of rapid drainage and channel expansion.

Date opened	Start WL (m AHD)	Drainage (m)	Drain T (hrs)	Drain rate (m/hr)	HG (m/m)	Q_d1 (ML/d)	Q_d2 (ML/d)	Stg. 2 T (hrs)	Stg. 2 drain rate (m/hr)	Start DO (ppm)	End DO (ppm)
<b>11/07/17</b>	<b>1.56</b>	<b>1.55</b>	<b>40</b>	<b>0.039</b>	<b>0.030</b>	<b>374</b>	<b>317</b>	<b>12</b>	<b>0.100</b>	<b>8.21</b>	<b>4.01</b>
17/06/19	1.38	1.10	60	0.018	0.025	183	157	14	0.073	4.20	1.40
30/06/16	1.44	1.23	62	0.020	-	141	210	24	0.045	9.15	5.84
06/08/15	1.63	1.57	72	0.022	-	421	508	22	0.058	10.24	5.44
30/06/14	1.55	1.39	70	0.020	0.023	1407	1866	24	0.050	8.56	7.09

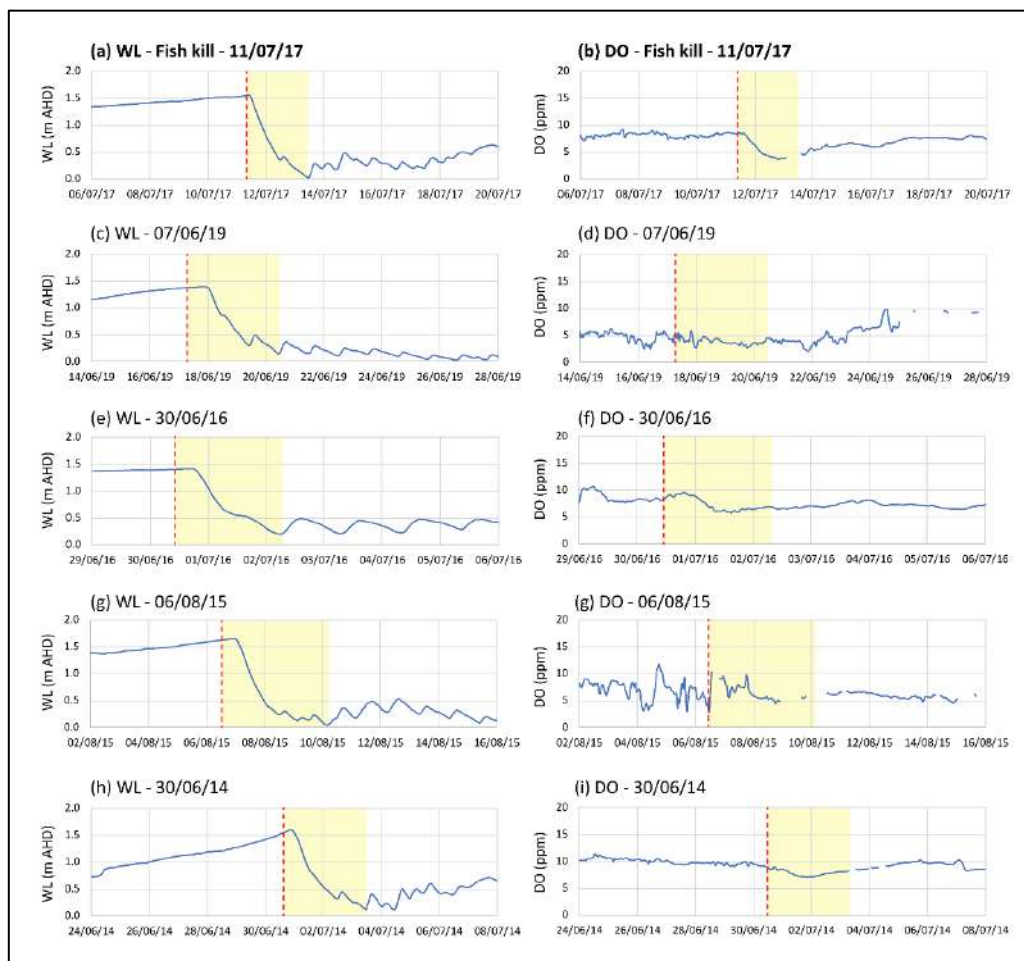


**Figure 5a-i.** Changes in water level (WL) and dissolved oxygen (DO) during historic artificial openings at Curdies Inlet. The red line is the time of each opening and the yellow box is the period of estuary drainage - taken as until the estuary stopped decreasing in water level.

## (b) Fish deaths via the loss of oxygenated water at the Gellibrand River

The Gellibrand River has also suffered historic fish deaths. Here fish deaths are suggested to occur due to the loss of the oxygen-rich top layer draining first when the estuary is in a stratified condition. This leaves below a dense, lower layer of deoxygenated water. Three fish death events at the Gellibrand had sufficient historic data to be analysed and compared to openings where fish deaths did not occur (Table 6; Figure 52):

(1) **22/02/2013 - major fish death**

<https://www.standard.net.au/story/1434216/open-and-shut-gellibrand-river-mouth-probe/>

(2) **11/04/2014 - minor fish death**

[http://www.estuarywatch.org.au/estuary\\_data\\_portal.php?action=view\\_estuary\\_event&estuary\\_event\\_id=1791&cma=ccma](http://www.estuarywatch.org.au/estuary_data_portal.php?action=view_estuary_event&estuary_event_id=1791&cma=ccma)

(3) **11/03/2016 - minor fish death**

<https://www.standard.net.au/story/3800044/river-opening-leads-to-fish-kill/>

The three fish deaths above all seemed to result from a rapid decrease in dissolved oxygen (DO) occurring during the drainage period. The decrease in DO occurred during Stage 2 of the opening sequence when drainage rates were most rapid and the channel cross-sectional area and discharge at the mouth was the largest. The available data is insufficient to provide a consistent reason why DO decreased rapidly after these three artificial openings that resulted in fish deaths. It must also be noted that the available data is taken from the Princetown Bridge monitoring station and so does not accurately reflect DO conditions across the whole estuary basin. Some hypotheses about why fish deaths occurred during these particular openings are as follows:

- **Low starting DO in the estuary (similar to descriptions by Becker et al 2009):** All openings where fish deaths had low starting DO (<4.80 ppm). This is consistently lower than openings where fish deaths did not occur. More data is required to establish a value for safe starting DO levels.
- **High HG/drainage rate combined with low starting DO:** While higher a HG at opening did not induce fish deaths alone, all openings where fish deaths occurred had a high starting HG combined with low starting DO. This means if the estuary drains rapidly, there is no buffer to protect against the loss of oxygen rich water which is likely to be lost more rapidly.
- **Lack of freshwater inflow in the day following opening:** Fish death events were followed by relatively low fluvial inflow in the two days after opening. This could result in less oxygen rich water being brought into replace what is lost via estuary drainage.
- **A prior long closure period:** If an estuary is closed for a longer period of time, it is more likely to be stratified.

**Table 6.** Data for historic openings with fish deaths (red text) and without fish deaths (black text) at the Gellibrand River. Parameter annotations are as per Table 5.

Date opened	Start WL (m AHD)	Drainage (m)	Drain T (hrs)	Drain rate (m/hr)	HG (m/m)	Q_d1 (ML/d)	Q_d2 (ML/d)	Stg. 2 T (hrs)	Stg. 2 drain rate (m/hr)	Start DO (ppm)	End DO (ppm)
22/02/13	1.51	1.36	42	0.032	-	144	42	21	0.054	3.05	0.65
11/04/14	1.48	1.30	30	0.043	0.049	141	141	8	0.141	4.79	0.50
11/03/16	1.39	1.21	48	0.025	0.019	146	142	19	0.059	3.10	2.50
1/04/15	1.55	1.25	30	0.042	-	163	153	22	0.051	7.33	4.87
11/03/16	1.38	1.20	28	0.043	0.019	149	150	18	0.063	6.71	2.68
12/05/16	1.87	1.31	24	0.055	0.035	480	599	23	0.049	7.23	3.77
13/04/17	1.78	1.42	51	0.028	0.020	539	417	26	0.043	6.54	4.15
19/04/18	1.74	1.50	40	0.038	0.036	382	328	26.00	0.043	8.08	4.16



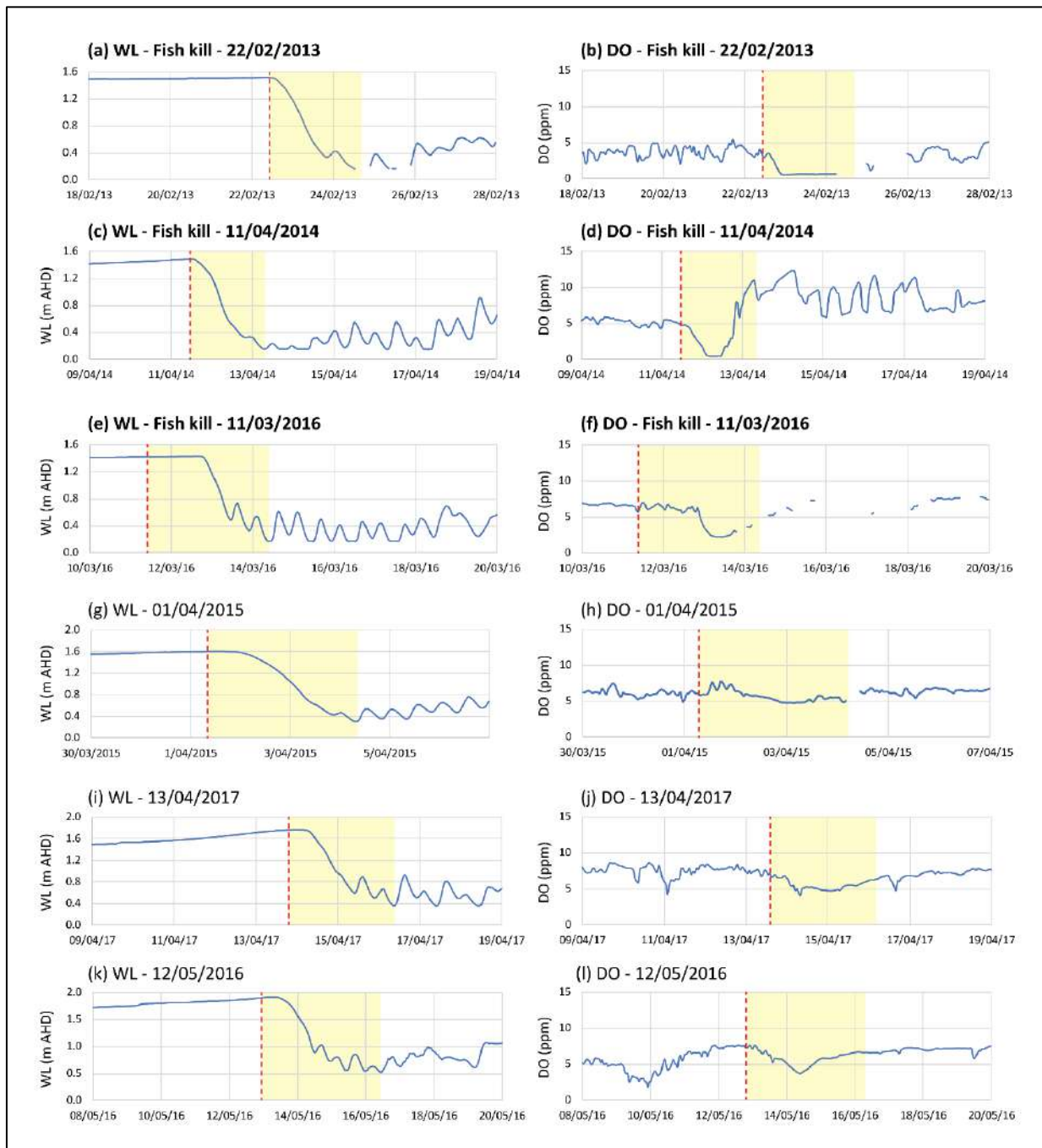


**Figure 6a-i.** Changes in water level (WL) and dissolved oxygen (DO) during historic artificial openings at Gellibrand River. The red line is the time of opening and the yellow box is the period of estuary drainage.